ZESZYTY
NAUKOWE
POLITECHNIKI
ŚLĄSKIEJ

Marek PAWEŁCZYK

FEEDBACK CONTROL OF ACOUSTIC NOISE AT DESIRED LOCATIONS

WYDAWNICTWO
POLITECHNIKI
ŚLĄSKIEJ

Gliwice 2005

POLITECHNIKA ŚLĄSKA
ZESZYTY NAUKOWE
Nr 1684

Marek PAWEŁCZYK

FEEDBACK CONTROL OF ACOUSTIC NOISE AT DESIRED LOCATIONS

Gliwice 2005

PL ISSN 0434-0760

Marek Pawełczyk
Institute of Automatic Control
Silesian University of Technology
ul. Akademicka 16
44-101 Gliwice, Poland
marek.pawelczyk@polsl.pl

To my Family

CONTENTS

SPIS TREŚCI

Objective

The objective of the research reported is to design and analyse optimal and adaptive feedback control algorithms appropriate for attenuating acoustic noise at desired locations. A group of acousto-electric plants characterised by small distances between the desired locations and corresponding available real microphones, compared to the wavelengths of the acoustic noise, is considered.

Structure

The monograph is organised as follows.

Chapter 1 constitutes an introduction. At the beginning the problem of acoustic noise is addressed and the idea of its active control is presented. The activity in this field is briefly summarised. Then, a group of acousto-electric plants is singled out. It will be dealt with in the remaining chapters. Finally, required assumptions are collected.

In *Chapter 2* the Internal Model Control system is addressed. Optimal control filters are derived for this structure using polynomial, frequency-domain and correlation-based approaches. However, contrary to most of the corresponding references imperfect plant modelling is assumed. The problem is formulated using general notation to allow for direct application to the systems designed in the next chapter. The optimal control systems are analysed in terms of performance and stability. Solutions to improve stability are recalled. Then, adaptive realisations are presented and analysed with focus on conditions for convergence of the algorithms. Overlapping problems of stability of the feedback loop and convergence of the adaptive algorithms are discussed. Methods for improving robustness are also included.

In *Chapter 3* three different structures of optimal and adaptive systems generating zones of quiet at desired locations, referred to as the Virtual Microphone Control systems are designed and analysed. First two of them use an estimate of the residual signal at the virtual microphone. The last one is composed of two stages – the so-called tuning and control stages.

Knowledge gained in the tuning stage is used to generate a command signal for the control stage. The systems are compared, spatial distribution of attenuation is examined and an alternative design methodology is abstracted. Finally, the problem of noise control at locations far from the secondary source is addressed.

Chapter 4 briefly addresses multi-channel realisations of all the control systems. Similarly to the previous chapters, the plant and disturbance are defined at the beginning and main assumptions are made. Then, optimal systems are designed using different approaches. Stability and performance of the systems is discussed and decentralised control is mentioned. Afterwards, adaptive systems are addressed.

Chapter 5 concerns laboratory experiments. It begins with presentation of the real active headrest – a representative of the considered group of acousto-electric plants. Properties of this plant are discussed and basic characteristics are presented. Then, attenuation results of tonal, multi-tonal and real noises obtained using the control systems in different configurations are provided. They are illustrated in the form of spatial distribution of attenuation areas.

In *Chapter 6* the research is summarised and conclusions are drawn.

Appendix A provides basic definitions and theorems.

In *Appendix B* simulation analysis is performed. The data come from laboratory experiments with the active headrest system. First, optimal control system designs using polynomial, frequency-domain and correlation-based approaches are considered. Then, adaptive systems are addressed. Influence of modelling errors, feedback loop and algorithm parameterisation are analysed. Virtual Microphone Control systems are also compared.

In *Appendix C* simulation results of optimal and adaptive control of tonal and real noises obtained using all the control systems are given. They are presented in the form of spatial distribution of attenuation.

References and *Glossary* are also provided.

Finally, the monograph is recapitulated in Polish and captions to figures and tables are presented in Polish.

All important conclusions drawn from the appendices are presented in the main text. There are, however, several references to the appendices, where more details on corresponding experiments can be found.

Contribution

Theoretical results on optimal and adaptive Internal Model Control system designed using different approaches are gathered, systemised and generalised to the case of imperfect plant model. Some conclusions, important for noise control are also drawn. Then, optimal and adaptive Virtual Microphone Control systems of different structures are designed and analysed in a coherent way for a group of acousto-electric plants. Although the general idea of such systems is known the presented solutions are new. Multi-channel structures of all the systems are also addressed. The systems are verified by means of simulation and on a real-world active headrest system characterised by non-minimum phase paths including significant time-delays.

The main contribution can be thus summarised as development and analysis of feedback control systems for generating zones of quiet at desired locations and their practical verification.

Declaration

The author when preparing the monograph has benefited from a rich set of publications on active noise control and control theory, mainly the excellent works (in alphabetical order): [Elliott_01], [Haykin_96], [KuoM_96], [MorariZ_89], [NiederlinskiMO_95], [Orfanidis_88], [Rafaely_97], [VaudreyBS_03]. Appropriate references to these and other works are provided. All remaining derivations, conclusions and experiments are results of the author's own research.

Acknowledgments

The author would like to thank the reviewers, Professor Leszek Trybus (Rzeszów University of Technology) and Professor Piotr Tatjewski (Warsaw University of Technology) who offered much useful feedback.

The author is also indebted to members of the Computer Control Systems Group who read the manuscript and provided precious comments and suggestions. Thanks are also addressed to the authorities and colleagues from the Department of Automatic Control, Electronics and Computer Science, the Institute of Automatic Control, and in particular the Computer Control Systems Group for encouragement to the research and pleasant atmosphere.

The author also owes acknowledgments to those institutions which supported him during the research. They are State Committee for Scientific Research (KBN), Ministry of National Education and Sport, Rector of the Silesian University of Technology, and FIAT.

Finally, the greatest thanks are to my family for patience, understanding and tremendous support.

Marek Pawełczyk

June 2005

CHAPTER 1

INTRODUCTION

1.1 ACOUSTIC NOISE

Sound may be defined as any pressure variations that the human ear can detect [BrüelKjær_01]. Sound is a common part of everyday life. It enables spoken communication, provides enjoyable experience, permits to make quality evaluations and diagnoses, alerts or warns. However, sometimes sound is unpleasant or unwanted and then it is called noise [Crocker_97]. Noise increases together with development of industry and transport. Generally, two types of noise can be distinguished in the environment – broadband and narrowband [KuoM_96]. Broadband noise is caused, for example, by turbulence and therefore distributes its energy across the frequency band. In turn, narrowband noise concentrates most of its energy at specific frequencies. This noise is related to rotating or reciprocating machines, so it is purely periodic (deterministic) or nearly periodic and may consist of one or many tones.

In addition to loss of concentration and annoyance, many people suffer from severe hearing damage due to high-level ambient noise in their working environment. Prolonged exposure to loud sound causes damage to the hair cells with the result that hearing ability becomes progressively impaired. Besides, it has also negative influence on other basic human systems. It has the potential to: cause stress reactions, lead to pathological alterations in the myocardium and the vascular walls [Ising_98], and deteriorate vision acuity [Harazin_98]. Therefore, it is justified to engage efforts in reducing noise reaching humans.

Commonly used passive barriers are practically unfeasible for low-frequency (e.g. industrial or road) noise because of the dependence between acoustic wavelength of the noise and thickness of the barriers required for absorption [NelsonE_94]. They are also not applicable if the listener needs to move over a noisy environment. Therefore, active solutions gain considerable interest in recent years.

1.2 Active noise control

In active noise control (ANC) an additional secondary sound source is used to cancel noise from the original primary source. The physical justification is given by Young's interference principle. According to this principle, interference of two out-of-phase sounds of equal amplitudes results in their mutual cancellation. The secondary source can also change the radiation acoustic impedance thereby reducing the sound power radiated [KuoM_96], [HansenS_97], [Elliott_01]. This theory, although formally very simple, is difficult to be directly applied in practice. There are many problems related to physical aspects of the cancellation phenomenon as well as related to control. Therefore, the term 'attenuation' or 'reduction' should be rather used instead of 'cancellation'. In control system terminology primary noise constitutes an output disturbance that is to be suppressed. In fact, a residual signal as the effect of primary and secondary sounds interference at a given point in space is controlled in the mean-square or peak sense. The first approach, considered in this monograph, directly corresponds to the primary goal, i.e. minimisation of the sound pressure level [Rafaely_97], [Elliott_01]. It can, however, lead to significant reinforcement of some frequency components of the disturbance. In turn, the second approach, barely mentioned, tends to equalise contribution of all frequency components to the residual noise, making its spectrum flatter. This may be perceived by the user as an unpleasant hissing noise.

In a diffuse acoustic field global active noise control in an entire enclosure is practically unfeasible [NelsonE_94]. The solution is thus local control in a particular area or some areas and creation of the so-called 'local zones of quiet', called further as the 'zones of quiet'. Actually, the control is performed at a given point in space and the attenuation propagates from this point in the form of a zone. However, it is often impossible to place an observer sensor at this point due to practical inconvenience or technological difficulty. Therefore, another sensor, called error or residual sensor, placed as close as possible to the desired point or area is used. The error sensor feeds back information about attenuation results, which can also be used to drive the secondary source (feedback control). Sometimes it is beneficial to employ a reference sensor to detect noise upstream, long before it reaches the area of interest (feedforward control). If the control algorithms are required to adapt to changes of the noise character or to variations of the plant physical properties the information from the error sensor supervises an adaptation (Figure 1.1). In applications, the primary source is usually not a loudspeaker and may often be distributed. It is rather a working mechanism or engine. In turn, the secondary source is usually a loudspeaker (loudspeakers, in general) and the

sensors are microphones providing a measure of the acoustic pressure at their location. If the reference microphone in feedforward control were able to detect the secondary sound it would introduce the so-called acoustic feedback, which might deteriorate the performance or even lead to instability of the entire control system [KuoM_96]. If possible, it is then suggested to substitute a tachometer or pyrometer for this microphone or employ a unidirectional microphone [TokhiL_92].

Local active noise control near the secondary source deserves particular interest. It is technologically feasible and acceptable. It requires small energy amount to drive the secondary source and therefore is also economically efficient. Moreover, the direct component of the secondary sound field dominates over the reverberant component. This gives good coupling between the secondary source and the observation point, where attenuation is desired [Rafaely_97]. Therefore, acoustic pressure increase at other locations is not significant. It should be, however, stressed that the error microphone is placed then in the intense near-field of the vibrating secondary source diaphragm where energy is stored, what can make the plant non-linear at low frequencies [BiesH_96].

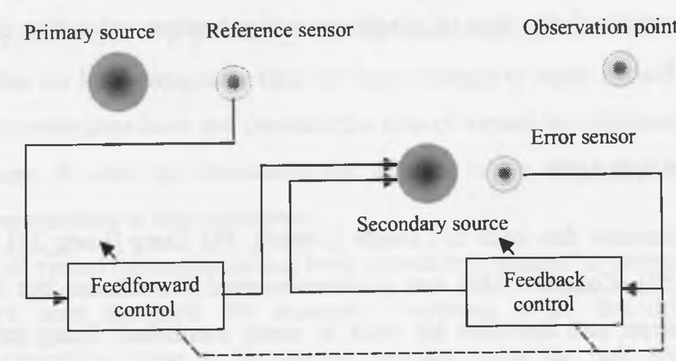

Figure 1.1 Active noise control strategies.

The distance between the error microphone and the observation point (area) is nonzero and can vary in time. As a consequence, the zone of quiet generated at the error microphone can poorly propagate to the observation point, where, by assumption, the user ear is located. Zones of quiet can have different and complicated shapes dependent on geometrical properties of the ANC system [Ahuja_91], [TokhiL_92]. Their distribution has been theoretically analysed for idealised conditions in [NelsonE_94], [Elliott_96], [GarciaEB_97], [Rafaely_97, 01] using the spatial correlation function of diffuse sound field. It follows from those considerations that these areas extend with respect to reinforcement areas when decreasing the frequency and increasing the distance from the secondary source. For instance, the 10-dB zone of quiet may reach about one-tenth of a wavelength for pure-tone sound fields. The zones of quiet additionally extend if they are generated at an acoustic barrier, which imposes zero acoustic pressure gradient at its surface, what 'flattens' the secondary sound field close to the barrier [GarciaEB_97], [RafaelyEG_99], [RafaelyE_99]. They can be further enlarged if the control system is set to operate on a pair or more closely spaced positions [GarciaEB_96].

One of the examples of acousto-electric plants where local control near the secondary source is performed is active headrest recognised as a test-plant in this monograph and presented in details in Chapter 5. In a prototype of this plant the headrest of a chair is equipped with loudspeakers generating secondary sounds for both channels, as well as microphones sensing interference effects. Such a device is already known in the literature [RafaelyGE_97], [GarciaEB_97]. However, the shape and arrangement of the necessary components of the headrest considered have been designed not to annoy the user and become closer to a market acceptable solution with the general aim to improve acoustic comfort by attenuating noise at the user ears.

Other examples of this type of plants are active headset and active phone. They are briefly referred to.

1.3 State of the Art

First ANC applications date back to Coanda [Coanda_30], Lueg [Lueg_36], and Olson and May [OlsonM_53]. Coanda's idea was a phase-inverted cancellation but his project was technically incorrect and therefore his work is rarely mentioned. Lueg attenuated a one-dimensional acoustic wave in a duct using feedforward from an upstream microphone. Olson and May applied feedback from a downstream microphone to attenuate ambient noise around the headrest in a seat.

First-generation applications were based on analogue designs. Advances in microelectronics, high-speed signal processors and filtering techniques during the 1980's precipitated a flurry of activity in digital control systems or hybrid – digital and analogue. In Poland first researches on ANC were undertaken in University of Mining and Metallurgy (AGH), Cracow (e.g. [Engel_84], [EngelK_95]), Central Institute for Labour Protection (CIOP), Warsaw (e.g. [Zawieska_91], [Makarewicz_93]), and Silesian University of Technology, Gliwice (e.g. [Ogonowski_94]).

In ANC a feedforward architecture is of considerable interest. Then, the control system is inherently stable if the control filter is stable. There are, however, two primary practical limitations. The reference signal highly correlated with the output disturbance should be available and it should not be influenced by the control signal. Violation of the first assumption decreases the performance while not satisfying the second assumption introduces a feedback loop that can become unstable during the adaptation [VaudreyBS_03]. The ANC systems considered here are often subject to noises upcoming from different directions and originating from various sources. On the other hand, they are designed to have a general usage or to be used in mobile applications. Therefore, it has been assumed that the reference signal coherent with such a noise is unavailable and the best-developed feedforward control as originally suggested by Lueg cannot be employed. Thus, the idea of Olson and May has been undertaken.

At the end of the 20th century Rafaely, Elliott and Garcia-Bonito have thoroughly analysed both acoustical and control limitations existing in ANC systems. They have also given recipes for optimal (fixed) controllers design using H_2/H_∞ approach to overcome stability and performance problems due to plant variations [RafaelyGE_97, 99], [GarciaEB_97], [RafaelyE_99], [Rafaely_01]. The analysis of generated zones of quiet leads to conclusion that for low frequencies they are large enough to reach human ears. For higher frequencies the researchers have put forward the idea of virtual microphones, which enables to shift the zones. It relies on attenuating the acoustic noise at desired locations without performing measurements at these locations.

The idea of virtual microphones has been extensively studied in recent years and some algorithms have been designed. For example, Holmberg et al., has designed a robust algorithm for cancelling noise at the desired location using the pole placement method [HolmbergRS_02]. He has included in the controller a model of the disturbance incorporating the Internal Model Principle. Tseng et al., has shown that best performance at the virtual microphone gives a controller which is open-loop unstable [TsengRE_02]. He has also proposed a method of designing open-loop stable H_2/H_∞ controllers, which is less conservative than that based on the small-gain theory but results in a convex optimisation problem. The researchers have verified their algorithms by implementing them on one active headrest channel. Kestell and co-workers have applied a weighted microphone array to estimate the sound pressure level or additionally particle velocity at a remote location using a forward-difference prediction method [KestellCH_99, 00, 01], [KestellHC_00], [MunnCHK_02]. Such methodology can be used to control acoustic energy density, which represents the total energy at a point, and not the potential energy only. Cazzolato has also proposed to tune the microphone weights with the Least Mean Squares (LMS) algorithm and has confirmed effectiveness of this approach by means of simulations [Cazzolato_02].

In case of fixed controllers, mainly based on the robust theory, independent systems can often control individual channels of a plant, e.g. the active headrest (single input – single output, or SISO approach) [RafaelyGE_97], [RafaelyEG_99], [RafaelyE_99], [TsengRE_02]. However, to the author knowledge, there is no multi-channel implementation of the H_2 / H_∞ systems. In the references where this approach is addressed it is arbitrarily assumed that the acoustic cross-coupling is negligible. Even single-channel version is usually verified only by simulations with reduced requirements according to stability constraints in face of plant perturbations, or with absence of analogue filtering.

In adaptive systems, due to existing acoustic coupling between the channels, a multi-channel, also referred to as the multi input – multi output (MIMO), approach to control is recommended for the sake of convergence as well as attenuation [Pawelczyk_02c, 02e]. Uncompensated paths usually varying in time create additional feedbacks in the control system [Elliott_01]. In the non-linear system, which in fact any adaptive system is, the feedbacks can generate a chaotic behaviour in a long-time horizon [FigwerB_03]. Such behaviour is particularly evident when the adaptive system is tuned to converge fast, what is very important for practical success of many ANC applications. Moreover, as it will be shown later, a MIMO system can provide higher noise attenuation. Furthermore, increasing the number of secondary sources and microphones can enhance the performance [Pawelczyk_03c].

1.4 Main assumptions

It is assumed that in Figure 1.1 the secondary source is a loudspeaker and the error and observer sensors are microphones, called in the sequel as the real and virtual microphones, respectively. Then, a sample acousto-electric plant with one secondary source and one real-virtual microphone pair, digitised with sampling interval T_S, can be presented in details as in Figure 1.2.

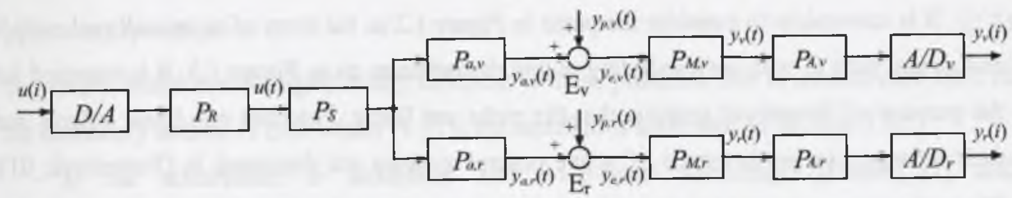

Figure 1.2 Detailed block diagram of the plant composed of real and virtual acousto-electric paths.

The notation in Figure 1.2 is as follows:

- Er, Ev – real and virtual microphones,
- *D/A* – digital-to-analogue converter,
- A/D_r, A/D_v – analogue-to-digital converters,
- P_R – low-pass analogue reconstruction filter,
- P_S – secondary source (a loudspeaker) with power amplifier,
- $P_{a,r}$, $P_{a,v}$ – real and virtual acoustic paths on the way from the loudspeaker to respective microphones,
- $P_{M,r}$, $P_{M,v}$ – real and virtual microphones with voltage amplifiers,
- $P_{A,r}$, $P_{A,v}$ – low-pass analogue anti-aliasing filters,
- $u(t)$ – continuous-time control signal,
- $u(i)$ – discrete-time control signal,
- $y_{p,r}(t)$, $y_{p,v}(t)$ – primary noises (unwanted sounds) at the real and virtual microphones,
- $y_{a,r}(t)$, $y_{a,v}(t)$ – secondary sounds generated by the secondary source at the real and virtual microphones,
- $y_{e,r}(t)$, $y_{e,v}(t)$ – sounds being interference effect of the primary and secondary sounds at the real and virtual microphones,
- $y_r(t)$, $y_v(t)$ – continuous-time output signals of the real and virtual microphones,
- $y_r(i)$, $y_v(i)$ – discrete-time output signals of the real and virtual microphones.

The low-pass analogue anti-aliasing and reconstruction filters are introduced to correctly sample and reconstruct signals [MitraK_93], [BendatP_93]. It is assumed that the filters are properly designed and sufficiently suppress frequency components higher than the Nyquist frequency. It should be mentioned here that the analogue filters could be omitted if a non-uniform sampling and oversampling methods were applied, thereby reducing the phase lag of the plant [Marvasti_01], [CzyzK_04]. However, non-uniform sampling requires extrapolation of the samples to uniformly spaced ones before further processing or application of modified transfer functions [Jury_70], [Gessing_96].

It is convenient to consider the paths in Figure 1.2 in the form of an overall real path S_r and virtual path S_v with corresponding output disturbances as in Figure 1.3. It is assumed for the purpose of theoretical analysis that the paths are linear. Potential non-linear effects and their influence on performance of active control systems are discussed in [Pawelczyk_01]. The paths are represented by rational transfer functions $S_r(z^{-1})$, $S_v(z^{-1})$ of complex variable z^{-1} or frequency responses, $S_r(e^{-j\omega T_S})$, $S_v(e^{-j\omega T_S})$, of the transfer functions, respectively. Frozen transfer functions can also be considered and additionally indexed with discrete time i if their parameters vary in time [Jury_70]. The output of each path can be computed as a solution to corresponding discrete-time difference equation with parameters being parameters of the transfer function and z^{-1} interpreted as a backward time-shift operator. In the signal processing literature an additional operator q^{-1} is sometimes used to distinguish from the complex variable. Models of the paths are also linear and noted with hats, respectively.

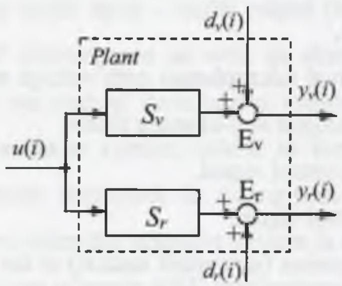

Figure 1.3 Comprehensive block diagram of the plant.

It is additionally assumed in some sections that both the paths and their models have finite impulse responses (FIR structure), even very long if necessary. This is a common assumption in majority of the ANC publications [Michalczyk_04]. Then, the paths and similarly the models can be represented by finite-length, M, vectors of their impulse responses, e.g.

$$\underline{s}_r = \left[s_{r,0}, s_{r,1}, \ldots, s_{r,M-1}\right]^T, \tag{1.1}$$

$$\underline{s}_v = \left[s_{v,0}, s_{v,1}, \ldots, s_{v,M-1}\right]^T. \tag{1.2}$$

It is also assumed that the distance between the real and virtual microphones is much less than the smallest wavelength in the disturbance. Then, the primary noise contribution to the acoustic field at the positions of these microphones can be considered the same, so that the output disturbance is [Rafaely_97]

$$d_v(i) = d_r(i) = d(i). \tag{1.3}$$

Secondary sound can be significantly different at these positions due to intense near field of the secondary source. A case where (1.3) is not satisfied is addressed in Section 3.5.5.

If the disturbance is stochastic and wide-sense stationary ([ChenG_91] and [BendatP_93]), it can be modelled as a zero-mean wide-sense stationary white noise signal, $e(i)$, passing through a minimum phase disturbance-shaping filter $F(z^{-1})$, sometimes called the 'synthesis filter' [BoxJ_70], i.e.

$$d(i) = F(z^{-1})e(i). \tag{1.4}$$

$F(z^{-1})$ can be generally a rational transfer function, although in majority of the ANC publications it is assumed to be an FIR filter.

The filter in (1.4) can be derived by factoring (Auto-) Power Spectrum Density (PSD), $S_{dd}(z^{-1})|_{z^{-1}=e^{-j\omega T_S}}$, of $d(i)$ into two components known as the spectral factors, $F(z^{-1})$ and $F(z)$, where the latter is the time-reversed form of the former [Elliott_01]:

$$S_{dd}(z^{-1}) = F(z^{-1})F(z)|_{z^{-1}=e^{-j\omega T_S}}. \tag{1.5}$$

Because of a real-value signal $S_{dd}(e^{-j\omega T_S})$ is real and non-negative, and hence it is usually written as $S_{dd}(e^{\omega T_S})$ [NiederlinskiKF_97]. According to [Papoulis_77] the spectral factors can be found provided $S_{dd}(e^{\omega T_S})$ satisfies the discrete form of the Paley-Wiener condition

$$\int_0^{2\pi} \left|\ln S_{dd}(e^{\omega T_S})\right| d\omega T_S < \infty. \tag{1.6}$$

It should also be stressed here that there are $2^{\deg F}$ different factorisations (1.5), where $\deg F$ is the degree of $F(z^{-1})$, but there is only one resulting in minimum phase shaping filter [Orfanidis_88]. Such solution is only accepted here. By adjusting variance of the white noise sequence the filter could be made of monic polynomials and then the factorisation is unique. This is, however, not the case in this work, where unit variance of $e(i)$ is assumed.

There are also other methods to find the disturbance-shaping filters, e.g. by stochastically modelling the disturbance [BoxJ_70], [NiederlinskiKF_93], performing Gram-Schmidt orthogonalisation of the disturbance, or Cholesky factorisation of its correlation matrix [Orfanidis_88]. However, they do not guarantee a minimum phase solution directly, and usually require additional spectral factorisation.

It is additionally assumed, for generality, that there is no access to results of noise control at the observation point, and the virtual microphone, Ev, is allowed to be used only for measurements during control system tuning and monitoring (Figure 1.3). It is also assumed, for the same reason, that the noise source is distributed or it is impossible to place a sensor next to it. Thus, in this research the real microphone, Er, is used exclusively in control.

1.5 Other assumptions

Optimal and adaptive control systems are designed and analysed in this research. They, wherever referred, require corresponding assumptions:

I.1. The optimal control system is linear and time-invariant, and the signals (the processes) are wide-sense stationary [Orfanidis_88], [BendatP_93]. The plant paths, their models and control filter are of IIR structure and they are represented by rational transfer functions.

I.2. The adaptive system is linear and time-invariant, i.e. the trajectories are frozen or, in practice, the plant and control filter variations are slow compared to the reference and residual signals over the time-scale of the filter and plant impulse responses [WangR_99b]. The plant paths, their models and control filter are of FIR structure and they are represented by vectors of impulse response parameters.

Exceptions to assumptions I.1 and I.2 will be commented.

For convergence analysis of the adaptive systems some of the following assumptions must be satisfied:

J.1. The convergence coefficient is very small or vanishes to zero (a consequence of frozen trajectories).

J.2. The control filter structure is known.

J.3. The control filter parameters are bounded.

J.4. The control filter input is persistently exciting.

J.5. The control filter input and variations of the control filter parameters are statistically independent.

J.6. Perfect cancellation is possible.

J.7. The feedback loop does not destabilise the system.

1.6 Summary

This chapter constitutes an introduction to the remaining chapters. Therefore first, the emerging problem of acoustic noise has been pointed out and the idea of active control has been addressed. Although it dates back to seven decades the last advances in signal

processing precipitated a flurry of activity in this field. This activity has been briefly summarised. However, many more references are provided in the following chapters when discussing particular problems. It has been emphasised that the global noise control is rarely feasible and creation of local zones of quiet is usually of interest. Moreover, the zones of quiet are of small dimensions, dependent, e.g. on noise wavelength and geometrical set-up of the plant. Hence, if it is impossible due to any reason to place a sensor in the area of interest, it is suggested to shift the zones using the idea of virtual microphones. An appropriate block diagram of the discretised real and virtual paths of the plant has been presented.

In the plethora of many different acousto-electric plants it has been found justified to single out a group that is characterised by small distances between considered points in space compared to the noise wavelengths. It can be assumed that the noise is the same at these points for such plants. PSD of the noise has been factored out into a disturbance-shaping filter.

Finally, assumptions used in the sequel have been collected.

CHAPTER 2

INTERNAL MODEL CONTROL SYSTEM

2.1 INTERNAL MODEL CONTROL SYSTEM STRUCTURE

Feedback control is considered in this monograph. Nevertheless, most well developed adaptive algorithms for active noise control that give best results require a reference signal [NelsonE_94], [KuoM_96], [HansenS_97]. Therefore, Internal Model Control (IMC) structure is most willingly used, in which that signal is estimated (Figure 2.1) [MorariZ_89]. It is also sometimes called as the 'feedback control with secondary path neutralisation' [KuoM_96].

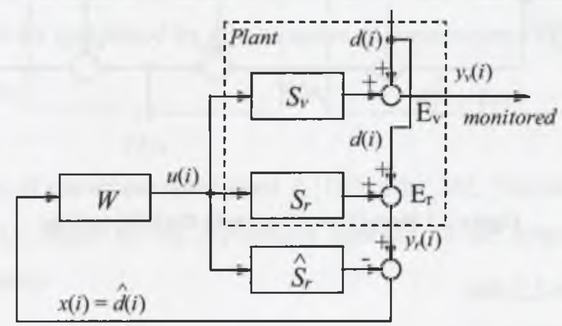

Figure 2.1 Basic structure of the IMC system.

"The immediate advantage of the internal model structure for the feedback controller is that the control filter that minimises the mean-square error can now be designed using the standard Wiener technique" [Elliott_01]. Namely, the reference signal can be a good estimate of the disturbance and hence satisfy the two conditions for good performance and stable control system, i.e. it can be highly correlated with the disturbance and uncontrollable [ElliottS_96]. The feedback system can be then reduced to a feedforward system, which is stable provided the control filter is stable since the acousto-electric plant is stable.

In this chapter the SISO IMC system is thoroughly analysed in the context of active noise control for the considered group of acousto-electric plants. Available knowledge is systemised and relevant conclusions are drawn. However, contrary to most of the related references the entire analysis is performed for a practical case where the plant model is imperfect. Optimal control is addressed in Section 2.2, whereas adaptive control is dealt with in Section 2.3. The considerations of this Chapter constitute also the background for design and analysis of control systems presented in Chapter 3. Multi-channel realisation is postponed to Chapter 4.

2.2 Optimal control

It is convenient for analysis of optimal control to present Figure 2.1 in the form as in Figure 2.2.

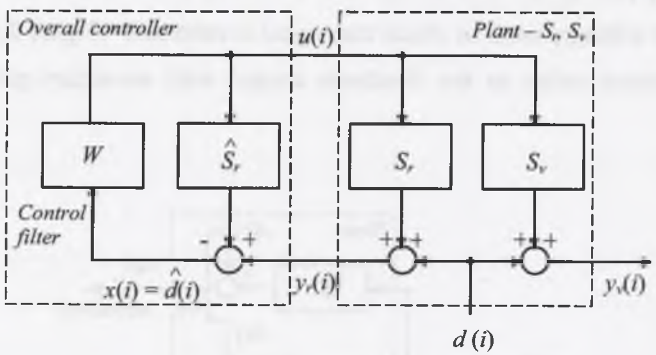

Figure 2.2 Signal flow diagram in the IMC system.

It follows from Figure 2.2 that

$$y_r(i) = d(i) + W(z^{-1}) S_r(z^{-1}) x(i), \tag{2.1}$$

$$x(i) = \frac{1}{1 + W(z^{-1})\hat{S}_r(z^{-1})} y_r(i), \tag{2.2}$$

$$u(i) = \frac{W(z^{-1})}{1 + W(z^{-1})\hat{S}_r(z^{-1})} y_r(i) = -H(z^{-1}) y_r(i), \tag{2.3}$$

where $H(z^{-1})$ is the overall IMC controller written in negative feedback notation. In the reminder the explicit dependence on the variable z^{-1} is dropped, where it does not make confusion to have a compact form of the equations. Taking (2.1) and (2.2) together gives

$$y_r(i) = \frac{1 + W\hat{S}_r}{1 + W(\hat{S}_r - S_r)} d(i) = V_r d(i), \tag{2.4}$$

where V_r is the Real-Output Sensitivity Function. Properties of the sensitivity function are discussed in [MorariZ_89].

Let the following general notation in (2.4) be introduced to allow for applying the derivations to other control structures considered in the next chapter:

$$\begin{cases} S_1 = \hat{S}_r \\ S_2 = \hat{S}_r - S_r \\ y = y_r \end{cases} \tag{2.5}$$

where $y(i)$ denotes a general signal under control or, in other words, controlled output signal. Then, relation (2.4) takes the form

$$y(i) = \frac{1 + WS_1}{1 + WS_2} d(i) = V d(i), \tag{2.6}$$

where V is the General-Output Sensitivity Function. Let the minimised cost function be defined to correspond to minimisation of the sound pressure level [Crocker_97]. This can be achieved by minimisation of the mean-square acoustic pressure. In the control system terminology this can be performed by minimisation of mean-square value of the signal under control, $y(i)$:

$$L = E\{y^2(i)\} \tag{2.7}$$

or squared H_2 norm of disturbance-weighted V [Orfanidis_88], [BendatP_93], [Rafaely_97]. In this definition $E\{.\}$ stands for the expectation operator. In the frequency domain this cost function corresponds to

$$L_\omega = \int_0^{2\pi} S_{yy}(e^{\omega T_s}) d\omega T_s, \tag{2.8}$$

where $S_{yy}(e^{\omega T_s})$ denotes PSD of $y(i)$.

2.2.1 Polynomial-based approach

Taking (2.6) and (1.4) into account, the cost function (2.7) can be expressed as

$$L = E\left\{\left[\frac{F + WS_1F}{1 + WS_2} e(i)\right]^2\right\}. \tag{2.9}$$

Taking first derivative of the term within the curly brackets and making it equal to zero allows to find the optimal control filter, which satisfies

$$F + W_{opt} S_1 F = 0 . \tag{2.10}$$

For IMC ($S_1 = \hat{S}_r$, see (2.5)) this result is analogous to the result of an optimisation problem with perfect real path model, what is usually assumed in the literature [Elliott_01], [SakaiM_03]. However, not necessarily perfect model appears explicitly here, instead of the real path itself. This result is also similar to the result of feedforward system with perfect cancellation of the intrinsic feedback [FraanjeVD_03]. The above analysis can also be interpreted as assuming that the real path model is perfect, then designing the optimum control filter and applying this filter to the case where the model is imperfect [AstromW_95]. A result equivalent to (2.10) can also be obtained if (2.6) is multiplied by $(1 + WS_2)$ and a modified signal

$$y_m(i) = (1 + WS_2) y(i) \tag{2.11}$$

is controlled. This could be, however, incorrectly interpreted as implicitly shaping spectrum of the residual signal. It is also worth stressing that although the cost function (2.9) has one global minimum, which satisfies (2.10), it can exhibit different shapes in the vicinity of this minimum, from very sharp if $S_2 = 0$ (no modelling errors, see (2.5)) to very flat if S_2 is significant (large modelling errors).

The optimum control filter, which removes all contribution of $d(i)$ to $y(i)$ could be directly found from (2.10) as

$$W_{opt} = -\frac{1}{S_1} . \tag{2.12}$$

However, in this case the overall IMC controller, H in (2.3), would have infinite gain. Moreover, if S_1 were non-minimum phase including a time delay the filter W_{opt} would be unstable and non-causal (Appendix A.2). This is the case in ANC. One of the possible solutions could be then the one presented in [NiederlinskiMO_95] and [Pawelczyk_99a] that modifies the cost function to include a control weighting term (Weighted Minimum Variance Control) or non-minimum phase part of the real path model (Minimum Variance Control for Non-minimum Phase Plants). The Minimum Variance Control for noise attenuation has been presented in details in [Pawelczyk_99a, 99b, 00a]. It has been found, however, to yield poorer results compared to these obtained with the techniques described in this monograph and it will not be considered further. It is also worth noting that in case of IMC not the real path itself is

inverted in (2.12) but its model, since $S_1 = \hat{S}_r$ [VaudreyBS_03]. Therefore, if possible, a minimum phase no-delay model sufficiently well matching the non-minimum phase real path with delay at frequencies of interest could be searched for. This would allow to obtain perfect cancellation due to (2.10) and (2.12). Such a model is, however, very difficult to find if broadband disturbance is considered.

To solve the problem given by (2.10) for general case, where the transfer function S_1 is non-minimum phase, this transfer function can be factorised into an inner and outer parts (Appendix A.7), so that

$$S_1 = S_1^{(i)} S_1^{(o)} . \tag{2.13}$$

The inner part, $S_1^{(i)}$, is an all-pass term and the outer part, $S_1^{(o)}$, is a minimum phase term [MorariZ_89], [Elliott_01]. The methods for inner-outer factorisation by means of spectral factorisation are presented, e.g. in [Vidyasagar_85], [Francis_87], [ZhangF_92], [AhlenS_94] and [IonsescuO_96]. Combining (2.10) and (2.13) results in

$$F + FW_{opt} S_1^{(o)} S_1^{(i)} = 0 . \tag{2.14}$$

Multiplying both sides by the time-reversed term $S_1^{(i)}(z)$, which is H_2 norm-preserving and does not change the cost function (2.9), and then taking into account that $S_1^{(i)}(z^{-1}) S_1^{(i)}(z) = 1$ yields

$$F(z^{-1}) S_1^{(i)}(z) + F(z^{-1}) W_{opt}(z^{-1}) S_1^{(o)}(z^{-1}) = 0 . \tag{2.15}$$

The causally-constrained sub-optimal control (Wiener-type) filter, $W_{opt+}(z^{-1})$, can be therefore found from

$$\left\{ F(z^{-1}) S_1^{(i)}(z) \right\}_+ + F(z^{-1}) W_{opt+}(z^{-1}) S_1^{(o)}(z^{-1}) = 0 , \tag{2.16}$$

what finally gives

$$W_{opt+}(z^{-1}) = -\frac{1}{F(z^{-1}) S_1^{(o)}(z^{-1})} \left\{ F(z^{-1}) S_1^{(i)}(z) \right\}_+ \equiv -\frac{1}{F(z^{-1}) S_1^{(o)}(z^{-1})} \left\{ \frac{F(z^{-1})}{S_1^{(i)}(z^{-1})} \right\}_+ . \tag{2.17}$$

The symbol $\{\cdot\}_+$ denotes that causal part is taken from $\{\cdot\}$ (Appendix A.6). Hence, such a filter is also called the single-sided filter [Orfanidis_88], [Elliott_01], [SakaiM_03], [FraanjeVD_03]. The variables have been included in above equations to avoid misunderstanding. This filter will be also called optimal in the sequel for simplicity.

With the presence of a perfectly modelled plant the term $[FS_1^{(o)}]^{-1}$ in (2.17) is referred to in classical Wiener filtering as a whitening filter, which operating on the control filter input generates the process of innovations [Orfanidis_88]. The signal obtained in such a way is not the same as the white noise $e(i)$ generating the disturbance signal (1.4) if the outer part differs from the plant itself, i.e. if there is an inner part. Nevertheless, it has the property of being uncorrelated from a sample to a sample, what is required to drive the optimal causal Wiener filter [Elliott_01]. Hence, the optimal filter can also be derived using the prewhitening method to design Wiener filter [Orfanidis_88].

Under optimal control and taking (2.13) and (2.16) into account, the minimum value of the cost function (2.9) is

$$L_{\min} = E\left\{\left[\frac{\left\{\frac{F}{S_1^{(i)}}\right\}_-}{1-\frac{S_2}{FS_1^{(o)}}\left\{\frac{F}{S_1^{(i)}}\right\}_+}e(i)\right]^2\right\}, \tag{2.18}$$

where $\{\}_-$ denotes non-causal part taken from $\{\}$. Now, let the system output under optimal control be calculated. From (2.6), (2.13) and (2.17) there is

$$y(i)_{opt} = \frac{F-\frac{S_1}{FS_1^{(o)}}\left\{\frac{F}{S_1^{(i)}}\right\}_+ F}{1-\frac{S_2}{FS_1^{(o)}}\left\{\frac{F}{S_1^{(i)}}\right\}_+}e(i). \tag{2.19}$$

The numerator can be further expressed as

$$F-\frac{S_1}{S_1^{(o)}}\left\{\frac{F}{S_1^{(i)}}\right\}_+ = F\frac{S_1^{(i)}}{S_1^{(i)}} - S_1^{(i)}\left\{\frac{F}{S_1^{(i)}}\right\}_+ = S_1^{(i)}\left[\frac{F}{S_1^{(i)}}-\left\{\frac{F}{S_1^{(i)}}\right\}_+\right]. \tag{2.20}$$

Since the following causal/non-causal decomposition is valid $\{\} = \{\}_+ + \{\}_-$, it finally gives

$$y(i)_{opt} = \frac{S_1^{(i)}\left\{\frac{F}{S_1^{(i)}}\right\}_-}{1-\frac{S_2}{FS_1^{(o)}}\left\{\frac{F}{S_1^{(i)}}\right\}_+}e(i). \tag{2.21}$$

If for IMC the modelling error were negligible ($S_2 = \hat{S}_r - S_r = 0$, see (2.5)), the optimum output signal would be

$$y_r(i)\Big|_{opt,\hat{S}_r=S_r} = \hat{S}_r^{(i)}\left\{\frac{F}{\hat{S}_r^{(i)}}\right\}_- e(i). \tag{2.22}$$

Furthermore, if a model of the real path were minimum phase, the non-causal part would be zero and the output would be also zero. However in general, both the system output and cost

function depend on the modelling error due to sub-optimality of the control filter (Figure 2.3). Therefore, it may happen that the modelling error significantly increases the cost function value and thereby reduces noise attenuation. However, it is also possible for a stable sub-optimal control system to yield better performance due to imperfect modelling. In an ANC application this results in generating higher attenuation for different acoustical conditions than those present when estimating the plant model.

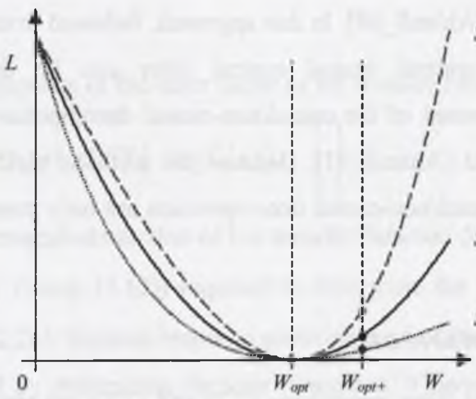

Figure 2.3 Influence of sub-optimal control and modelling errors on the cost function value.

The user is rather more interested in noise attenuation at the ear, i.e. at the virtual than at the real microphone. It follows from Figure 2.2 that

$$y_v(i) = S_v W x(i) + d(i), \tag{2.23}$$

$$x(i) = -\frac{1}{1+W(\hat{S}_r - S_r)}d(i). \tag{2.24}$$

Taking (2.23) and (2.24) together gives

$$y_v(i) = \left[1+\frac{S_v W}{1+W(\hat{S}_r - S_r)}\right]d(i) = \frac{1+W(\hat{S}_r - S_r + S_v)}{1+W(\hat{S}_r - S_r)}d(i) = V_v d(i), \tag{2.25}$$

where V_v is the Virtual-Output Sensitivity Function.

Implementation of the optimal filter given by (2.17) requires, in addition to the inner-outer factorisation, extraction of the causal part. This operation can be performed with partial fraction expansion or, faster, by using the contour inversion formula to compute impulse response parameters for non-negative indices and then summing the series up [Orfanidis_88]. The causal Wiener filter can also be evaluated with a polynomial-based approach developed by Kučera [Kucera_79]. For a given problem structure the equations have been derived there using the method of 'completing the squares'. However, this method often leads to tedious calculations. The 'completing the squares' method has also been used in the frequency domain, e.g. by Grimble [Grimble_85]. Another method to solve this problem is to apply a variational approach utilizing orthogonality principle in the frequency domain [AhlenS_91]. An alternative direct polynomial-based solution to the optimal control filter can be obtained by applying the method originally developed by Ahlén and Sternad for the special case of input estimation problem [AhlenS_89]. In that approach, followed from a technique presented in [AstromW_84], the optimal causal control filter can be determined by solving a Diophantine equation instead of the causal/non-causal decomposition, as it has also been noted in [Grimble_85] and [AhlenS_91]. Because the methods yield equivalent results the equations based on the causal/non-causal decomposition are only presented in the remainder for coherence.

2.2.2 Frequency-domain approach

The optimal causal control filter minimising (2.7) and (2.8) can also be determined in the discrete frequency domain by applying the methodology presented in [Haykin_96], [KuoM_96] and [Elliott_01], and taking the considerations from the previous subsection into account:

$$W_{opt+}(n) = -\frac{1}{F(n)S_1^{(o)}(n)}\left\{\frac{F(n)}{S_1^{(i)}(n)}\right\}_+ , \tag{2.26}$$

where n is the frequency bin number. The causal part is calculated as [Elliott_01]

$$\left\{\frac{F(n)}{S_1^{(i)}(n)}\right\}_+ = DFT\left[\ell(n)\cdot IDFT\left(\frac{F(n)}{S_1^{(i)}(n)}\right)\right], \tag{2.27}$$

where

$$\ell(n) = \begin{cases} 1 & n \geq 0 \\ 0 & n < 0 \end{cases}. \tag{2.28}$$

The Discrete Fourier Transform (DFT) and its inverse (IDFT) can be computed using one of the Fast Fourier Transform (FFT) algorithms, provided the number of frequency bins, N, is large enough for the causal part of the impulse response of the expression in curly brackets to decay to zero before the $N/2$ sample [Orfanidis_88], [BendatP_93]. Also the spectral factorisation, (1.5), can be performed in the discrete frequency domain by using the cepstral

method [OppenheimS_75], [Elliott_01]. The minimum phase factor $F(n)$ is then obtained from its magnitude (square root of PSD of the disturbance) as

$$F(n) = \exp\left\{DFT\left[\ell_0(n)\cdot IDFT\left(\ln(S_{dd}(n))\right)\right]\right\}, \tag{2.29}$$

where

$$\ell_0(n) = \begin{cases} 1 & n > 0 \\ 1/2 & n = 0 \\ 0 & n < 0 \end{cases}. \tag{2.30}$$

Similarly, frequency response of the outer factor of the transfer function S_1 is calculated as

$$S_1^{(o)}(n) = \exp\left\{DFT\left[2\,\ell_0(n)\cdot IDFT\left(\ln(|S_1(n)|)\right)\right]\right\}, \tag{2.31}$$

since it has the same magnitude as that of the transfer function S_1. It further allows for easy calculation of $S_1^{(i)}(n)$ (using (2.13)) required to determine the frequency response of the optimal causal filter, (2.26). Impulse response parameters of a filter yielding such a frequency response can be found by minimising the sum (weighted, if necessary) of the squared error between the actual and the desired responses at frequency bins. This can be done using, e.g. iterative search with the Gauss-Newton method, available in the Matlab package (*invfreqz()* function) [DennisS_83].

2.2.3 Correlation-based approach

The optimal causal control filter designed with the polynomial or frequency-domain approach is unconstrained, i.e. it has infinite impulse response (IIR). The unconstrained filter can obviously be truncated or approximated by a constrained one, if necessary. Causal and constrained (FIR) optimal control filter can be directly designed using the correlation-based approach described, e.g. in [KuoM_96] and [Elliott_01], and correctly applied to control system with the general output given by (2.6). It is assumed for the purpose of this approach that the transfer function S_1 is of FIR structure of order M. The optimal constrained causal control filter takes then the form

$$\underline{w}_{opt+} = -E\left\{\underline{\hat{r}}(i)\underline{\hat{r}}^T(i)\right\}^{-1} E\left\{\underline{\hat{r}}(i)d(i)\right\}, \tag{2.32}$$

where:

$$\hat{r}(i) = \underline{s}_1^T\underline{d}(i), \tag{2.33}$$

and the vectors are defined as:

$$\underline{w}_{opt+}=\left[w_0, w_1, \ldots, w_{N-1}\right]^T_{opt+}, \tag{2.34}$$

$$\underline{s}_1=\left[s_{1,0}, s_{1,1}, \ldots, s_{1,M-1}\right]^T, \tag{2.35}$$

$$\underline{\hat{r}}(i)=\left[\hat{r}(i), \hat{r}(i-1), \ldots, \hat{r}(i-N+1)\right]^T, \tag{2.36}$$

$$\underline{d}(i)=\left[d(i), d(i-1), \ldots, d(i-M+1)\right]^T. \tag{2.37}$$

According to (2.33) the signal $\hat{r}(i)$ is the disturbance signal filtered by S_1 and not simply the real path. This is an important difference compared to solutions found in the literature, e.g. [KuoM_96], [HansenS_97], [Rafaely_97], [Elliott_01]. The hats have been introduced to indicate that S_1 is generally composed with path models – see (2.6) and respective equations in Chapter 3. Even if the paths appear in some of the equations they are unknown and should be substituted with their models. Such notation coincides also with the notation used for adaptive systems (Section 2.3). The optimal filter, (2.32), is thus expressed in terms of the inverted autocorrelation matrix of the filtered-disturbance signal and the vector of cross-correlation between the filtered-disturbance signal and the disturbance itself. Practical implementation of (2.32) in a feedback system requires estimation of these auto- and cross-correlations, preferably from auto- and cross-spectral densities, respectively. The filter can also be computed using, e.g. the Levinson's algorithm [Orfanidis_88].

The optimal filter (2.32) could also be derived with the help of the 'correlation cancelling principle', sometimes called the 'orthogonality principle' or 'Wiener-Hopf condition'. It aims at removing the correlation between the output signal and the control filter input [Orfanidis_88].

2.2.4 Optimal control of deterministic disturbances

A correctly sampled, i.e. satisfying the Shannon-Kothielnikov theorem, periodic disturbance can be represented (decomposed) as the finite sum of harmonics with frequencies being integer multiples of the fundamental frequency of the signal [BendatP_93]. In particular case the signal can be a single harmonic, i.e. a tone originating from a rotating or reciprocating machine, or a series of not related tones generated by several sources operating with different frequencies. In the latter case there is no fundamental frequency. Hence, a periodic signal can be generally written as

$$d(i)=\sum_{l=1}^{P} D_l \sin(\omega_l T_S i+\psi_l), \tag{2.38}$$

where P is the number of tones, and ω_l, D_l, ψ_l are the angular frequency, amplitude and phase, respectively, of the l-th tone. An optimal causal control filter minimising mean-square value of the output signal (2.6) should therefore satisfy

$$\underset{l\in\{1,\,2,\,\ldots,\,P\}}{\forall}\quad 1+W_{opt+}(e^{-j\omega_l T_S})S_1(e^{-j\omega_l T_S})=0, \tag{2.39}$$

regardless of the amplitude and phase of every tonal component. Representing complex values of the responses of W_{opt+} and S_1 in terms of magnitudes and phases gives

$$\underset{l\in\{1,\,2,\,\ldots,\,P\}}{\forall}\quad 1+\left|W_{opt+}(e^{-j\omega_l T_S})\right|e^{j\varphi_l}\left|S_1(e^{-j\omega_l T_S})\right|e^{j\theta_l}=0, \tag{2.40}$$

where φ_l and θ_l are the phases of the optimal causal control filter and S_1, respectively, at the frequency ω_l. Provided the order of the control filter is sufficiently large, solution to the problem given by (2.40) always exists and is not unique:

$$\underset{l\in\{1,\,2,\,\ldots,\,P\}}{\forall}\quad \begin{cases}\left|W_{opt+}(e^{-j\omega_l T_S})\right|=\left|S_1(e^{-j\omega_l T_S})\right|^{-1},\\ \varphi_l=\theta_l+\pi+p_l\cdot(2\pi)\end{cases} \tag{2.41}$$

where p_l are integers. Because the above conditions need only to be satisfied at individual frequencies, parameters p_l can always be chosen to obtain a causal control filter of sufficiently large order even if S_1 is non-minimum phase including a considerable delay (see Appendix B.5 for an example). It is worth stressing here that for optimal IMC the stationary multi-tonal noise can be perfectly cancelled regardless of plant modelling errors.

There are also other solutions to the problem of control of multiple tones. One of them is to process the signal in a bank of parallel channels, each responsible for a single tone selected with an appropriate band-pass filter. The tones are individually controlled by the so-called 'phase shifters'. Such approach has been extensively studied in [Pawelczyk_02a]. Another solution is to apply the Internal Model Principle by incorporating model of the disturbance in the design [NiederlinskiMO_95], [BodsonJD_01], [BrownZ_04].

2.2.5 Stability and robustness of optimal control systems

Stability analysis can generally be performed using a number of methods [Kaczorek_93]. One of them is to analyse zeros of the characteristic equation. For IMC it takes the form (see (2.4))

$$1+\left(\hat{S}_r-S_r\right)W=0 \tag{2.42}$$

or, for the general notation (see (2.5))

$$1+S_2W=0\,. \tag{2.43}$$

However, if the exact transfer function S_2 is unknown and the only knowledge on it is available from experiments, the most suitable methods are based on Nyquist or Bode plots of S_2W. It also follows from (2.6) that the general system would tend to a feedforward-type system, surely stable for stable plant and control filter, provided

$$S_2W\approx 0\,. \tag{2.44}$$

For IMC this means that the modelling error or strictly the term $(\hat{S}_r-S_r)W$ should be close to zero [Elliott_01]. Then, potential instability of the feedback loop would be avoided. Therefore, it is of vital interest to protect against unjustified excessive rise of the filter coefficients, particularly if modelling errors exist due to, e.g. changes in the acoustic environment. The protection is also important for internal stability guaranteeing all signals bounded in the control system. For IMC this is determined by the characteristic equation (2.42) and the denominator of (2.3) (Appendix A.1). A limitation of the control filter gain can be done by modifying the minimised cost functions (2.7) and (2.8) to respective forms [KuoM_96], [Elliott_01]:

$$L=E\{y^2(i)\}+\beta\,\underline{w}^T\underline{w}\,, \tag{2.45}$$

$$L_\omega=\int_0^{2\pi}\left[S_{yy}(e^{\omega T_S})+\beta\left|W(e^{-j\omega T_S})\right|^2\right]d\omega T_S\,. \tag{2.46}$$

Such method can also improve the numerical conditioning of the optimal solution, e.g. in case of presence of dominating tones in the disturbance. The equations for the optimal control filters in the polynomial, (2.17), and frequency-domain, (2.26), approaches retain the same form with the exception that the spectral factors are obtained from

$$F(z^{-1})F(z)=S_{dd}(z^{-1})+\left.\frac{\beta}{S_1(z^{-1})S_1(z)}\right|_{z^{-1}=e^{-j\omega T_S}}, \tag{2.47}$$

$$F(n)=\exp\left\{DFT\left[\ell_0(n)\cdot IDFT\left(\ \ln\left(S_{dd}(n)+\beta/\left|S_1(n)\right|^2\right)\right)\right]\right\}, \tag{2.48}$$

respectively, instead by using (1.5) (see [Elliott_01] for a similar problem). In turn, in the correlation-based approach the control filter is calculated according to

$$\underline{w}_{opt+}=-\left[E\left\{\hat{\underline{r}}(i)\hat{\underline{r}}^T(i)\right\}+\beta\mathbf{I}_N\right]^{-1}E\left\{\hat{\underline{r}}(i)d(i)\right\}. \tag{2.49}$$

It can have a unique solution even if the disturbance signal is not sufficiently rich (not persistently exciting [NiederlinskiKF_93]) and $E\left\{\hat{\underline{r}}(i)\hat{\underline{r}}^T(i)\right\}$ is singular. This kind of regularisation is equivalent to adding to the filtered-disturbance signal a low-level wide-sense stationary white noise of variance β, uncorrelated to *e*(*i*) (see [Orfanidis_88] for a similar problem).

It follows from the equations for the optimal control filter, (2.17), (2.26), that if the magnitude of frequency response of S_1, being a real path model for IMC, had deep valleys at some frequencies the filter would have high gains at those frequencies. Then, the overall control system might become unstable due to (2.43) in case of changes in the plant response. Therefore, if the bound of the plant perturbations, referred to as the uncertainty, is known it can be reasonable to take it into account in the design procedure to guarantee robust stability [MorariZ_89], [Elliott_01]. Following the reasoning, let the general plant S (for IMC $S=S_r$) be described as the nominal plant S_o with the multiplicative uncertainty δS [MorariZ_89], [Weinmann_91], [DoyleFT_92]

$$S(e^{-j\omega T_S})=S_o(e^{-j\omega T_S})\left[1+\delta S(e^{-j\omega T_S})\right] \tag{2.50}$$

and the upper bound of the uncertainty be

$$\forall_{\omega T_S}\ \overline{\delta S}(e^{\omega T_S})\geq\left|\delta S(e^{-j\omega T_S})\right|. \tag{2.51}$$

Due to such properties of the ANC plant like possible significant changes of both magnitude and phase this description of uncertainties is much more suitable then using the additive uncertainty [MorariZ_89], [Rafaely_97]. Conservatively, it can be assumed that all plant responses at all frequencies are within a disc with centre $S_o(e^{-j\omega T_S})$ and radius $\overline{\delta S}(e^{\omega T_S})\left|S_o(e^{-j\omega T_S})\right|$ (this describes a larger set of plants than practically possible). Then, the well-known necessary and sufficient condition for robust stability is [MorariZ_89], [DoyleFT_92]

$$\left\|T_o(e^{-j\omega T_S})\overline{\delta S}(e^{\omega T_S})\right\|_\infty<1, \tag{2.52}$$

where $\|\cdot\|_\infty$ denotes the H_∞ norm (Appendix A.5), and T_o is the Complementary Sensitivity Function for the nominal plant [MorariZ_89]. Assuming lack of modelling errors for the nominal plant, i.e. $\hat{S}=S_o$, the expression (2.50) can be interpreted as a description of uncertainty of a model for the perturbed plant. Then, in the particular case of IMC the Complementary Sensitivity Function reduces to (Figure 2.2)

$$T_{r,o}(e^{-j\omega T_s}) = -\hat{S}_r(e^{-j\omega T_s})W(e^{-j\omega T_s}) \tag{2.53}$$

and the condition (2.52) for robust stability becomes [MorariZ_89]

$$\left\| \hat{S}_r(e^{-j\omega T_s})\overline{\delta S}_r(e^{\omega T_s})W(e^{-j\omega T_s}) \right\|_\infty < 1. \tag{2.54}$$

This equation allows also to evaluate a bound on the control filter that guarantees assumed stability margin. According to (2.44) and using the above notation the IMC system 'tends' to a feedforward-type system provided

$$\hat{S}_r(e^{-j\omega T_s})\overline{\delta S}_r(e^{\omega T_s})W(e^{-j\omega T_s}) \approx 0, \tag{2.55}$$

although the problems of internal stability remain [MorariZ_89]. It has been shown in [Rafaely_97] that the uncertainty ((2.50) and (2.51)) constrains both achievable disturbance attenuation and possible disturbance enhancement obtained in a robustly stable feedback control system. One of the important conclusions from the analysis is that if the multiplicative uncertainty is less than unity perfect cancellation is possible at corresponding frequencies in a robustly stable control system and it is limited otherwise.

Description of the plant changes in terms of multiplicative uncertainty and related constraints on robust stability allow formulating another cost function. Taking into account that

$$S_{yy}(e^{\omega T_s}) = \left|V(e^{-j\omega T_s})F(e^{-j\omega T_s})\right|^2, \tag{2.56}$$

it can be written [Rafaely_97]

$$L_\omega = \int_0^{2\pi}\left[\left|V(e^{-j\omega T_s})F(e^{-j\omega T_s})\right|^2 + \beta_2\left|T_o(e^{-j\omega T_s})\overline{\delta S}(e^{\omega T_s})\right|^2\right]d\omega T_s, \tag{2.57}$$

where $V(e^{-j\omega T_s})$ is the frequency response of the General-Output Sensitivity Function, β_2 is a weighting coefficient, and PSD of the white noise is constant and unity. If F in (1.4) were assumed to be made of monic polynomials, non-unity variance of the white noise should also be taken into account. This cost function exhibits a trade-off between noise attenuation (first term in the integral) and robust stability (second term). It has been motivated by the H_∞ condition for robust performance, which guarantees robust stability at the same time [MorariZ_89], [DoyleFT_92], [SkogestadP_96]. In the polynomial-based approach the optimal filter minimising (2.57) remains the same in form. However, the disturbance shaping

filter, $F(z^{-1})$, is obtained now as a solution to the more general spectral factorisation, which for IMC takes the form [Elliott_01]:

$$S_{dd}(z^{-1}) + \beta_2\overline{\delta S}_r(z^{-1})\overline{\delta S}_r(z) = F(z^{-1})F(z)\Big|_{z^{-1}=e^{-j\omega T_S}}. \tag{2.58}$$

Similarly, in the frequency-domain approach it holds then

$$F(n) = \exp\left\{FFT\left[\ell_0(n)\cdot IDFT\left(\ln\left(S_{dd}(n) + \beta_2\left|\overline{\delta S}_r(n)\right|^2\right)\right)\right]\right\}. \tag{2.59}$$

According to [ElliottS_96], minimisation of the cost function given by (2.57) is equivalent to minimisation, in the mean-square sense, of the control system output described by (2.6) with the control filter input being the disturbance signal added to additional exogenous white noise, $e_\delta(i)$. This noise should be uncorrelated to $e(i)$, have variance β_2 and be shaped by the upper bound of the multiplicative uncertainty. Then, in the correlation-based approach the optimal causal and constrained control filter is

$$\underline{w}_{opt+} = -E\left\{\hat{\underline{r}}_\delta(i)\hat{\underline{r}}_\delta^T(i)\right\}^{-1}E\left\{\hat{\underline{r}}_\delta(i)d(i)\right\}, \tag{2.60}$$

where

$$\hat{r}_\delta(i) = \hat{S}_r\left[d(i) + \overline{\delta S}_r e_\delta(i)\right] \tag{2.61}$$

(see [Rafaely_97] and [ElliottS_96] for a similar problem). Better performance can be, however, obtained if the H_2 cost function without the robust term, (2.8), is minimised subject to the H_∞ constraint (2.52). This strategy is known as the H_2/H_∞ control problem. It has been discussed in [MorariZ_89] and extensively studied for ANC in [Rafaely_97] and [RafaelyE_99]. Searching for the solution is proposed there with the 'sequential quadratic programming – SQP' method implemented under *fmincon()* function of the Matlab package [Grace_95]. The general idea is to assume perfect plant model to obtain a simple form of the H_2 cost function subject to the H_∞ constraint, (2.52). For the SQP method the problem should be formulated as a convex one to find the global solution [RobertsV_73]. Another idea is to design the optimal control filter without any constraints and then cascade it with a low-order low-pass discrete filter [MorariZ_89].

It is worth noticing here that in the robustly stable designs presented in the quoted references the cost function includes PSD of the disturbance in the form of F, which should be known or estimated. A similar but more general problem can be defined as minimisation of H_2 or H_∞ norm of the sensitivity function itself, independently of the disturbance, over assumed frequency band. Such problem has been considered for continuous-time control in [Pawelczyk_02b, 02d, 02g]. It addresses also the case where the disturbance is non-stationary or, if originating from many sources, may change due to switching on and off some of them. An appropriate solution will be briefly referred to at the end of Chapter 3.

Some modifications of the H_2 cost function, other than those given by (2.46) and (2.57), can also be applied to enhance robustness of the optimal solution. One of the ways is to include control signal weighting [NiederlinskiMO_95], [Pawelczyk_99a]. Such approach is less conservative than that with control filter weighting because it limits the power sent to the loudspeaker, usually concentrated at some frequencies and not the entire filter [Rafaely_97]. In turn, in [SternadA_93] the optimal control filter solving the general LQ problem has been found with the aid of the variational method in the frequency domain. Another solution could be to transform the problem to a state-space form and design a Kalman filter even if the measurements were non-stationary [AhlenS_91]. A Wiener-type filter could also be designed in such case by applying an approach based on the *LU* Cholesky factorisation of the covariance matrix of the input [Orfanidis_88].

2.3 ADAPTIVE CONTROL

The optimal control filter in the IMC system does not depend in fact on the plant but on its model. Hence, it may seem that it can be successfully implemented in an application as a fixed one, regardless of plant time variations. However, there are some additional aspects. First, the optimal causal filter is defined for every frequency of the broadband disturbance. Second, the causal filter is in fact sub-optimal for the non-minimum phase model. The first problem makes the filter difficult to be implemented exactly even for a stationary disturbance. In practice, parameters of the disturbance originating from an operating machine or vehicle are at least slightly changing in time. Additionally, they cannot be measured with perfect precision to perform optimal control. The second problem may be more serious. The sub-optimal filter does not lead to the minimum of the cost function. According to (2.6) the cost function may exhibit significantly different shapes at the minimum, dependent on the plant modelling error (Figure 2.3). In most ANC applications and particularly these considered here the acoustic field response being a part of the response of the acousto-electric plant is subject to change. With the fixed control filter this may produce significantly different values of the cost function, (2.18), and therefore attenuation results. The control filter implemented as adaptive is tuned to satisfy the general purpose, namely to control the noise components that

contribute mostly to the overall mean-square value of the output signal. Moreover, it can be capable to retune in case of non-stationarity of the disturbance or changes of the plant response. Hence, adaptive controller is often a remedy to the above problems.

In this section basic parameter-update algorithms are briefly presented with focus on the most popular Filtered-Reference LMS. Then, convergence and stability problems are dealt with.

2.3.1 FILTERED-REFERENCE LMS ALGORITHM

The Filtered-Reference LMS algorithm has been originally developed for feedforward systems, where the reference signal, $x(i)$, being the control filter input and correlated with the disturbance, $d(i)$, is not estimated but is measured or synthesised. The derivation is presented in many references, e.g. [Haykin_96], [KuoM_96], [HansenS_97], [Elliott_01]. It is briefly reported below to set the background for the following analysis.

Under assumption I.2 defined in Section 1.5 the order of the general path and the control filter can be exchanged for analysis, as in Figure 2.4.

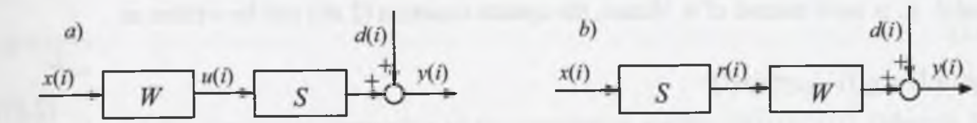

Figure 2.4 Exchanging the plant and control filter for analysis.

Then, the acoustic noise cancellation problem with the presence of acousto-electric path at the control filter output can be considered as the classical electrical noise cancellation problem with the control filter input being the reference signal filtered by the path response. Hence, the output of the entire system can be expressed as

$$y(i) = d(i) + \underline{w}^T \underline{r}(i) , \tag{2.62}$$

where

$$r(i) = \underline{s}^T \underline{x}(i) \tag{2.63}$$

and appropriate vectors are defined with the rules set in (2.34)-(2.37). Due to the above assumption the cost function (2.7) is quadratic in terms of the filter parameters. The parameters can be then updated in the opposite direction to the gradient of the cost function, so that

$$\underline{w}(i+1) = \underline{w}(i) - \frac{\mu}{2}\frac{\partial L}{\partial \underline{w}(i)}, \tag{2.64}$$

where μ is a greater than zero 'convergence coefficient' called also the 'step size' or 'learning rate' [HaykinW_03]. Taking (2.7) and (2.62) into account the gradient can be calculated as

$$\frac{\partial L}{\partial \underline{w}(i)} = -2E\{\underline{r}(i)y(i)\}. \tag{2.65}$$

Estimation of the cross-correlation term would require a lengthy averaging procedure, difficult to perform on-line. Therefore, a simplified alternative is used in the form of the LMS algorithm where the gradient is estimated by the instantaneous value $\underline{r}(i)y(i)$, which is a noisy but unbiased estimate [Morgan_80], [WidrowSS_81], [WidrowS_85], [Orfanidis_88], [Haykin_96], [HaykinW_03]. Then, the update equation becomes

$$\begin{cases} \underline{w}(i+1) = \underline{w}(i) - \mu\underline{r}(i)y(i) \\ \underline{r}(i) = \underline{s}^T\underline{x}(i). \end{cases} \tag{2.66}$$

In practice, the path impulse response, $\underline{s}$, is unknown and the impulse response of its FIR model, $\hat{\underline{s}}$, is used instead of it. Hence, the update equation (2.66) can be written as

$$\begin{cases} \underline{w}(i+1) = \underline{w}(i) - \mu\hat{\underline{r}}(i)y(i) \\ \hat{\underline{r}}(i) = \hat{\underline{s}}^T\underline{x}(i). \end{cases} \tag{2.67}$$

This form of LMS is referred to as the Filtered-Reference LMS or, more commonly, Filtered-x LMS (FXLMS) since the reference signal is usually denoted as $x(i)$ (Figure 2.5).

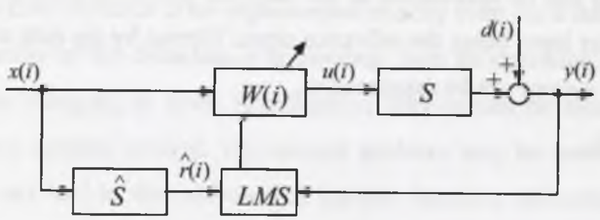

Figure 2.5 The Filtered-Reference LMS algorithm.

2.3.1.1 Convergence analysis

Before proceeding further it is now worth pointing to the underlying problem of convergence of the adaptive algorithm. In stochastic systems convergence of two random variables can be defined in different sense [ChenG_91], [Macchi_95]:

1) convergence 'with probability one' or 'almost surely – a.s.',
2) convergence 'in probability',
3) 'weak' convergence,
4) convergence 'in the mean-square sense',
5) convergence 'in the mean',
6) convergence 'of the mean'.

Definitions and mutual relations of these convergence types are presented in Appendix A.8. Nevertheless, it is worth mentioning that the convergence 'with probability one' is the strongest, whereas the convergence 'of the mean' is the poorest.

Provided that the assumptions J.1-J.5 defined in Section 1.5 are satisfied and the plant is perfectly modelled, the sufficient condition for convergence 'of the mean' of the control filter parameters updated with the FXLMS algorithm to optimal filter parameters takes the form

$$\mu < \frac{2}{\lambda_{\max}}, \tag{2.68}$$

where $\lambda_{\max}$ is the maximum eigenvalue of the correlation matrix $E\{\hat{\underline{r}}(i)\hat{\underline{r}}^T(i)\}$ [Macchi_95]. In the sequel, the notion 'convergence of the algorithm (system)', instead of 'convergence of the control filter parameters' will be often used. Under the same assumptions the sufficient condition for convergence of the algorithm 'in the mean-square sense' is stronger [Macchi_95], [Elliott_01]

$$\mu < \frac{2}{N \cdot E\left\{\hat{r}^2(i)\right\}}. \tag{2.69}$$

It has been experimentally shown that the reliable upper bound of the convergence coefficient should be modified to

$$\mu < \frac{2}{(N+k)E\left\{\hat{r}^2(i)\right\}}, \tag{2.70}$$

where k is the overall plant delay [ElliottN_89], [Elliott_01]. It is convenient for implementation purposes to rewrite the above equation using available quantities, i.e. estimate

$E\left\{\hat{r}^2(i)\right\}$ by averaging the data over the control filter length, so that

$$\mu < \frac{2}{(1+k/N)\underline{\hat{r}}^T(i)\underline{\hat{r}}(i)}. \tag{2.71}$$

This leads to the Normalised FXLMS algorithm [KuoM_96]

$$\underline{w}(i+1) = \underline{w}(i) - \mu_n \frac{\underline{\hat{r}}(i)}{\underline{\hat{r}}^T(i)\underline{\hat{r}}(i) + \varsigma} y(i) \tag{2.72}$$

with the upper bound of its convergence coefficient being

$$\mu_n < \frac{2}{(1+k/N)} \tag{2.73}$$

and additionally included regularisation parameter $0 \le \varsigma << 1$. A generalisation of Normalised LMS algorithm is the Affine Projection Algorithm described, e.g. in [HaykinW_03].

The necessity of relying on a practically imperfect model instead of the plant itself may lead to degradation of the correlation between the filtered-reference signal, $\hat{r}(i)$, and the system output, $y(i)$, which is responsible for updating the filter parameters in the proper direction ((2.64) and (2.65)), what implies convergence [SnyderH_94]. Hence, the eigenvalues λ_l (l = 1, 2, ..., N) of the cross-correlation matrix $E\left\{\underline{\hat{r}}(i)\underline{r}^T(i)\right\}$ determine behaviour of the adaptive algorithm. The classical FXLMS algorithm with imperfect modelling, if convergent, converges to the following solution

$$\underline{w}(\infty) = -E\left\{\underline{\hat{r}}(i)\underline{r}^T(i)\right\}^{-1} E\left\{\underline{\hat{r}}(i)d(i)\right\}, \tag{2.74}$$

regardless weather it operates in a feedforward or feedback structure. However, it is different than the optimal solution, (2.32), [Elliott_01]. If the assumptions J.1-J.5 hold and all the eigenvalues λ_l (not entirely real) of the cross-correlation matrix have positive real parts the sufficient condition for convergence 'of the mean' is [Morgan_80], [Elliott_01]

$$\underset{l}{\forall} \ \mu < \frac{2\operatorname{Re}(\lambda_l)}{|\lambda_l|^2}. \tag{2.75}$$

The convergence coefficient should be further limited if the plant is highly resonant or the disturbance highly correlated [BoucherEN_91].

The above discussion on the upper bound of the convergence coefficient may seem to violate the primary assumption of very slow adaptation required to derive the FXLMS algorithm. However, it turns out in practice that this algorithm "behaves more robustly than it was originally assumed" [Elliott_01] (see Appendices B.7 and B.8 for examples).

Each eigenvalue, λ_l, of the cross-correlation matrix can be associated with a mode of the FXLMS algorithm [KuoM_96], [Elliott_01]. It follows from the above evaluation that if for an excited mode of the algorithm the corresponding eigenvalue has negative real part the algorithm can diverge. Hence, it is important to provide an easily interpretable and reliable convergence condition addressing the modelling problem. It has been shown in [WangR_99b] that under the assumptions J.1-J.5 the sufficient but not necessary condition for convergence 'with probability one' of the FXLMS algorithm to the stable equilibrium point given by (2.74) is that $\hat{S}(z^{-1})/S(z^{-1})$ is SPR (Appendix A.4), or equivalently

$$\underset{\omega T_S}{\forall} \operatorname{Re}\left\{\hat{S}(e^{-j\omega T_S})S^*(e^{-j\omega T_S})\right\} > 0. \tag{2.76}$$

The proof has been performed using the Ljung's Ordinary Differential Equations (ODE) method [LjungS_83]. However, "the ODE method does not give information on the transient behaviour of the algorithm". If the assumption about vanishing to zero convergence coefficient is not satisfied the control filter parameters converge to the stable equilibrium point (2.74) 'in probability' [WangR_99b]. The condition (2.76) directly implies that the so-called 'phase error' between the control-to-output path and its estimate (the plant and the model, respectively, for feedforward control) must not exceed $\pm\pi/2$ at all frequencies [WangR_99b]. Hence, the so-called 'phase condition' takes the form

$$\underset{\omega T_S}{\forall} \left| \angle\{S(e^{-j\omega T_S})\} - \angle\{\hat{S}(e^{-j\omega T_S})\} \right| < \frac{\pi}{2}, \tag{2.77}$$

where $\angle\{.\}$ stands for the phase of $\{.\}$. This condition is also valid for tonal disturbances, for which it was derived much earlier [Morgan_80], [Burgess_81], [ElliottN_93].

After convergence, the value of the cost function differs form the minimal one obtained with optimal control and the so-called 'excess mean-square error' is proportional to μ [Orfanidis_88], [Macchi_95], [KuoM_96], [HaykinW_03]:

$$L_\infty - L_{\min} \sim \mu. \tag{2.78}$$

However, as it has been shown in many experiments, e.g. in [SaitoS_96] and [Elliott_01], this degradation is rather marginal for small μ and feedforward systems, provided the modelling errors are not so significant for the algorithm to diverge. For feedback systems and non-minimum phase plants the adaptive system may even produce a smaller value of the cost function due to sub-optimality of the fixed realisation (Figure 2.3). Moreover, the convergence coefficient (or both μ_n and ς in the Normalised modification, (2.72)) can be controlled to enable fast response in face of tracking necessity and small excess mean-square error after convergence [HaykinW_03]. Recent investigations show that for the adaptive LMS-based algorithm the steady-state mean-square value can be reduced because of non-linear effects, compared to that obtained with the optimal filter of the same length even for minimum phase plants [HaykinW_03].

Average behaviour of the estimate of the mean-square value of the output signal, associated with each stable l-th mode significantly excited to influence this value, can be expressed by a time constant. The time constant takes the following form

$$\tau_l = \frac{1}{2\mu\lambda_l} \tag{2.79}$$

for perfect plant model; time constant of the parameter update is doubled [HaykinW_03]. So the spread of the time constants can be written in terms of the spread of eigenvalues of the cross-correlation matrix [Orfanidis_88], [Macchi_95], [Haykin_96], [Elliott_01]:

$$\frac{\tau_{\min}}{\tau_{\max}} = \frac{\lambda_{\max}}{\lambda_{\min}}. \tag{2.80}$$

The eigenvalue spread is further determined by spectral properties of the disturbance and frequency response of the plant (or rather the perfect plant model):

$$\frac{\lambda_{\max}}{\lambda_{\min}} \le \frac{\max\limits_{\omega}\left\{\left|\hat{S}(e^{-j\omega T_s})\right|^2 S_{dd}(e^{\omega T_s})\right\}}{\min\limits_{\omega}\left\{\left|\hat{S}(e^{-j\omega T_s})\right|^2 S_{dd}(e^{\omega T_s})\right\}}. \tag{2.81}$$

The inequality can be substituted by equality for long filters.

Convergence of the adaptive algorithm can be characterised by convergence time. It is formally defined to be "the number of steps (samples) required for the power of the transient error to decrease below the steady-state error level" [Macchi_95]. However, practically, it is often defined as the number of samples required for the cost function value to be acceptably reduced [ElliottSN_87]. Sometimes, it is also expressed as the number of samples corresponding to an integer multiple (usually 3 or 4) of time constants of the excited modes, required for the cost function to differ marginally from its steady state value [Macchi_95]. Convergence time of an adaptive LMS-based algorithm depends strongly on μ, which is chosen dependent on properties of the plant and its model for a given disturbance.

Conclusions drawn from experimental analysis for the IMC system are reported in Section 2.3.5.

Another notion, often used to describe convergence is the 'convergence rate' defined in different ways in the literature. For example, it is the Euclidean norm of the parameter estimation error [ChenG_91], [Niederlinski_95], [Macchi_95]. Next time, it is the reciprocal of the time constant of the exponential-like trajectory [SastryB_89]. Sometimes it is simply defined as the reciprocal of the time required for the error to decrease below an assumed level, or the reciprocal of the convergence time.

2.3.1.2 Improvement of convergence

Convergence conditions for an adaptive control system with the FXLMS algorithm can be relaxed if the cost function being minimised is redefined as in (2.45). This results in the following parameter-update equation [KuoM_96], [Elliott_01]

$$\underline{w}(i+1) = (1-\beta\mu)\underline{w}(i) - \mu\hat{\underline{r}}(i)y(i). \tag{2.82}$$

Due to the first term on the RHS ($0 << 1-\beta\mu < 1$) this algorithm is referred to in the literature as the Leaky FXLMS. It converges provided real parts of the eigenvalues of the matrix $E\left\{\hat{\underline{r}}(i)\underline{r}^T(i) + \beta\mathbf{I}_N\right\}$ are positive. In this case, the sufficient condition for convergence 'with probability one', (2.76), modifies to [Elliott_01]

$$\underset{\omega T_s}{\forall} \quad \mathrm{Re}\left\{\hat{S}(e^{-j\omega T_s})S^*(e^{-j\omega T_s})\right\} + \beta > 0 \tag{2.83}$$

under the assumptions J.1-J.3, J.5 defined in Section 1.5. Hence, this algorithm is able to converge even in case of significant phase errors provided the weighting coefficient β is large enough. It should be emphasised that the leakage improves robust stability but degrades the performance. Hence, the weighting coefficient β is a trade-off between performance and robustness as in the optimal system. It has been mentioned while analysing the optimal control that this modification of the cost function is equivalent to properly injecting an exogenous white noise to the system [Rafaely_97].

Similar results to that of the Leaky FXLMS can be obtained with an adaptive realisation of the optimal H_2 / H_∞ approach. It is derived by transforming the constrained optimisation problem to an unconstrained one using penalty or barrier functions in the frequency domain, [Fletcher_87], and minimising the new cost function with the steepest descent method [Rafaely_97]. The obtained algorithm adapts to non-stationary disturbance and is robust to *plant perturbations. It may give important benefit. Properly designed it may protect against* unacceptable reinforcement of some frequency component, or obey other constraints. The amplification of noise at some frequencies might sometimes be severe in classical H_2 approach. However, the important drawback of the adaptive H_2 / H_∞ control system is its complexity and computational load, what makes it rarely used.

The convergence and performance problems can also be relaxed to some extend by applying to FXLMS some of the known modifications of the LMS algorithm that update the convergence coefficient, e.g. Correlation LMS, Normalised LMS (with controlled relaxation coefficient), Variable-step-size LMS or others [KuoM_96], [HaykinW_03]. The Correlation FXLMS algorithm has been found particularly useful and successfully verified in [Pawelczyk_03a, 04a]. Control filter parameters are updated according to

$$\begin{cases} \underline{w}(i+1) = \underline{w}(i) - \mu(i)\hat{\underline{r}}(i)y(i) \\ \mu(i+1) = \upsilon_1 \vartheta(i) \\ \vartheta(i+1) = \upsilon_2 \vartheta(i) + (1-\upsilon_2)\hat{\underline{r}}(i+1)y(i+1) \end{cases} \tag{2.84}$$

where υ_1 is a "scale factor" and υ_2 is a "smoothing factor introduced to deal with the nonstationary character of the adaptation error process" [KuoM_96]. This modification allows to keep tracking capabilities, reduce mean-square value of the controlled output in the steady state and make the overall system stable in case of practical changes of the plant response and disturbance non-stationarity [ShanK_88], [KuoM_96].

Convergence rate of the adaptive algorithm can be significantly improved (convergence time reduced) by making the convergence coefficient a function inversely proportional to PSD estimate of the filtered-reference signal,

$$S_{\hat{r}\hat{r}}(n) = \left|\hat{S}(n)\right|^2 S_{xx}(n) \tag{2.85}$$

([Orfanidis_88] and [BendatP_93]) or at least inversely proportional to $|\hat{S}(n)|^2$. Such approach reduces the spread of time constants of the algorithm modes. It can be efficiently performed using one of the following solutions:

- control filter update in the frequency domain – then an individual convergence coefficient for each frequency bin, *n*, can be used ([KuoM_96]),
- control filter update in the time domain with the correction term transformed back from the frequency domain, where it was calculated and decomposed to obtain a causal part [ElliottR_00],

- control filter update in the time domain, where instead of filtering the reference signal by the plant model, $\hat{S}$, it is filtered by $\hat{S}/|\hat{S}|^2$, which has the magnitude equal to that of the inverse of $\hat{S}$ and the same phase [Michalczyk_04].

Another way to improve convergence rate is to apply the Newton LMS (however, the initial convergence rate is higher for the LMS itself), Fast RLS (e.g. RLSL, FK, FAEST, FTF – their computational complexity is of $O(N)$, whereas for RLS itself the complexity is of $O(N^2)$), Lattice RLS or Lattice LMS algorithms [Orfanidis_88], [HaykinW_03]. Obviously, filtering the reference signal as in the FXLMS algorithm is still necessary. Among these algorithms the Lattice ones deserve particular attention. Similarly to Newton LMS, their convergence time is independent on the eigenvalue spread, (2.80), and therefore they respond very fast [VeenaN_04]. Moreover, they provide high computational efficiency, numerical stability and accuracy. Additionally, due to modularity of structure, the filter order can be easily changed, if necessary [MitraK_93].

Recent investigations show that convergence rate of the LMS algorithm depends significantly on initial conditions and for proper choice it can be significantly higher than for the algorithms mentioned above [HaykinW_03]. Moreover, LMS "is an algorithm that is robust with respect to disturbance variation, a property of which RLS, for example, cannot boast", [HaykinW_03]. In fact, it has been proven to be an H_∞ optimal algorithm in this sense [HassibiSK_96]. Although this optimality is not unique, LMS is the only algorithm that is also risk-sensitivity optimal, i.e. "under Gaussian assumption of the disturbance, it minimises the expected exponential of the prediction error energy" [HaykinW_03]. The above features justify widespread use of the LMS in adaptive filtering practice.

2.3.2 Other LMS-based algorithms

Dependent on the structure of the control filter, computational load and demands related to the residual signal, some LMS-based algorithms and realisations have been developed. They are briefly described in the following subsections.

2.3.2.1 Filtered Recursive LMS

The optimal control filter designed using the polynomial or frequency-domain approach is of IIR structure (see (2.17) and (2.26), respectively). The denominator of this filter depends on spectral properties of the disturbance and response of the path model (model of the control-to-output path for IMC). In case of the considered group of acousto-electric plants frequency responses of their paths do not exhibit evident separate modes. However, the disturbance-shaping filter can have zeros close to the unit circle. Therefore, generally, impulse response of the optimal filter can have a large number of significant parameters that should be taken into account if this filter is going to be correctly approximated by an FIR filter.

The IIR filter when implemented as adaptive should be updated with the Filtered Recursive LMS algorithm. It is usually called as the Filtered-u LMS algorithm or FULMS since the reference and control signals are often gathered in a common vector denoted as U. FULMS has been originally developed by Eriksson and takes the form:

$$\begin{cases} \underline{w}^N(i+1) = \underline{w}^N(i) - \mu \underline{\hat{r}}(i) y(i) \\ \underline{w}^D(i+1) = \underline{w}^D(i) - \mu \underline{\hat{u}}_f(i) y(i) \\ \hat{r}(i) = \underline{\hat{s}}^T \underline{x}(i) \\ \hat{u}_f(i) = \underline{\hat{s}}^T \underline{u}(i). \end{cases} \tag{2.86}$$

where W^N and W^D are numerator and denominator, respectively, of the overall control filter (Figure 2.6) [ErikssonAG_87], [Eriksson_91], [KuoM_96].

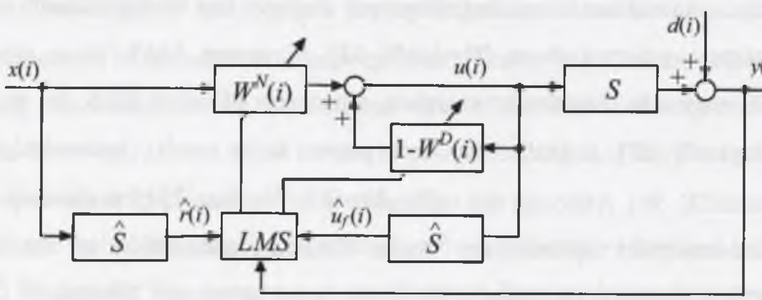

Figure 2.6 The Filtered Recursive LMS algorithm.

The cost function, (2.7), is now non-quadratic with respect to control filter parameters, what may results in convergence to a local minimum [Shynk_89]. A sufficient condition for global convergence of the FULMS algorithm has been first derived in [WangR_99]. Provided the assumptions J.1-J.6 defined in Section 1.5 are satisfied and

$$\mathrm{Re}\left\{ \frac{S}{W^D_{opt+} \hat{S}} \right\} > 0, \tag{2.87}$$

then by Ljung's ODE theorem the FULMS algorithm converges 'with probability one' to the unique equilibrium point.

In [JacobsonJMS_01], the authors claim that the problem of convergence in case of modelling errors can be avoided by simply applying the Normalised Recursive LMS algorithm ([KuoM_96]), instead of Filtered Recursive LMS. They have proven that if the assumptions J.1-J.6 are satisfied and the plant is SPR, then the Normalised Recursive LMS algorithm converges 'with probability one' to the global unique equilibrium point. Unfortunately, the assumption about properties of the plant is unjustified for acousto-electric plants, particularly belonging to the considered group.

Due to demanding convergence conditions, presence of local minima and higher complexity of the Recursive LMS-based algorithms, a common practice in majority of active control literature and also in this research is to implement the control filter as a sufficiently long approximating FIR filter and apply the FXLMS algorithm for updating its parameters. This coincides with the correlation-based approach. Potential loss in performance is marginal [Michalczyk_04]. Following subsections are devoted to some representations or extensions of FXLMS.

2.3.2.2 Filtered-Error LMS

Any modifications to the adaptive algorithm, (2.67), should not substantially deteriorate the estimate of the cross-correlation, (2.65), between the filtered-reference signal and the system output to guarantee update of the control filter parameters in the opposite direction to the gradient of the cost function, (2.64). This conclusion allows to derive an algorithm in which the controlled output (error) is filtered instead of the reference signal (see [Pawelczyk_03e] for detailed derivation and comparison to FXLMS). The adaptation is performed according to the following law

$$\begin{cases} \underline{w}(i+1) = \underline{w}(i) - \mu \underline{x}(i-M) \hat{y}_f(i) \\ \hat{y}_f(i) = \underline{\hat{s}}_f^T \underline{y}(i), \end{cases} \tag{2.88}$$

where $\underline{\hat{s}}_f$ is the vector of flipped parameters of the general plant model, i.e. the vector of $z^{-M}\hat{S}(z)$ (Figure 2.7). This algorithm, derived using a different method is known in the literature as the Filtered-Error LMS (FELMS) [KuoM_96], [Elliott_01]. It has, in fact, little advantage over FXLMS for SISO systems, but it is often used for MIMO systems where if properly implemented requires much less computations than FXLMS.

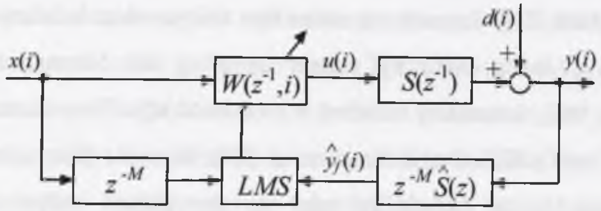

Figure 2.7 The Filtered-Error LMS algorithm.

2.3.2.3 Shaped-Error LMS

In this subsection a modification of the FXLMS algorithm that allows to shape spectrum of the output signal, $y(i)$, in a desired way is considered. Such problem is important for two reasons. First, warning or alarming sounds can be generated in the controlled frequency band. With classical FXLMS they might be cancelled to the acoustic floor level as they are usually tonal and therefore are well tackled by discrete adaptive systems. Second, the user may prefer hearing less attenuated sound and not to be fed with a kind of very unpleasant wide-band hissing noise. By applying the methodology mentioned in the previous subsection, an appropriate algorithm can be derived (see [Pawelczyk_03e] for detailed derivation and analysis). The adaptation procedure takes the form

$$\begin{cases} \underline{w}(i+1) = \underline{w}(i) - \mu \underline{\hat{r}}_q(i) y_q(i) \\ \hat{r}_q(i) = \underline{q}^T \underline{r}(i) \\ y_q(i) = \underline{q}^T \underline{y}(i), \end{cases} \tag{2.89}$$

where $\underline{q}$ is the vector of impulse response parameters of the output-shaping filter, Q (Figure 2.8).

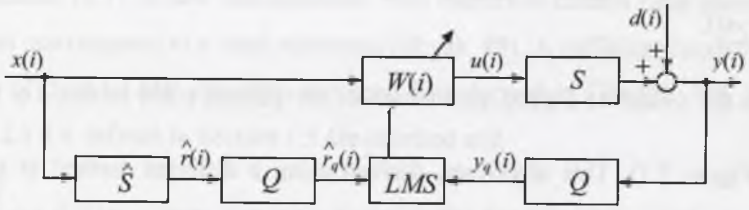

Figure 2.8 The Shaped-Error LMS algorithm.

This algorithm, derived using a different method is known in the literature as the Shaped-Error LMS (SELMS) [KuoM_96], [Elliott_01]).

2.3.2.4 Frequency-domain FXLMS

Sometimes it can be beneficial to perform adaptation in the frequency domain [Shynk_92], [Haykin_96], [KuoM_96], [Rafaely_97], [ElliottR_97, 00], [Elliott_01]. Then, blocks of data as long as the control filter length must be acquired to perform FFT. Due to the block processing frequency-domain implementation allows more accurate calculation of the gradient of the cost function, (2.65), than using the instantaneous values provided both the plant and disturbance properties do not change over the block length. The filter is updated every block length and it remains constant over this horizon. Such way of implementation significantly reduces the computational load, particularly for long filters, since convolution is omitted. However, if the overall control algorithm is performed in frequency domain an additional large delay of the block length is introduced because control signals are calculated once for such time. To avoid this disadvantage the algorithm can be modified. So the control filter can be updated in frequency domain once per block and then transformed back into time domain. Finally, the control signal is calculated in each sample as convolution of impulse response of the control filter with the reference signal (see the above references). During the processing care should be taken to avoid circular effects and obtain causal implementations [BendatP_93].

While performing adaptation in the frequency domain different convergence coefficients can be used for different frequencies, what can significantly improve the convergence rate (reduce the convergence time). On the other hand, having frequency responses of the control filter and plant model, both the performance and stability can be easily monitored and proper precautions undertaken.

2.3.3 Adaptive control of deterministic disturbances

"Although the Filtered-Reference LMS algorithm has been motivated by the need to control stochastic disturbances, it can also provide a very efficient method of adapting a feedforward controller for single-frequency disturbances" [Elliott_01]. Indeed, it has been confirmed in many references that this algorithm is suitable for any disturbance, stochastic or deterministic, in any control structure provided there is a reference signal (measured, synthesised or estimated), which is correlated with the disturbance (see Chapter 5 for results of real-world experiments and Appendix C for simulation results) [Macchi_95]. The convergence condition is then much weaker than that for stochastic disturbance because (2.77) needs only to be satisfied for the individual frequencies. It had been derived much earlier than the condition for stochastic disturbance [Morgan_80], [Burgess_81], [ElliottN_93].

If the disturbance has only harmonic content it is also possible to design an adaptive gradient algorithm directly updating the control signal. Such algorithm is particularly efficient if the sampling frequency is properly chosen with respect to the fundamental frequency of the disturbance [KuoM_96], [Elliott_01]. Another method is to apply individually a cosine-wave generator for each tone and a two-parameter control filter updated with FXLMS minimising a pseudo-error signal instead of the residual signal [KuoM_96], [DiegoGFP_04].

Adaptive control of deterministic disturbances in the form of multiple tones can also be performed in a filter bank composed of parallel channels, each processing an individual frequency [HaykinW_03]. Such solution has been originally suggested in [Conover_56] and also extensively studied in [Pawelczyk_02a] in the context of feedforward systems. It has also been shown that the adaptive algorithm can be significantly simplified to the form of Delayed-x LMS algorithm, where instead of filtering the reference signal in (2.67) it is only shifted by an integer delay [Pawelczyk_00c]. The multi-rate signal processing technique with octave filters have been applied additionally to widen the attenuation band.

There are also other solutions in literature to the problem of adaptive control of deterministic disturbances. They are presented, e.g. in [NiederlinskiMO_95], [BodsonD_97], [MarinoST_03], [BrownZ_04].

2.3.4 Adaptive IMC system analysis

In the proceeding sections different parameter update algorithms have been presented and discussed, including FXLMS with some modifications or representations, and FULMS. In the sequel the classical form of the FXLMS algorithm will be considered, bearing in mind that it can be performed in one of the other forms, dependent on application. Hence, the assumption I.2 as defined in Section 1.5 remains valid.

IMC in adaptive version has been first studied by Walach and Widrow [WalachW_83], [Widrow_86]. Control filter parameters are updated using (2.67), where $\underline{\hat{s}} = \underline{\hat{s}}_r$ and the reference signal is not measured but estimated as (Figure 2.2)

$$x(i) = y_r(i) - \underline{\hat{s}}_r^T \underline{u}(i) \tag{2.90}$$

Therefore, the overall adaptive IMC system with the FXLMS algorithm can be presented as in Figure 2.9.

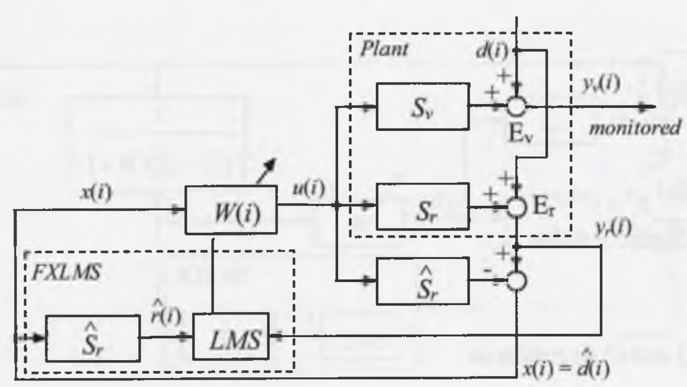

Figure 2.9 The IMC system with the FXLMS algorithm.

A simplified analysis of the adaptive IMC system is presented below. Further discussion of this system, including different convergence conditions and role of the convergence coefficient, is postponed to the following subsection.

In order to take advantage of the results of adaptive feedforward control system analysis it is convenient to redraw the system from Figure 2.9 to a feedforward-type structure with the input $d(i)$ as presented in Figure 2.10.

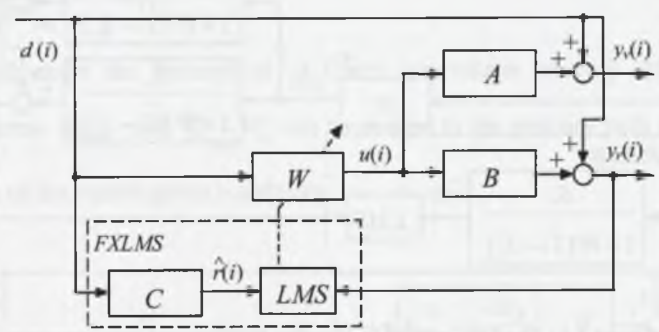

Figure 2.10 Adaptive feedforward-type structure.

According to this figure:

$$y_v(i) = (1 + AW)d(i), \tag{2.91}$$

$$y_r(i) = (1 + BW)d(i), \tag{2.92}$$

$$\dot{r}(i) = Cd(i). \tag{2.93}$$

Taking (2.25) and (2.4) into account gives, respectively,

$$A = \frac{S_v}{1+W(\hat{S}_r - S_r)}, \tag{2.94}$$

$$B = \frac{S_r}{1+W(\hat{S}_r - S_r)}. \tag{2.95}$$

It follows from Figure 2.9 that

$$\hat{r}(i) = \hat{S}_r\, x(i). \tag{2.96}$$

Combining (2.2) and (2.4) results in

$$\hat{r}(i) = \hat{S}_r \frac{1}{1+W\hat{S}_r} \cdot \frac{1+W\hat{S}_r}{1+W(\hat{S}_r - S_r)} d(i) = \frac{\hat{S}_r}{1+W(\hat{S}_r - S_r)} d(i). \tag{2.97}$$

Taking (2.93) into account yields

$$C = \frac{\hat{S}_r}{1+W(\hat{S}_r - S_r)}. \tag{2.98}$$

Finally, the block diagram from Figure 2.10 takes the form as in Figure 2.11.

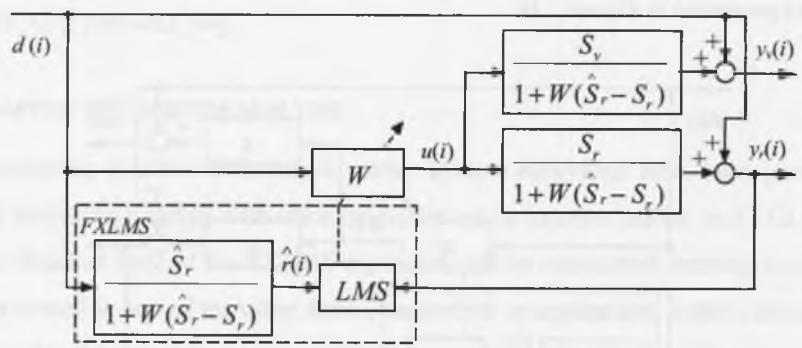

Figure 2.11 The IMC system in adaptive feedforward-type structure.

In case of feedforward control with the FXLMS algorithm a convenient convergence condition is given by (2.77). However, it is seen from Figure 2.11 that for the IMC system the control filter modifies the control-to-output path and may have the impact on convergence of the adaptive algorithm. This figure can be further rewritten by shifting the common denominator of transfer functions A, B and C in front of the control filter as in Figure 2.12. So it is clear that in this structure the assumption J.5 from Section 1.5 concerning independence of the control filter input on the control filter, required to derive the convergence phase condition, is not satisfied.

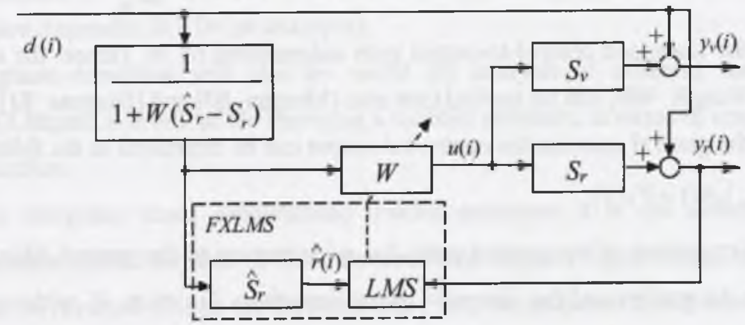

Figure 2.12 The IMC system in adaptive feedforward-type structure – another representation.

The convergence analysis can be then approximately tackled by adopting the method presented in [VaudreyBS_03]. Let the so-called control path be defined as the path from the control filter input to the system output in Figure 2.11, i.e.

$$B_W = BW. \tag{2.99}$$

It is non-linearly dependent on control filter W for the structure considered. However, it can be successfully approximated by a linear term of Taylor series expansion at a frozen W_0

$$B_W \cong B_W\big|_{W_0} + \frac{\partial B_W}{\partial W}\bigg|_{W_0} (W - W_0). \tag{2.100}$$

This is justified under the assumption of frozen trajectories or very slow adaptation, in practice. The terms $B_W\big|_{W_0}$ and $\frac{\partial B_W}{\partial W}\big|_{W_0} W_0$ can be shifted to the primary path as in Figure 2.13, with no change of the convergence conditions.

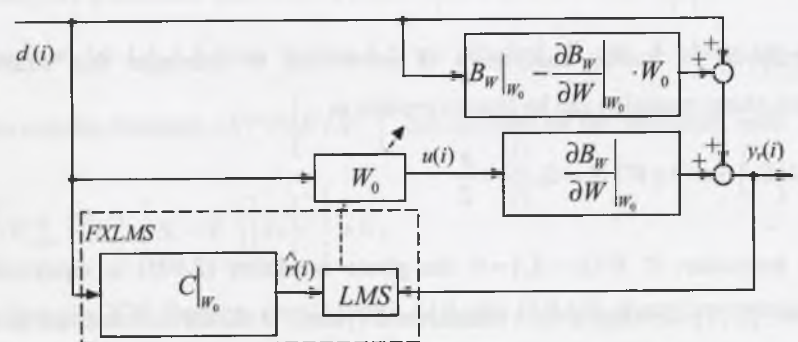

Figure 2.13 The Linearised IMC system in adaptive feedforward-type structure.

Then, B_W can be considered as linearly dependent on W because $\left.\frac{\partial B_W}{\partial W}\right|_{W_0}$ is independent on W. This makes the linearised control-to-output path independent on W. Hence, the convergence analysis of [WangR_99b] can be applied (see also [Morgan_80] and [Burgess_81]).

Using the general notation the controlled output can be expressed in the following form

$$y(i) = (1 + B_W)\, d(i) = V\, d(i). \tag{2.101}$$

Therefore, the gradient of the control path, B_W, with respect to the control filter, W, can be calculated as the gradient of the General-Output Sensitivity Function, V, with respect to the control filter, what according to (2.6) gives

$$\frac{\partial B_W}{\partial W} = \frac{\partial V}{\partial W} = \frac{S_1 - S_2}{(1 + W S_2)^2}. \tag{2.102}$$

For IMC itself and recalling (2.5) the gradient takes the form

$$\frac{\partial B_W}{\partial W} = \frac{S_r}{\left[1 + W(\hat{S}_r - S_r)\right]^2}. \tag{2.103}$$

Let now the assumptions J.1-J.5, J.7 from Section 1.5 hold for the linearised system. Then, following the reasoning from [WangR_99b] and [VaudreyBS_03], it suffices for convergence of the FXLMS algorithm that the phase angle ($\angle$) of gradient of the General-Output Sensitivity Function does not differ from phase angle of filter C in Figure 2.11 and Figure 2.13 by more than $\pm\pi/2$, i.e.

$$\left| \angle\left\{ \frac{S_r}{\left[1 + W(\hat{S}_r - S_r)\right]^2} \right\} - \angle\left\{ \frac{\hat{S}_r}{1 + W(\hat{S}_r - S_r)} \right\} \right| < \frac{\pi}{2}. \tag{2.104}$$

For the purpose of further analysis it is convenient to rearrange this equation. The convergence phase condition can be then expressed as

$$\left| \angle\{S_r\} - \angle\{\hat{S}_r\} - \angle\left\{1 + W\left(\hat{S}_r - S_r\right)\right\} \right| < \frac{\pi}{2}. \tag{2.105}$$

Hence, in particular, if $W(\hat{S}_r - S_r) \approx 0$ the phase condition (2.105) is equivalent to the classical one, (2.77), developed for a feedforward system. It should be noted that limitation of the control filter gain, what is advantageous for stability of the feedback loop (see (2.44)), may also reduce the phase error and protect against divergence of the FXLMS algorithm. On

the other hand, the last term on the LHS of (2.105) may sometimes help to satisfy the phase condition (see Appendix B.7 for an example).

The phase condition will also be useful for analysis of different control systems designed in Chapter 3. It will allow choosing a suitable structure, in terms of convergence, for given application.

While designing more sophisticated control structures it is not always clear what transfer function should be used to filter the reference signal (Figure 2.9). Then, the above analysis can be reversed to ease up the synthesis. First, the gradient (2.102) can be calculated and then the filter C (as in Figure 2.10) sufficiently simple and providing small phase error can be designed. Finally, the required transfer function used to filter the reference signal can be found.

2.3.5 Convergence and stability of adaptive IMC system

Adaptive internal model-based systems (IMC and the control systems considered in Chapter 3) are very difficult to be fairly analysed. They operate with non-stationary signals due to the adaptation loop, have structural feedback loop and are generally employed to face time variations of the plant and non-stationarity of the disturbance. Therefore, their analysis is usually subject to a variety of constraints that often significantly limit practical application of found conditions. Some of the conditions developed over last years are briefly summarised below.

Convergence analysis of the IMC system with control filter parameters updated using the FULMS algorithm has been provided in [FraanjeVD_03]. It is an extension of the analysis of [WangR_99] performed there for systems where perfect noise cancellation is possible. Assuming that: J.1-J.4, J.7 from Section 1.5 are satisfied, S_r and $\hat{S}_r$ have the same inner factor, the transfer function $z\hat{S}_r^{(o)}F\left\{F/\hat{S}_r^{(i)}\right\}_-^*$ has no poles on the unit circle, and

$$\mathrm{Re}\left\{ S_r \left\{ \left[W_{opt+}^D - W_{opt+}^N\left(S_r - \hat{S}_r\right)\right] \hat{S}_r \right\}^{-1} \right\} > 0, \tag{2.106}$$

then, by Ljung's ODE theorem (see [LjungS_83]), the FULMS algorithm operating in IMC structure converges 'with probability one' to the unique global equilibrium point.

A simplified convergence analysis for IMC with the FXLMS algorithm has been presented in [SakaiM_03]. The proof has been carried out in the frequency domain. Assuming that J.1-J.4, J.7 are satisfied, the order of the FIR control filter tends to infinity (is much larger then the order of the FIR plant and its model), both the plant and its model are minimum phase with the same known delay, and

$$\mathrm{Re}\left[\hat{S}_r^*(n)S_r(n)+\frac{1}{F(n)}\left\{e^{j\Omega n}F(n)\right\}_+ e^{j\Omega n}\hat{S}_r^*(n)\left(\hat{S}_r^*(n)-S_r(n)\right)\right]>0, \tag{2.107}$$

then the FXLMS algorithm converges 'of the mean' to a local stable equilibrium point (Ω is the basic frequency bin and n is the number of a frequency bin).

In the previous subsection the phase condition for convergence 'with probability one', (2.105), has been derived after linearising the control path. It has been found particularly useful in analysis. It is a counter-part to the condition (2.107) but it is more general since the latter is valid only for a minimum phase plant and its model. What is also important, under comparable assumptions the phase condition refers to stronger convergence. Condition (2.105) implicitly includes properties of the disturbance via W, whereas in (2.107) they are included explicitly.

The above brief review demonstrates high complexity of the stability problems in adaptive ANC systems related to imperfect modelling. It has been assumed hitherto in the form of J.7 that presence of the feedback loop does not destabilise the overall system, namely the modelling error is not too large. Taking into account other assumptions, it can be concluded that any analysis known to the author is of limited value due to a variety of restrictive constraints. It is believed that more reliable analysis can be approached using, e.g. the tool presented in [ChenG_91] based on conditional expectations and particularly on the martingale method. "The martingale method is a powerful tool for analysing recursive identification algorithms and stochastic adaptive control systems". It has been successfully used, e.g. in [Niederlinski_95] and [FilatovU_04]. Such analysis still remains an open problem.

Another methodology to overcome the problems due to imperfect plant modelling is to update the model simultaneously with adaptation of the control filter. Several algorithms have been proposed for the on-line adaptation of the plant model. They usually require injecting to the system additional wideband noise uncorrelated with the disturbance, what exhibits close analogy to interpretation of the Leaky FXLMS algorithm (see (2.82), (2.83) and following comments). Appropriate algorithms can be found, e.g. in [ErikssonA_89], [Rafaely_97], [Figwer_03], [VeenaN_04]. There are also some trials to identify the plant model without the additional noise but the result is generally not unique [WidrowS_85], [TapiaK_90], [NowlinGT_02], [ZhangG_04]. Usefulness of the algorithms mentioned above is usually

comparable to the Leaky FXLMS in terms of the convergence itself. They can, however, improve the convergence rate. Some of them are particularly appreciated in feedback internal model-based structures. Then, in addition to updating the control filter parameters the plant model constitutes a part of the overall feedback controller. If changes of the plant are large enough stability of the feedback loop may be impaired (see (2.43)). For changes of the plants under consideration (Chapter 5), application of these algorithms is unnecessary and Leaky FXLMS supported with the Correlation or Normalised modification suffices to overcome stability-related problems. The on-line model identification algorithms will not be dealt with in the sequel.

It has been assumed in J.1 for the convergence analysis that the convergence coefficient is very small or vanishes to zero. On the other hand, the adaptive system is also responsible for responding to time-variations of the plant or non-stationarity of the disturbance. However, since the model of the plant is required to adapt the controller as well as estimate the reference signal variations of the plant are more crucial. In case of too small convergence coefficient the so-called 'lag effect' may appear, which can degrade the performance, even if the system remains stable [Macchi_95]. In turn, too large coefficient increases the excess mean-square error or can even lead to divergence as the upper bounds demonstrate. It has been shown in [Macchi_95] that the optimal coefficient is related to so-called 'non-stationarity degree' introduced to describe time variations, and the tracking capability of the LMS-based algorithm behaves much better when facing random time-variations than a deterministic trend.

A further insight into the stability related problems can be gained and behaviour of the adaptive algorithm can be examined with simulation analysis. However, it should be emphasised at the very beginning that stability, similarly to convergence, is an asymptotic property of a system. Therefore, any analysis performed over a short time horizon can rather refer to a tendency towards instability (or divergence) and the conclusions cannot be straightforwardly generalised.

Three potential sources of instability of an adaptive LMS-based feedback ANC system should be considered [VaudreyBS_03]:

1) the structural feedback loop,
2) the phase error violating the convergence condition,
3) too large convergence coefficient μ.

The first two problems originate directly from imperfect modelling and sometimes can be difficult to overcome. Moreover, they can influence each other. These problems have been experimentally examined for a simulated minimum phase plant in [VaudreyBS_03] and for non-minimum phase plant including time delay in Appendix B.7. For example, even if the phase error (2.105) is small and the filter tends to converge to the optimal solution roots of the characteristic equation (2.43) can leave the unit circle on the z plane during adaptation or, equivalently, frequency response of the open loop can encircle the Nyquist point. Then, an increase of the output signal results in a change of the control filter, what can further violate the phase condition (2.105). It has been shown that due to presence of the adaptive filter such condition can be self-correcting during adaptation and decrease the phase error. Moreover, it can even be less conservative than in case of feedforward systems (2.77). It has also been demonstrated that even in case of the phase error between the plant and the model significantly exceeding $\pi/2$, the adaptive algorithm of the IMC structure can converge. This is because the phase condition (2.105) may be satisfied, although instability due to the feedback loop may appear [VaudreyBS_03]. On the other hand, even very small phase error between the plant and the model may lead to divergence, particularly for a larger convergence coefficient.

The third potential source of instability, i.e. the convergence coefficient, has great impact on the convergence itself and the convergence time (rate). This dependence has been verified by means of simulations for the IMC system with imperfect modelling and reported in Appendix B.8. In these investigations the convergence time has been defined as the number of samples required for an examined tone of 250 Hz to be attenuated by 20 dB. It has been found that for small convergence coefficient increase of its value decreases convergence time and the dependence is reciprocal,

$$t_C \sim \mu^{-1}, \tag{2.108}$$

regardless of plant modelling error. For small values of μ the plant dynamics has little effect and only the plant gain and control filter length influence the scaling in (2.108). Then, there exists an optimal value of μ in terms of the smallest convergence time (highest convergence rate). Minimum value of t_C depends both on the plant gain and delay for a given μ. However, the optimum value of μ and the range of its values are mainly limited by the delay, what corresponds to (2.73). This has been confirmed in analysis performed in [ElliottSN_87] for a simplified case of a feedforward system with the plant being a pure delay and tonal reference signal. It has been experimentally found there that the optimal μ is inversely

proportional to the overall path delay expressed in samples. Continuing the analysis from Appendix B.8, further increase of the convergence coefficient increases the convergence time due to fluctuations of the residual signal (or excess mean-square error, (2.78)). Finally, after crossing the critical value the adaptive system suddenly diverges.

Summarising the entire stability and convergence considerations, and potential related problems it is suggested to support additionally the adaptive algorithm with a heuristic supervisory loop, regardless of any modifications. This loop can be used to monitor the convergence and performance, and reset the algorithm or change some settings, if necessary (see Section 5.3.5.3 for an example). This is particularly important for the considered acousto-electric applications to avoid any unpleasant and annoying sound effects.

2.4 SUMMARY

In this chapter Internal Model Control system has been considered. It seems particularly useful for active control if no reference signal correlated with the disturbance is available or can be synthesised, because it allows to estimate the disturbance, the better the more accurate the real path model is. Consequently, design and analysis methods similar to those used for feedforward systems can be applied. This structure is also advantageous due to minimisation of the effect of non-linearity caused by the D/A converter saturation [MorariZ_89]. Examples illustrating design and analysis of this system are presented in Appendices B.1-B.8. They have been simulated on the basis of real data obtained from laboratory measurements.

First, optimal causal control filters minimising mean-square value of the residual signal at the real microphone have been designed using different approaches. Polynomial-based approach requires spectral factorisation of the disturbance PSD estimate, inner-outer factorisation of the real path model and causal/non-causal decomposition (alternatively, solving a Diophantine equation). Next, the frequency-domain and correlation-based approaches have been employed. All the solutions have been found equivalent (Appendices B.3 and B.4). It should be emphasised that the designs with all the approaches have been performed, contrary to majority of the references, without assuming perfect plant modelling. The problem of control of deterministic noise has been considered separately. It has been explained and confirmed by simulations in Appendix B.5 that the solution to this problem is not unique provided the control filter order is sufficiently large. Moreover, it does not depend on the plant but only on its model. Then, stability of the feedback loop and numerical conditioning of the optimal solution have been analysed. Literature-based modifications have been discussed. They generally involve including a weighting term due to filter parameters, control signal, or upper bound of the multiplicative uncertainty, if it is known.

Next, adaptive control systems have been addressed. The most commonly used algorithm, known as FXLMS, has been presented. It has been stressed that its properties depend on the choice of the convergence coefficient and plant modelling errors. Therefore, various sufficient conditions for convergence defined in different sense have been provided. Some modifications of this algorithm relaxing the conditions have also been presented. Among them, the Leaky FXLMS algorithm deserves particular attention. Other LMS-based adaptive algorithms have also been mentioned. Their choice is application-specific. Afterwards, FXLMS has been applied for updating parameters of the control filter in the IMC system. It has been emphasised that such system is very difficult for analysis due to interacting problems of stability of the structural feedback loop and convergence of the adaptive algorithm. Therefore, any analysis found in the available references requires restrictive assumptions concerning the physical plant and signals, which usually do not correspond to the ANC applications. Also the simplest and convenient convergence phase condition derived for a feedforward system without intrinsic feedback cannot be directly applied. It has been, however, shown that similar analysis can be performed after linearising the control path. Then, a phase condition explicitly including the control filter has been obtained. Its relevance has been confirmed by means of simulation experiments (Appendix B.7). Moreover, its idea is helpful for designing FXLMS-based parameter update procedures for other more complicated structures and comparing their convergence properties for a given application. It has also been shown that the convergence coefficient, control filter length, plant delay and gain have crucial impact on convergence time. The conclusions have been supported by simulation experiments reported in details in Appendix B.8.

Both optimal and adaptive IMC systems respond similarly for frequencies contributing to the noise being controlled and invariant plant. The attenuation results are also similar. In case of changes of the plant the adaptive filter retunes accordingly (Appendices B.3-B.5). The fixed optimal filter, although dependent on the unchanged plant model and not the plant itself is in fact sub-optimal for non-minimum phase model. As a result the system performance depends strongly on the modelling errors.

Simulation analysis presented in Appendix C.2 demonstrates that the zones of quiet generated by the optimal or adaptive IMC systems are located at the real microphone.

For considered frequencies they are of small dimensions and propagate poorly. Hence, if they are expected at other locations appropriate control systems should be designed.

The entire analysis presented in this chapter constitutes the background for following chapters. Therefore, both the optimal and adaptive solutions have been expressed using general symbols that can be substituted by symbols appropriate for the other algorithms.

Chapter 3

Virtual Microphone Control Systems

3.1 The idea of Virtual Microphone Control systems

The IMC system presented in Chapter 2 has been designed to minimise mean-square value of the residual (output) signal at the real microphone. The secondary sound operates at the same time on the acoustic noise at the position of the user ear. In the worst case this can result in sound reinforcement at that position. In many applications placing another microphone directly at the ears is not accepted. It is then justified to make efforts to design a dedicated system. The purpose is to minimise the mean-square value of the noise at the desired location while performing measurements of sound interference results at another location. This can be done by employing the general idea of Virtual Microphone Control (VMC) systems (Figure 3.1). In this chapter optimal and adaptive VMC systems in three different structures are designed for the considered group of acousto-electric plants.

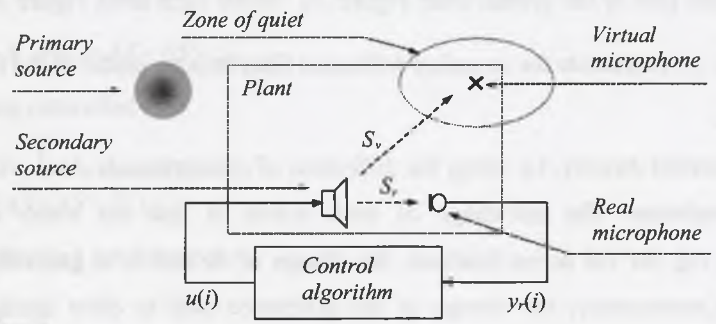

Figure 3.1 The idea of a VMC system.

3.2 Structure 1

In this section a VMC system structure, similar to that of [Rafaely_97] and [TsengRE_02] is considered as presented in Figure 3.2. However, the approach to optimal control is completely different in Subsection 3.2.1. Adaptive realisation, not addressed in the literature, is presented in Subsection 3.2.2. For this system, referred to as the VMC1 system, the controlled signal being estimate of the residual signal at the virtual microphone constitutes also the control filter input.

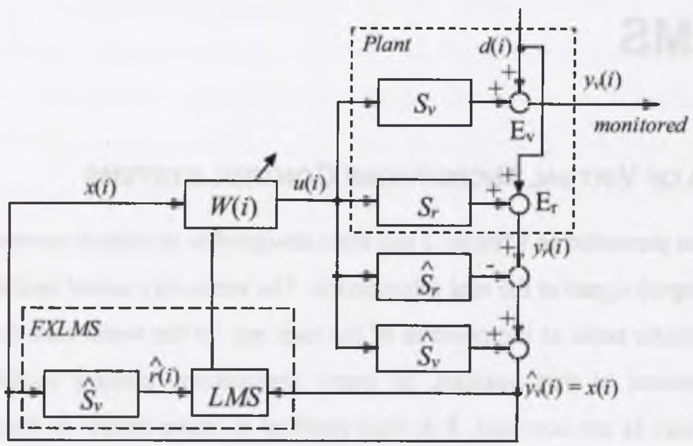

Figure 3.2 The VMC1 system with the FXLMS algorithm.

3.2.1 Optimal control

By analogy to IMC, it is convenient for analysis of optimal control to present the non-adaptive (fixed) part of the system from Figure 3.2 in the form as in Figure 3.3. The model $\widehat{\Delta S}$ in Figure 3.3 represents the so-called difference filter being a model of the difference path

$$\Delta S = S_r - S_v . \tag{3.1}$$

It can be identified directly, i.e. using the difference of measurements done with the real and virtual microphones. The advantage of such notion is that for many active control applications, e.g. for the active headrest, the change of S_r and S_v is generally in the same 'direction'. Consequently, the change of the difference path is often much smaller than changes of the paths themselves.

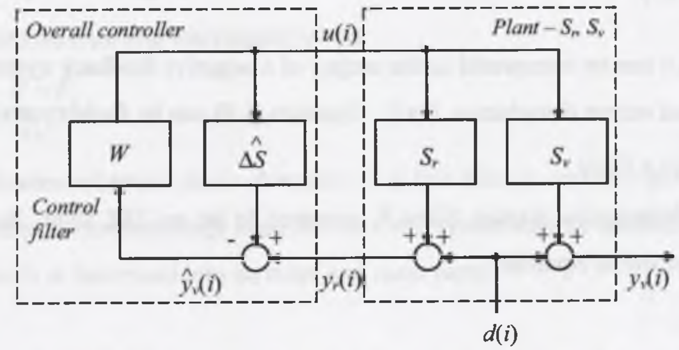

Figure 3.3 Signal flow diagram in the fixed part of the VMC1 system.

In this structure mean-square value of the estimated signal at the virtual microphone, $\hat{y}_v(i)$, is minimised. It follows from Figure 3.3 that:

$$\hat{y}_v(i) = \frac{1}{1 + W\widehat{\Delta S}} y_r(i) , \tag{3.2}$$

$$u(i) = \frac{W}{1 + W\widehat{\Delta S}} y_r(i) = -H y_r(i) , \tag{3.3}$$

$$y_r(i) = d(i) + S_r u(i) , \tag{3.4}$$

and H is the overall controller in negative feedback notation. Substituting for $u(i)$ from (3.3) into (3.4) gives

$$y_r(i) = \frac{1 + W\widehat{\Delta S}}{1 + W(\widehat{\Delta S} - S_r)} d(i) = V_r d(i) . \tag{3.5}$$

Taking (3.2) and (3.5) together and noticing that, after (3.1),

$$\widehat{\Delta S} - S_r = \hat{S}_r - S_r - \hat{S}_v = \widehat{\Delta S} - \Delta S - S_v , \tag{3.6}$$

the signal being controlled is

$$\hat{y}_v(i) = \frac{1}{1 + W(\widehat{\Delta S} - \Delta S - S_v)} d(i) . \tag{3.7}$$

Making the following substitutions:

$$\begin{cases} S_2 = \widehat{\Delta S} - \Delta S - S_v \\ y = \hat{y}_v \end{cases} \tag{3.8}$$

and taking (1.4) into account allows expressing this problem in a general compact form

$$y(i) = \frac{F}{1+WS_2} e(i) . \tag{3.9}$$

Thus, signal $y(i)$ can be interpreted as the output of a negative feedback system with plant S_2, controller W and output disturbance $Fe(i)$. Equation (3.9) can be further rewritten as

$$y(i) = -WS_2 y(i) + Fe(i) . \tag{3.10}$$

Let now the disturbance-shaping filter F, assumed to be an FIR filter, be split using the following Diophantine equation

$$F = F_1 + z^{-k} F_2 , \tag{3.11}$$

where k is the time delay of S_2 (a sampled acousto-electric path has always a time delay of one sample, at least). Degrees of the polynomials are (see also [NiederlinskiMO_95], [Pawelczyk_00a])

$$\begin{cases} \deg F_1 = k-1 \\ \deg F_2 = \deg F - k \end{cases} . \tag{3.12}$$

The assumption about FIR structure of F is only for notational convenience and it does not restrict the considerations. If F were a rational transfer function, both sides of (3.10) could be multiplied by its stable denominator and only the numerator would be split. From these equations it follows

$$y(i) = \left[-WS_2 y(i) + z^{-k} F_2 e(i)\right] + \left[F_1 e(i)\right], \tag{3.13}$$

where the two components separated by squared brackets are uncorrelated because S_2 contains a delay of k samples and W is without delay. Therefore, the cost function (2.7) can be expressed as

$$L = E\left\{\left[-WS_2 y(i) + z^{-k} F_2 e(i)\right]^2\right\} + E\left\{\left[F_1 e(i)\right]^2\right\}, \tag{3.14}$$

where the second component on the RHS is unable to be controlled. Hence, the optimal filter minimising the cost function is determined by

$$W_{opt} = \arg\min_W E\left\{\left[-WS_2 y(i) + z^{-k} F_2 e(i)\right]^2\right\}. \tag{3.15}$$

Substituting for $y(i)$ from (3.9) gives

$$W_{opt} = \arg\min_W E\left\{\left[\left(-WS_2 \frac{F}{1+WS_2} + z^{-k} F_2\right) e(i)\right]^2\right\}. \tag{3.16}$$

Taking the first derivative of the term within the curly brackets and making it zero results in the expression that can be used to derive the optimal filter:

$$-W_{opt} S_2 F + z^{-k} F_2 + z^{-k} F_2 W_{opt} S_2 = 0 . \tag{3.17}$$

Taking (3.11) into account and rearranging yields

$$W_{opt} = \frac{z^{-k} F_2}{S_2 F_1} = \frac{F - F_1}{S_2 F_1} . \tag{3.18}$$

However, due to non-minimum phase character of S_2 this filter is unstable and non-causal. To solve this problem the methodology used for the IMC system can be applied. Therefore, the transfer function S_2 is factorised into an inner and outer parts

$$S_2 = S_2^{(i)} S_2^{(o)} . \tag{3.19}$$

Then, applying the factorisation to (3.17) the (sub-) optimal stable and causal control filter can be derived

$$W_{opt+} = \frac{1}{F_1 S_2^{(o)}} \left\{ \frac{F - F_1}{S_2^{(i)}} \right\}_+ \tag{3.20}$$

and the optimal estimated residual signal at the virtual microphone, (3.9), is

$$y(i)_{opt} = \frac{F}{1 + \frac{S_2^{(i)}}{F_1}\left\{\frac{F-F_1}{S_2^{(i)}}\right\}_+} e(i) . \tag{3.21}$$

If the causality condition in (3.21) were removed the optimal signal would be

$$y(i)_{opt|cond} = F_1 e(i) \tag{3.22}$$

and it would have the smaller mean-square value the smaller the time delay of the transfer function S_2 were (see (3.8)). This coincides with the result of Minimum Variance Control for minimum phase plants [NiederlinskiMO_95], [Pawelczyk_00a].

The user is interested in noise control at the ear (virtual microphone) located often at a position different than that where the models have been acquired. Therefore, it is necessary to examine the Virtual-Output Sensitivity Function, V_v. Combining (3.3), (3.5) and (3.8) results in

$$u(i) = \frac{W}{1+WS_2} d(i) . \tag{3.23}$$

It follows from Figure 3.3 that

$$y_v(i) = d(i) + S_v u(i) . \tag{3.24}$$

Taking (3.23) and (3.24) together gives finally

$$y_v(i)=\frac{1+W(S_2+S_v)}{1+WS_2}d(i)=\frac{1+W\left(\hat{\Delta S}-\Delta S\right)}{1+W\left(\hat{\Delta S}-\Delta S-S_v\right)}d(i)=V_v d(i). \tag{3.25}$$

For stability of the system the following characteristic equation (see (3.8))

$$1+W\left(\hat{\Delta S}-\Delta S-S_v\right)=0 \tag{3.26}$$

cannot have unstable zeros or $W(\hat{\Delta S}-\Delta S-S_v)$ cannot encircle the Nyquist point, assuming the control filter is stable. Hence, even if the modelling error, $\hat{\Delta S}-\Delta S$, of the difference path is negligible, the limitation is still restrictive due to S_v (for comparison see the condition for the IMC system, (2.42)).

3.2.2 ADAPTIVE CONTROL

For the adaptive VMC1 system, control filter parameters are updated according to (2.67), where $\underline{\hat{s}}=\underline{\hat{s}}_v$, $y(i)=x(i)$ and the reference signal is estimated as

$$x(i)=\hat{y}_v(i)=y_r(i)-\underline{\hat{\Delta s}}^T\underline{u}(i) \tag{3.27}$$

($\underline{\hat{\Delta s}}$ is a vector of impulse response parameters of the difference filter).

It is convenient for analysis to redraw the system from Figure 3.2 to a feedforward-type structure with input $d(i)$, similarly as in Figure 2.10.

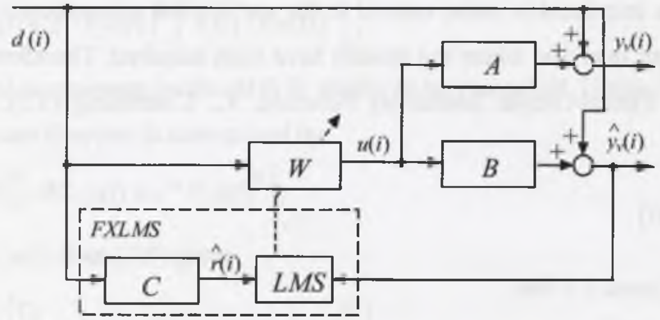

Figure 3.4 Adaptive feedforward-type structure.

According to the diagram from Figure 3.4:

$$y_v(i)=(1+AW)d(i), \tag{3.28}$$

$$\hat{y}_v(i)=(1+BW)d(i), \tag{3.29}$$

$$\hat{r}(i)=Cd(i). \tag{3.30}$$

Taking (3.25) and (3.7) into account gives, respectively,

$$A=\frac{S_v}{1+W\left(\hat{\Delta S}-\Delta S-S_v\right)}, \tag{3.31}$$

$$B=-\frac{\hat{\Delta S}-\Delta S-S_v}{1+W\left(\hat{\Delta S}-\Delta S-S_v\right)}. \tag{3.32}$$

It follows from Figure 3.2 that

$$\hat{r}(i)=\hat{S}_v x(i)=\hat{S}_v\hat{y}_v(i). \tag{3.33}$$

Taking (3.7) into account yields

$$C=\frac{\hat{S}_v}{1+W\left(\hat{\Delta S}-\Delta S-S_v\right)}. \tag{3.34}$$

Finally, the block diagram from Figure 3.4 takes the form as in Figure 3.5.

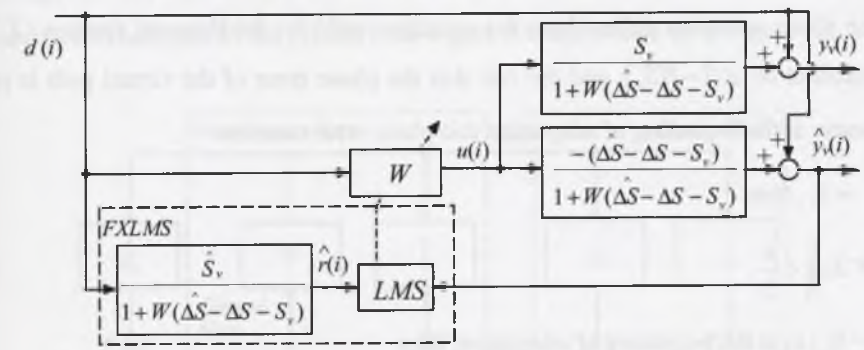

Figure 3.5 The VMC1 system in adaptive feedforward-type structure.

Then, the gradient of the control path with respect to the control filter, (2.102), can be expressed as (see (3.8) and note that $S_1=0$ here)

$$\frac{\partial B_W}{\partial W}=\frac{\Delta S-\hat{\Delta S}+S_v}{\left[1+W(\hat{\Delta S}-\Delta S-S_v)\right]^2}. \tag{3.35}$$

Following the reasoning from Section 2.3.4 and using (3.34) together with (3.35) it suffices for convergence that

$$\left|\angle\left\{\frac{\Delta S-\hat{\Delta S}+S_v}{\left[1+W(\hat{\Delta S}-\Delta S-S_v)\right]^2}\right\}-\angle\left\{\frac{\hat{S}_v}{1+W(\hat{\Delta S}-\Delta S-S_v)}\right\}\right|<\frac{\pi}{2}. \tag{3.36}$$

Rearranging, the convergence phase condition is

$$\left|\angle\left\{\Delta S-\hat{\Delta S}+S_v\right\}-\angle\left\{1+W(\hat{\Delta S}-\Delta S-S_v)\right\}-\angle\left\{\hat{S}_v\right\}\right|<\frac{\pi}{2}. \tag{3.37}$$

It has been assumed until now that the difference path is directly modelled, (3.1), and its modelling error has been considered. However, the above phase condition can also be equivalently written in terms of modelling errors of the real path by applying (3.6), so that

$$\left|\angle\left\{S_r-\hat{S}_r+\hat{S}_v\right\}-\angle\left\{1+W(\hat{S}_r-S_r-\hat{S}_v)\right\}-\angle\left\{\hat{S}_v\right\}\right|<\frac{\pi}{2}. \tag{3.38}$$

Below some special cases are considered:

a) If $\hat{\Delta S}=\Delta S$, then

$$\left|\angle\{S_v\}-\angle\left\{\hat{S}_v\right\}-\angle\{1-WS_v\}\right|<\frac{\pi}{2}. \tag{3.39}$$

Thus, the phase condition differs from the condition valid for feedforward systems (2.77) by the component of $\angle\{1-WS_v\}$ and the fact that the phase error of the virtual path is present here. Hence, at the beginning of adaptation this phase error remains.

b) If $\hat{S}_r=S_r$, then

$$\left|\angle\left\{1-W\hat{S}_v\right\}\right|<\frac{\pi}{2}. \tag{3.40}$$

c) If $W=0$, i.e. at the beginning of adaptation, then

$$\left|\angle\left\{S_r-\hat{S}_r+\hat{S}_v\right\}-\angle\left\{\hat{S}_v\right\}\right|<\frac{\pi}{2}. \tag{3.41}$$

3.3 Structure 2

In this section a VMC system structure, referred to as VMC2, modified according to Figure 3.2 is considered. The difference is that the reference signal being the control filter input is an estimate of the disturbance as in IMC, instead of the estimate of the residual signal at the

virtual microphone (Figure 3.6) [Pawelczyk_03a, 03f]. Optimal and adaptive control systems are addressed in Subsections 3.3.1 and 3.3.2, respectively.

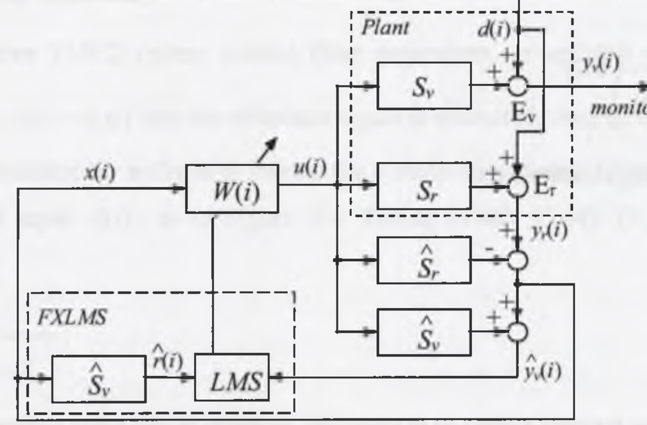

Figure 3.6 The VMC2 system with the FXLMS algorithm.

3.3.1 Optimal control

By analogy to IMC and VMC1 it is convenient for analysis of optimal control to present the non-adaptive (fixed) part of the system from Figure 3.6 in the form as in Figure 3.7.

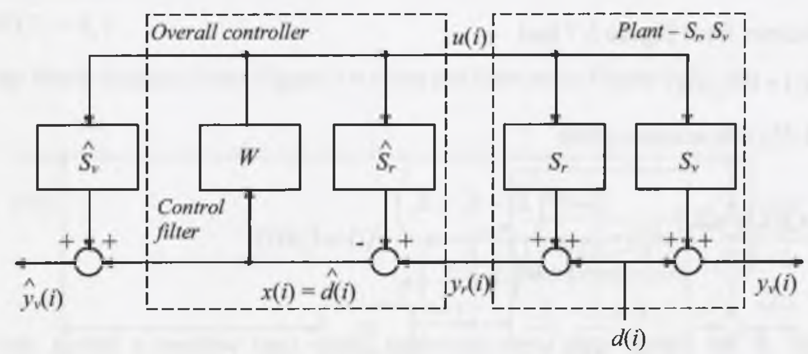

Figure 3.7 Signal flow diagram in the fixed part of the VMC2 system.

It follows from Figure 3.7 that

$$\hat{y}_v(i)=x(i)+W\hat{S}_v\,x(i), \tag{3.42}$$

$$x(i)=\frac{1}{1+W\left(\hat{S}_r-S_r\right)}d(i)\,. \tag{3.43}$$

Hence, the controlled estimated residual signal at the virtual microphone is

$$\hat{y}_v(i)=\frac{1+W\hat{S}_v}{1+W\left(\hat{S}_r-S_r\right)}d(i)\,. \tag{3.44}$$

Making the following substitutions:

$$\begin{cases}\hat{S}_v=S_1\\ \hat{S}_r-S_r=S_2\\ \hat{y}_v=y\end{cases} \tag{3.45}$$

and taking (1.4) into account allows to express this problem in the same compact form, (2.6), as for IMC and use the derivations presented in Chapter 2.

Then, the optimum causal control filter minimising the mean-square value of the system output is given by (2.17) (also by (2.26) and (2.32) for the other design approaches), the overall controller in negative feedback notation – by (2.3), and the estimated residual signal at the virtual microphone – by (2.21). For this particular structure the model of the virtual path needs to be factorised into an inner and outer parts [Pawelczyk_05a]:

$$S_1=\hat{S}_v=\hat{S}_v^{(i)}\hat{S}_v^{(o)}\,. \tag{3.46}$$

It follows from Figure 3.7 that

$$y_v(i)=d(i)+WS_vx(i)\,. \tag{3.47}$$

Taking (3.43) into account gives

$$y_v(i)=\frac{1+W(S_2+S_v)}{1+WS_2}d(i)=\frac{1+W\left(\hat{S}_r-S_r+S_v\right)}{1+W\left(\hat{S}_r-S_r\right)}d(i)=V_vd(i)\,. \tag{3.48}$$

If a model of the virtual path were minimum phase (and without a delay), the causality operator in (2.17) could be omitted and the optimal filter would be

$$W_{opt}=-\frac{1}{\hat{S}_v}\,. \tag{3.49}$$

Then, the controlled signal, (3.44), would be identically equal zero, although not the signal $y_v(i)$.

Due to similarity of the structures, stability of VMC2 is subject to the same constraints as for IMC (Section 2.2.5).

3.3.2 Adaptive control

For the adaptive VMC2 system control filter parameters are updated according to (2.67), where $\hat{\underline{s}}=\hat{\underline{s}}_v$, $y(i)=\hat{y}_v(i)$ and the reference signal is estimated using (2.90).

It is convenient for analysis to redraw the system from Figure 3.6 to a feedforward-type structure with input $d(i)$, as in Figure 3.4. Taking (3.48), (3.44), (3.29) and (3.30) into account gives

$$A=\frac{S_v}{1+W\left(\hat{S}_r-S_r\right)}\,, \tag{3.50}$$

$$B=\frac{S_r-\hat{S}_r+\hat{S}_v}{1-W\left(S_r-\hat{S}_r\right)}\,. \tag{3.51}$$

It follows from Figure 3.6 that

$$\hat{r}(i)=\hat{S}_vx(i)\,. \tag{3.52}$$

Taking (3.43) into account yields

$$C=\frac{\hat{S}_v}{1+W(\hat{S}_r-S_r)}\,. \tag{3.53}$$

Finally, the block diagram from Figure 3.4 takes the form as in Figure 3.8.

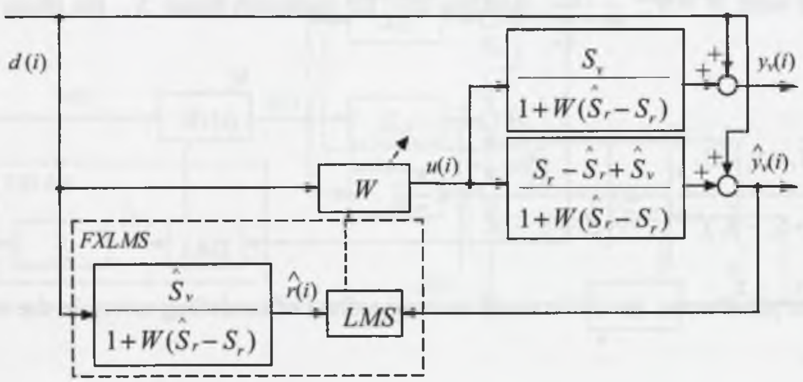

Figure 3.8 The VMC2 system in adaptive feedforward-type structure.

Then, the gradient of the control path with respect to the control filter, (2.102), can be expressed as (see (3.45))

$$\frac{\partial B_W}{\partial W} = \frac{\hat{S}_v - (\hat{S}_r - S_r)}{\left[1 + W(\hat{S}_r - S_r)\right]^2}. \tag{3.54}$$

Following the reasoning from Section 2.3.4 and using (3.53) together with (3.54) it suffices for convergence that

$$\left| \angle\left\{ \frac{\hat{S}_v - (\hat{S}_r - S_r)}{\left[1 + W(\hat{S}_r - S_r)\right]^2} \right\} - \angle\left\{ \frac{\hat{S}_v}{1 + W(\hat{S}_r - S_r)} \right\} \right| < \frac{\pi}{2}. \tag{3.55}$$

Rearranging, the convergence phase condition is

$$\left| \angle\left\{\hat{S}_v + S_r - \hat{S}_r\right\} - \angle\left\{1 + W(\hat{S}_r - S_r)\right\} - \angle\left\{\hat{S}_v\right\} \right| < \frac{\pi}{2}. \tag{3.56}$$

Some special cases are considered below:

a) If $\hat{S}_r = S_r$, then

$$\left| \angle\left\{\hat{S}_v\right\} - \angle\left\{\hat{S}_v\right\} \right| = 0. \tag{3.57}$$

Thus, the phase error is equal zero, regardless of modelling errors in the virtual path.

b) If $W = 0$, i.e. at the beginning of adaptation, then

$$\left| \angle\left\{\hat{S}_v + S_r - \hat{S}_r\right\} - \angle\left\{\hat{S}_v\right\} \right| < \frac{\pi}{2}. \tag{3.58}$$

c) If there were $W = W_{opt} = -\frac{1}{\hat{S}_v}$, possible only for minimum phase $\hat{S}_v$, the phase condition would be

$$\left| \angle\left\{ \frac{\hat{S}_v^2\left(\hat{S}_v + S_r - \hat{S}_r\right)}{(\hat{S}_v + S_r - \hat{S}_r)^2} \right\} - \angle\left\{ \frac{\hat{S}_v^2}{\hat{S}_v + S_r - \hat{S}_r} \right\} \right| < \frac{\pi}{2}. \tag{3.59}$$

Hence, the phase error, would be equal zero regardless of modelling errors in the virtual and real paths.

3.4 Structure 3

The VMC systems considered hitherto minimise mean-square value of the estimated signal at the virtual microphone. In optimal (fixed) realisation the noise model is explicitly present in the control filter in the form of disturbance-shaping filter. Plant modelling error influences also the system output. When being adaptive the systems are able to retune and in such sense they have general character. There is, however, a number of applications where the noise can be assumed stationary over a long time horizon, e.g. at the end of a ventilation duct, in some workplaces like control rooms, etc. Therefore, it is justified to design a dedicated algorithm for this type of environments.

In the algorithm considered here it is assumed that in the tuning stage (Figure 3.9) the control filter, W_t, is designed to minimise mean-square value of the signal at the virtual microphone. At the same time a signal $y'(i)$ is estimated as the difference of the signal at the real microphone and estimated disturbance filtered by an additional filter K. It is known that in a stable linear ANC system the disturbance is at least as 'rich' as the residual signal. Therefore, if the filter K of sufficient order is designed or adapted to minimise mean-square value of $y'(i)$ it 'stores' the information what the signal at the real microphone is when the noise at the virtual microphone is attenuated. In the control stage (Figure 3.10), by filtering the estimate of the disturbance this filter is used to produce a command signal to that measured by the real microphone. Then, the error signal in the form of $y'(i)$ is minimised in the mean-square sense by the control filter W_c [Pawelczyk_03f, 04a].

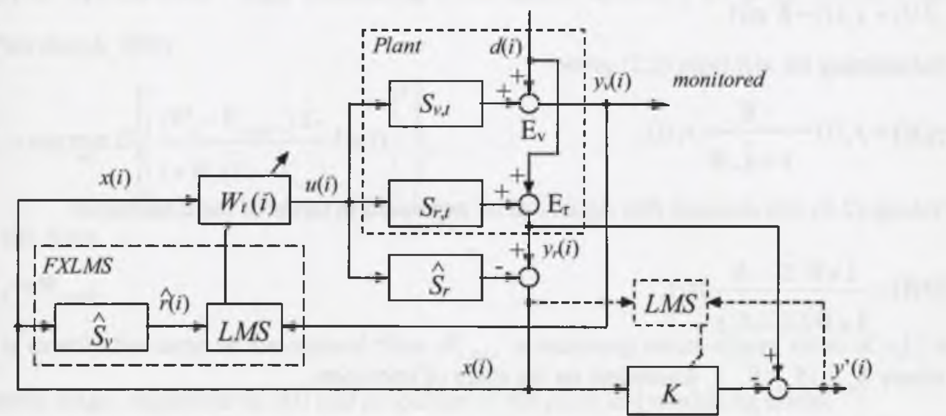

Figure 3.9 The VMC3 system with the FXLMS algorithm – tuning stage.

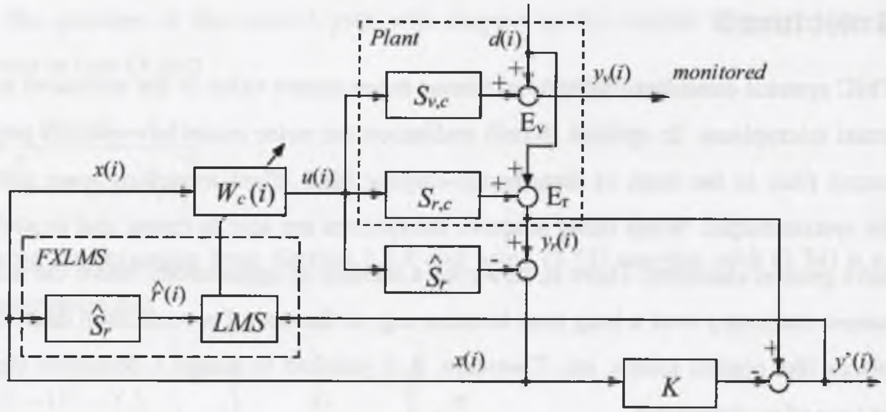

Figure 3.10 The VMC3 system with the FXLMS algorithm – control stage.

For generality, both the real and virtual paths in the tuning and control stages are distinguished to account for different responses during tuning and actual operation. The model of the real path remains the same for both stages. No model of the virtual path is used. Optimal control is considered in Subsection 3.4.1 followed by adaptive control in Subsection 3.4.2.

3.4.1 Optimal control

The main part of the system from Figure 3.9 and Figure 3.10 is analogous to the IMC system (Figure 2.1) so the signal flow diagram from Figure 2.2 remains valid. However, an additional signal, $y'(i)$, is estimated. It follows from Figure 3.9 and Figure 3.10 that

$$y'(i) = y_r(i) - K\,x(i). \tag{3.60}$$

Substituting for $x(i)$ from (2.2) gives

$$y'(i) = y_r(i) - \frac{K}{1+\hat{S}_r W}\,y_r(i). \tag{3.61}$$

Taking (2.4) into account, this signal can be expressed in terms of the disturbance

$$y'(i) = \frac{1+W\hat{S}_r - K}{1+W(\hat{S}_r - S_r)}\,d(i), \tag{3.62}$$

where $S_r \in \{S_{r,t}; S_{r,c}\}$, dependent on the stage of operation.

In the tuning stage ($S_r = S_{r,t}$, $W = W_t$) mean-square value of $y'(i)$ is minimised with the additional filter K satisfying (see also (1.4)) [Pawelczyk_05b]

$$K_{opt} = \arg\min_{K} E\left\{\left[\frac{1+W_t\hat{S}_r - K}{1+W_t(\hat{S}_r - S_{r,t})}Fe(i)\right]^2\right\}. \tag{3.63}$$

Taking the first derivative of the term within the curly brackets and making it zero results in optimal causal filter

$$K_{opt} = 1 + \hat{S}_r W_{t,opt+}. \tag{3.64}$$

Moreover, it is minimum phase no matter whether the paths and their models are minimum or non-minimum phase because the polynomial $1+\hat{S}_r W_t$ must be minimum phase for $y'(i)$ to be bounded – see (3.61) and Appendix A.1. It is assumed in (3.64) that the control filter, W_t, minimising $y_r(i)$ in the meantime is optimal and causal, i.e. $W_t = W_{t,opt+}$.

In the control stage ($S_r = S_{r,c}$, $W = W_c$, see also Figure 3.10) $K = K_{opt}$ is still valid, but W_c is designed to minimise mean-square value of a different signal, i.e. $y'(i)$. According to Figure 3.10, the following holds (see (3.62))

$$y'(i) = \frac{1+W_c\hat{S}_r - K_{opt}}{1+W_c(\hat{S}_r - S_{r,c})}\,d(i). \tag{3.65}$$

Substituting for H_{opt} from (3.64) yields

$$y'(i) = \frac{(W_c - W_{t,opt+})\hat{S}_r}{1+W_c(\hat{S}_r - S_{r,c})}\,d(i). \tag{3.66}$$

Hence, the optimal filter $W_{c,opt+}$ minimising mean-square value of $y'(i)$ in the control stage, i.e. [Pawelczyk_05b]

$$W_{c,opt} = \arg\min_{W_c} E\left\{\left[\frac{(W_c - W_{t,opt+})\hat{S}_r}{1+W_c(\hat{S}_r - S_{r,c})}Fe(i)\right]^2\right\}, \tag{3.67}$$

takes the form

$$W_{c,opt+} = W_{t,opt+}. \tag{3.68}$$

So it is exactly the same as the optimal filter $W_{t,opt+}$ minimising mean-square value of $y_r(i)$ in the tuning stage, regardless of $d(i)$ and properties of the plant and modelling errors.

Because the main part in the tuning stage is exactly the same as in the VMC2 structure, one may write (see (3.48))

$$y_v(i) = d(i) + \frac{W_t S_{v,t}}{1+W_t(\hat{S}_r - S_{r,t})} d(i) = \frac{1+W_t(\hat{S}_r - S_{r,t} + S_{v,t})}{1+W_t(\hat{S}_r - S_{r,t})} d(i) = V_t d(i). \tag{3.69}$$

Making the following substitutions:

$$\begin{cases} \hat{S}_r - S_{r,t} + S_{v,t} = S_1 \\ \hat{S}_r - S_{r,t} = S_2 \\ y_v = y \end{cases} \tag{3.70}$$

and taking (1.4) into account allows to express this problem in the same general compact form as for IMC, (2.6), and benefit from the derivation presented in Chapter 2.

Then, the optimum causal control filter minimising the mean-square value of the system output is given by (2.17) (also by (2.26) and (2.32) for the other design approaches), the overall controller in negative feedback notation – by (2.3), and the residual signal at the virtual microphone – by (2.21). For this particular structure the compound transfer function needs to be factorised into an inner and outer parts

$$S_1 = \hat{S}_r - S_{r,t} + S_{v,t} = (\hat{S}_r - S_{r,t} + S_{v,t})^{(i)} (\hat{S}_r - S_{r,t} + S_{v,t})^{(o)}. \tag{3.71}$$

Because of (3.68)) the signal at the virtual microphone, $y_v(i)$, is the same in both stages if the modelling error is also the same, so that

$$y_v(i)_{opt,c} = y_v(i)_{opt,t}. \tag{3.72}$$

Otherwise, taking (2.17), (2.19), (3.70) into account yields

$$y_v(i)_{opt,c} = \frac{1 - \frac{\hat{S}_r - S_{r,c} + S_{v,c}}{S_1^{(o)}} \left\{ \frac{F}{S_1^{(i)}} \right\}_+}{1 - \frac{(\hat{S}_r - S_{r,c})}{F S_1^{(o)}} \left\{ \frac{F}{S_1^{(i)}} \right\}_+} e(i). \tag{3.73}$$

Due to similarity of the structures, stability of VMC3 is subject to the same constraints as for IMC (Section 2.2.5).

3.4.2 ADAPTIVE CONTROL

Due to (3.68) it seems not necessary to make the control filter adaptive in the control stage. However, $W_{t,opt+}$ is sub-optimal only and the adaptivity is valuable to respond to changes in the plant paths and to make the overall system stable, i.e. to guarantee that the polynomial

$1+W_c(\hat{S}_r - S_{r,c})$ is stable.

In the tuning stage of the adaptive VMC3 system, control filter parameters are updated according to (2.67), where $\underline{\hat{s}} = \underline{\hat{s}}_v$, $y(i) = y_v(i)$ and the reference signal is estimated using (2.90). In turn, in the control stage $\underline{\hat{s}} = \underline{\hat{s}}_r$ and $y(i) = y'(i)$.

It is convenient for analysis to redraw the main part of the system from Figure 3.9 and Figure 3.10 to a feedforward-type structure with input $d(i)$ [Pawelczyk_05b]. Due to similarity to the IMC structure and bearing in mind that $y_v(i)$ is being controlled in the tuning stage the transfer function, B_t, is given by (2.95) (Figure 2.10). The transfer function C_t, by analogy to (2.98), is

$$C_t = \frac{\hat{S}_v}{1+W_t\left(\hat{S}_r - S_{r,t}\right)}. \tag{3.74}$$

Taking (3.70) into account, the gradient of the Sensitivity Function to the controlled signal with respect to the control filter, W_t, (2.102), can now be expressed as

$$\frac{\partial V_{v,t}}{\partial W_t} = \frac{\partial B_{W,t}}{\partial W_t} = \frac{S_{v,t}}{\left[1+W_t(\hat{S}_r - S_{r,t})\right]^2}. \tag{3.75}$$

Following the reasoning from Section 2.3.4 and using (3.74) together with (3.75), it suffices for convergence that

$$\left| \angle \left\{ \frac{S_{v,t}}{\left[1+W_t(\hat{S}_r - S_{r,t})\right]^2} \right\} - \angle \left\{ \frac{\hat{S}_v}{1+W_t(\hat{S}_r - S_{r,t})} \right\} \right| < \frac{\pi}{2}. \tag{3.76}$$

Rearranging, the convergence phase condition in the tuning stage is

$$\left| \angle\{S_{v,t}\} - \angle\{\hat{S}_v\} - \angle\left\{1+W_t(\hat{S}_r - S_{r,t})\right\} \right| < \frac{\pi}{2}. \tag{3.77}$$

A special case can be considered for $\hat{S}_r = S_{r,t}$, which is rather a reasonable assumption. Then, the phase condition as that for a feedforward system, (2.77), is valid with the exception that the phase error of the virtual path is present here. Filtering the reference signal by $\hat{S}_v$ in the tuning stage (Figure 3.9) is thus straightforward.

It is assumed for the control stage that the filter K has been rewritten according to (3.64) when the control filter, W_t, had converged to $W_{t,\infty}$, or K has been adapted with an additional LMS algorithm in the tuning stage (Figure 3.9). Then, the controlled signal, $y'(i)$, is given by (3.66) with $W_{t,opt+}$ replaced by $W_{t,\infty}$. Thus, the gradient of the Sensitivity Function to the currently considered controlled output, $y'(i)$, with respect to the control filter, W_c, takes the form

$$\frac{\partial V'}{\partial W_c} = \frac{\hat{S}_r\left[1+W_{t,\infty}(\hat{S}_r - S_{r,c})\right]}{\left[1+W_c(\hat{S}_r - S_{r,c})\right]^2}. \tag{3.78}$$

Following the reasoning from Section 2.3.4 again and using (2.98) together with (3.78), it suffices for convergence that

$$\left|\angle\left\{\frac{\hat{S}_r\left[1+W_{t,\infty}(\hat{S}_r - S_{r,c})\right]}{\left[1+W_c(\hat{S}_r - S_{r,c})\right]^2}\right\} - \angle\left\{\frac{\hat{S}_r}{1+W_c(\hat{S}_r - S_{r,c})}\right\}\right| < \frac{\pi}{2}. \tag{3.79}$$

Rearranging, the convergence phase condition in the control stage is

$$\left|\angle\left\{1+W_{t,\infty}\left(\hat{S}_r - S_{r,c}\right)\right\} - \angle\left\{1+W_c\left(\hat{S}_r - S_{r,c}\right)\right\}\right| < \frac{\pi}{2}. \tag{3.80}$$

Some special cases can be considered.

a). If $\hat{S}_r = S_{r,c}$ or W_c in the control stage converges to $W_{c,\infty} = W_{t,\infty}$ completely cancelling $y'(i)$, the phase error in (3.80) tends to zero.

b). If $W_c = 0$, i.e. at the beginning of adaptation, it holds

$$\left|\angle\left\{1+W_{t,\infty}(\hat{S}_r - S_{r,c})\right\}\right| < \frac{\pi}{2}. \tag{3.81}$$

Therefore, it is strongly recommended to start the adaptation in the control stage with initial condition of the control filter being final value of the updated control filter in the tuning stage, $W_{t,\infty}$.

3.5 NOISE CONTROL AT THE VIRTUAL MICROPHONE - COMMENTS

3.5.1 COMPARISON OF VMC SYSTEMS

The VMC1 system exhibits features of the classical feedback system. In turn, VMC2 and VMC3 have features similar to those of IMC. In VMC1 and VMC2 an estimate of the residual signal at the virtual microphone is directly minimised in the mean-square sense, whereas VMC3 is composed of two stages. Summarising the conditions for stability of the feedback loop ((3.26) and (2.42)) and for convergence of the adaptive algorithm ((3.37) and (3.56)) one can conclude that the VMC2 system is more appropriate to the problem of noise control than VMC1. For the data used for simulation optimal control filters in VMC1 and VMC2 respond similarly, particularly for frequencies significantly contributing to the noise (Appendix B.9). Attenuation and distribution of zones of quiet is also comparable (Appendices C.3 and C.4). However, in case of adaptive realisation VMC2 outperforms VMC1. It should be stressed here that for the FXLMS algorithm to properly update the control filter, the reference signal being the control filter input should be correlated with the disturbance. In VMC1 the reference signal is equivalent to the controlled signal. Therefore, if the algorithm tends to minimise this signal the correlation can be degraded, particularly for deterministic disturbances, what can impair the adaptation and result in increasing the output signal. Such process can be repetitive. It can be relaxed by using, e.g. the adaptive dual control synthesis [FilatovU_04].

The VMC2 and VMC3 systems are substantially different. However, an important relation between them can be found. For simplicity, one can assume that in the tuning stage of VMC3, while neglecting estimation errors, the following relations are valid:

$$\begin{cases} \hat{S}_r = S_{r,t} \\ \hat{S}_v = S_{v,t} \end{cases}. \tag{3.82}$$

Hence, the transfer function S_1 for both VMC2 and VMC3 is the same (compare (3.45) and (3.70)). Consequently, the optimal control filters in these systems are then equivalent (both in the tuning and control stages). Although the paths can differ from their models significantly in the control stage, the equations for the residual signal at the virtual microphone are also exactly the same for VMC2 and VMC3 (compare (3.48) and (3.69)). The potential of VMC3 is particularly evident in adaptive systems where the information stored in the additional filter, K, and the proper initial condition of the control filter in the control stage allow for much higher convergence rate and stable operation for substantial changes in the path responses (compare (3.56) and (3.80)). As simulation experiments demonstrate the signal $y'(i)$ in VMC3 can be attenuated to the quantization noise level even for a broadband disturbance, whereas $\hat{y}_v(i)$ in VMC2 can be then attenuated by barely a few dB. Zones of quiet are of larger dimensions for VMC3 (Appendices C.4 and C.5). The condition for stability of the structural feedback loop is the same for both systems and given by (2.43).

3.5.2 Attenuation in Terms of Sensitivity Function

Active noise control systems considered in this monograph aim generally at reducing mean-squared pressure of the acoustic noise at the desired location, i.e. at the virtual microphone [Rafaely_97]. Taking Parseval's Theorem or Wiener-Kinchine's relationship into account it can be proven that the overall attenuation of this quantity can be expressed in terms of the Virtual-Output Sensitivity Function [Pawelczyk_02b]

$$J_v = -10\log_{10}\left(\frac{\int_{-\pi}^{+\pi}\left|V_v(e^{-j\omega T_S})\right|^2 S_{dd}(e^{\omega T_S})\,d\omega T_S}{\int_{-\pi}^{+\pi} S_{dd}(e^{\omega T_S})\,d\omega T_S}\right)\ \text{[dB]}. \tag{3.83}$$

In turn, the frequency-dependent noise attenuation at the virtual microphone takes the following form

$$J_v(\omega) = -10\log_{10}\left(\frac{S_{y_v y_v}(e^{\omega T_S})}{S_{dd}(e^{\omega T_S})}\right) = -20\log_{10}\left(\left|V_v(e^{-j\omega T_S})\right|\right)\ \text{[dB]}. \tag{3.84}$$

Concluding, the smaller $\left|V_v(e^{-j\omega T_S})\right|$ over required frequency band the better attenuation of the primary noise over that band (and the smaller sensitivity of the system to changes of the path response [Horowitz_63]). Equations (3.83) and (3.84) can include SPL weighting to account for different audibility of different frequency components. Analogous conclusions can be drawn for the real microphone in terms of the Real-Output Sensitivity Function [Rafaely_97], [Pawelczyk_02b].

It has been found that the Virtual- and Real-Output Sensitivity Functions for respective control systems can be related as [Pawelczyk_05a]

$$V_v = V_r(1+\delta V), \tag{3.85}$$

where

- VMC1:

$$\delta V = \frac{(S_v - S_r)W}{1+\Delta\hat{S}W} = -\frac{\Delta S W}{1+\Delta\hat{S}W}, \tag{3.86}$$

- IMC, VMC2, VMC3:

$$\delta V = \frac{(S_v - S_r)W}{1+\hat{S}_r W} = -\frac{\Delta S W}{1+\hat{S}_r W}. \tag{3.87}$$

In the above equations δV can be interpreted as the multiplicative change of the Real-Output Sensitivity Function due to the distance between the real and virtual microphones. Taking (3.84) and (3.85) into account the frequency-dependent attenuation at the virtual microphone can be expressed as

$$J_v(\omega) = -20\log_{10}\left(\left|V_r(e^{-j\omega T_S})\right|\cdot\left|1+\delta V(e^{-j\omega T_S})\right|\right) = J_r(\omega) - 20\log_{10}\left(\left|1+\delta V(e^{-j\omega T_S})\right|\right). \tag{3.88}$$

Thus the term $-20\log_{10}\left(\left|1+\delta V(e^{-j\omega T_S})\right|\right)$ can be treated as the spatial attenuation gradient (due to change of the virtual path) [Pawelczyk_05c].

3.5.3 Alternative Design Methodology

All the optimal causal and stable control filters designed above depend on the disturbance. Therefore, they are valid only for (wide-sense) stationary noise. If the noise changes, parameters of the filters must be recalculated. Global minimisation of the respective Sensitivity Function mapping the disturbance to the controlled output, $y(i)$, leads to non-causal and unstable filters due to properties of the acousto-electric paths. One of the solutions to cope with varying disturbances is to consider a general broadband disturbance (1.4) modelled as a white noise shaped by a band-pass disturbance-shaping filter. This filter can be a spectral factor (1.5) of an assumed PSD of rectangular shape covering frequency band of interest. Presence of such a filter in all optimal control filters would allow controlling noise of dominating components located in the assumed frequency band. This can also be interpreted as weighting the Sensitivity Function [MorariZ_89]. Another solution to control noise over an assumed frequency band has been presented and thoroughly analysed in [Pawelczyk_04b, 05c] for the VMC1 system. However, it does not coincide with the main design methodology used in this research and, therefore, it is only briefly characterised below.

Taking advantage of (3.84) and using (3.7), the performance criterion is defined as

$$\max_{\underline{w}} L(\underline{w}) = \max_{\underline{w}}\left\{\frac{1}{n_u - n_l + 1}\sum_{n=n_l}^{n_u} 20\log_{10}\left|1+W(n)\left(\Delta\hat{S}(n) - \Delta S(n) - S_v(n)\right)\right|\right\}. \tag{3.89}$$

In this expression n is the frequency bin number, $\underline{w}$ is the vector of impulse response parameters of W, and indices n_l and n_u denote bin numbers representing lower and upper bounds, respectively, of the assumed frequency band. The following constraints are also imposed for:

- stability margin

$$20\log_{10}\left|W(n_\pi)\left(\hat{\Delta S}(n_\pi)-\Delta S(n_\pi)-S_v(n_\pi)\right)\right|\le-\chi,\ \varphi(n_\pi)=-\pi \tag{3.90}$$

- acceptable noise reinforcement above required frequency band

$$\min_{\underline{w}}\left\{20\log_{10}\left|1+W(n)\left(\hat{\Delta S}(n)-\Delta S(n)-S_v(n)\right)\right|\right\}\ge J_{\min,u},\ n=n_u+1,n_u+2,..,n_{\max} \tag{3.91}$$

- acceptable noise reinforcement below required frequency band

$$\min_{\underline{w}}\left\{20\log_{10}\left|1+W(n)\left(\hat{\Delta S}(n)-\Delta S(n)-S_v(n)\right)\right|\right\}\ge J_{\min,l},\ n=1,2,..,n_l-1. \tag{3.92}$$

Parameter n_π denotes the frequency bin number for which the phase of the open-loop system equals $-\pi$, $n_{\max}$ represents the highest monitored frequency, $\chi_{\min}>0$ (in [dB]) stands for the stability margin, and $J_{\min,u}<0$ and $J_{\min,l}<0$ (both in [dB]) limit noise reinforcement beyond the assumed frequency band. Summing up attenuations for subsequent frequencies in (3.89) and defining the stability constraint by a scalar stability margin (3.90) instead of using the uncertainty description makes the requirements milder than in classical H_∞ or mixed H_2/H_∞ designs presented in [Rafaely_97], [RafaelyGE_97], [TsengRE_02] (for known PSD estimate of the disturbance). This allows to find a stable and causal control filter of a simpler structure. The stability margin, $\chi_{\min}$ in (3.90) is, however, suggested to be determined by analysing the uncertainties. The problem defined by equations (3.89)-(3.92) can be simplified if under nominal conditions the difference filter is perfect, $\hat{\Delta S}=\Delta S$, or the modelling of the real path is perfect, $\hat{S}_r=S_r$ (see (3.6)).

Due to the general disturbance it is important for this algorithm to reduce the delay of the discretised plant. This can be obtained when executing the algorithm in the continuous-time domain, where the analogue filters from Figure 1.2 strongly contributing to the overall phase lag are absent. Further reduction of the delay can be obtained by decreasing the distance between the loudspeaker and microphones. Therefore, the above algorithm has been verified in the continuous-time domain to control noise over a wide frequency band in the VMC1

structure for a phone [Pawelczyk_04b, 05c], in a classical feedback structure for an active headset system [Pawelczyk_02b, 02g], and in a hybrid structure together with discrete-time adaptive algorithm for an active headset system [PawelczykW_01], [Pawelczyk_02d, 03b]. The assumptions made have been satisfied and high performance obtained.

The same strategy could also be applied for the VMC2 structure although the equations (3.89)-(3.92) would be more complicated because of the form of (3.44).

3.5.4 Tracking a desired signal

All the presented structures and algorithms have been designed under the assumption that the desired (command) signal at the position of the ear is zero, what denotes silence. In some applications the desired signal should be, however, different from zero and correspond to transmitted voice, music, warning or alarming signal, etc. The closed-loop system modifies response from the loudspeaker to the user ear and, as experiments show, makes the signal not understandable. Therefore, a feedforward filter shaping the desired signal and compensating for influence of the control algorithm, thereby improving intelligibility of the transmitted sound should be employed. The filter should be designed as the inverse of the transfer function from the desired signal to the output signal at the virtual microphone. It can be expected that for active control applications such filter is unstable and non-minimum phase. However, if there is no acoustic interference with the transmitted voice, as e.g. for a phone, phase response of the filter is not important. Then, spectral factorisation can be performed, both on numerator and denominator, giving stable and minimum phase filter. Details on design of such filter have been presented in [Pawelczyk_04b, 05c].

3.5.5 Noise control at a larger distance

It has been assumed in Chapter 1 that the distance between the real and virtual microphones is much less than the smallest wavelength in the disturbance. To the author knowledge, such assumption constitutes the explicit or implicit basis of any VMC system designs reported in the literature, e.g. [Rafaely_97], [RafaelyGE_97], [Elliott_01], [TsengRE_02], [HolmbergRS_02]. It implies that the primary noise at these microphones can be considered the same as in (1.3). If the distance were larger the primary noise at the real and virtual microphones could differ significantly. Therefore, a filter mapping the noise at the real microphone to that at the virtual microphone should be used

$$d_v(i)=F_v d_r(i)\,. \tag{3.93}$$

Then, it would appear as a component of any Virtual-Output Sensitivity function discussed in this chapter. Relation (3.93) has been addressed in [GarciaEB_96], [RoureA_99] and [TsengRE_02]. However, the authors admit that such filter depends on the acoustic environment, and therefore it is difficult to be found in general case. To illustrate this problem it suffices to consider a very practical example, where the direct acoustic wave generated by the noise source dominates over reflected waves at the positions of the real and virtual microphones, i.e. the source and the microphones are closer than the reverberation distance [Rafaely_01]. Then, if the real microphone is closer to the primary source, the noise at the virtual microphone could be estimated with a causal filter (Figure 3.11a).

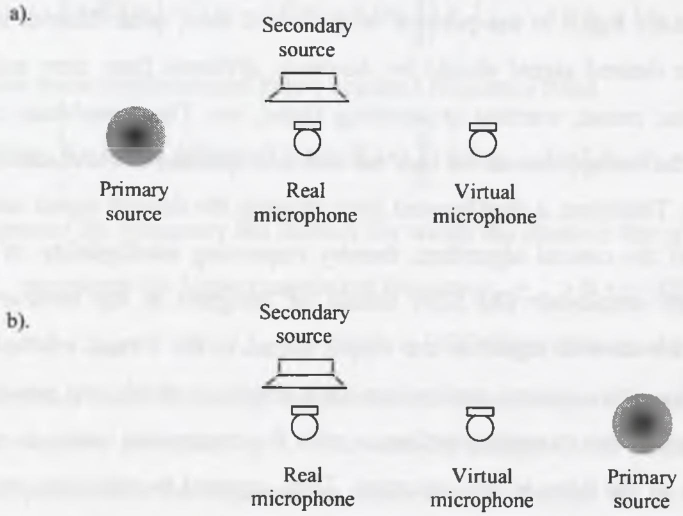

Figure 3.11 Sample arrangements of the real and virtual microphones with respect to the primary source.

If, after a while, the virtual microphone becomes located closer to the primary source (e.g. the user has turned), prediction is required to estimate the noise at the virtual microphone based on measurements from the real microphone (Figure 3.11b). In this example the disturbance-shaping filter, *F*, in (1.4) may also change what implies redesigning the optimal VMC systems. However, adaptive systems are immune to this problem. In turn, change of the F_v filter affects estimate of the residual signal at the virtual microphone controlled in the VMC1 and VMC2 systems, both in optimal and adaptive realisations

$$\hat{y}_v(i) = F_v\left(y_r(i) - \hat{S}_r u(i) \right) + \hat{S}_v u(i) . \tag{3.94}$$

In case of the VMC3 system the tuning stage should be repeated.

In another example a reverberant enclosure can be considered. Then, mapping the disturbance for a larger distance between the real and virtual microphones may be subject to significant errors degrading performance of the control systems [NelsonE_94]. To overcome this problem an array of closely spaced real microphones might be used to estimate the sound pressure level (and/or particle velocity, see Section 1.3) at the virtual microphone using a forward-difference prediction method [KestellCH_99, 00, 01], [KestellHC_00], [MunnCHK_02], [Cazzolato_02]. To cope with varying acoustic environment the microphone weights can be adapted. However, the authors of this concept limit the experiments to very small distances from the array, e.g. 100 mm for a broadband noise of frequencies up to 300 Hz, what corresponds to about one-tenth of the largest wavelength [Cazzolato_02]. The authors claim that this method has also the potential to predict noise at the virtual microphone if it is placed upstream from the microphone array (compare Figure 3.11b), although it is eased up, in fact, by the small distance.

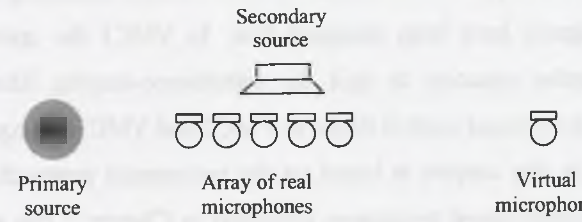

Figure 3.12 Employment of array of real microphones to estimate noise at the virtual microphone.

Concluding the above analysis, the idea of VMC systems is a powerful tool for generating zones of quiet at desired locations for the considered group of acousto-electric plants. If high attenuation is required at a larger distance from the secondary source it is suggested to provide the user with a wireless real microphone and use the designed systems to shift the zones by a shorter distance. It is also worth stressing here that 'small distance' is a relative term referring to acoustic wavelength of the noise. For low-frequency industrial noises generates by some devices the zones can be successfully shifted by more than 1 m. However, there is additional limitation. A larger distance between the primary source and the microphones, even the wireless ones, results in a larger discrete-time delay and thereby poorer performance for broadband broadband noise.

3.6 Summary

In this chapter Virtual Microphone Control systems have been designed in three different structures. The first one, VMC1, has the form of classical feedback with the controlled signal being the control filter input. The second, VMC2, and the third, VMC3, systems are similar to the Internal Model Control system, where estimate of the disturbance drives the control filter. Therefore, if the real path is well modelled these systems exhibit features of the feedforward system and therefore suitable design methods have been applied. The third structure has been equipped with an additional filter that stores knowledge about the noise being controlled together with the plant and is used to produce the command signal for the output measured by the real microphone. This structure has been designed to cope with stationary noise better. In turn, in VMC1 and VMC2 an estimate of the residual signal at the virtual microphone is controlled.

For all the VMC systems the optimal control filters minimising mean-square value of the considered signals have been designed first. In VMC1 the optimal solution requires solving a Diophantine equation to split the disturbance-shaping filter. Assuming lack of modelling errors the optimal control filters in VMC2 and VMC3 are equivalent. Although the design presented in this chapter is based on the polynomial approach, both the frequency-domain and correlation-based techniques presented in Chapter 2 can also be applied taking advantage of the general notation. Moreover, the stability analysis methodology of Chapter 2 remains valid.

Next, the adaptive VMC systems that update control filter parameters with the FXLMS algorithm have been considered. Similarly as in Chapter 2 convergence phase conditions have been derived. It has been emphasised that the adaptive VMC1 system can operate less effectively than the other systems. This is a result of the fact that the correlation between the control filter input and the disturbance becomes degraded for VMC1 when the adaptive algorithm converges. The VMC2 and VMC3 systems are immune to this problem provided the modelling of the real path is sufficiently good. The convergence condition for VMC3 is, however, weaker than that for VMC2. The considerations from Chapter 2 concerning modifications of the FXLMS algorithm remain valid. Also the conclusions about dependence of the convergence time on the convergence coefficient are similar (Appendix B.8).

Finally, the problem of noise control at the virtual microphone has been summarised. Equations for the spatial attenuation gradient due to change of the virtual path have been derived and alternative design methodology, particularly useful for continuous-time systems,

has been briefly described. It has been shown that the optimal system efficiently controlling non-stationary noise can be designed provided frequency band of the noise is known. The problem of tracking a desired signal, e.g. guaranteeing intelligibility of the transmitted speech has also been addressed. A special feedforward filter compensating for influence of the control loop should be designed in such case. The chapter has been finished with discussion of noise control at a distance larger than assumed in Chapter 1. In this case the primary noise at the real and virtual microphones cannot be considered the same and a filter mapping the noise from one position to another should be used in the design. It has been stressed that due to physical aspects it is difficult to find such a filter for general case. Moreover, both optimal and adaptive control systems should be redesigned even in case of change of position of the primary source with respect to the microphones. Even application of an array of real microphones does not solve the problem.

CHAPTER 4

MULTI-CHANNEL CONTROL SYSTEMS

4.1 MAIN ASSUMPTIONS

For many active noise control applications the use of a single pair of microphone and loudspeaker does not suffice to obtain satisfactory performance, i.e. generate a zone of quiet of acceptable dimensions [NelsonE_94]. Moreover, for some applications, presence of an obstacle, e.g. the head in an active headrest system, constitutes a barrier for the zone of quiet at one side to propagate to the other side. Therefore, more microphones and loudspeakers are often necessary. In the most general case a coupling between subsequent pairs (channels) should be taken into account resulting in a multi-channel system referred to also as the multi-input multi-output (MIMO) system.

Let the following notation be introduced:

- G – the number of real and virtual microphones (plant outputs),
- I – the number of secondary sources (plant inputs).

A sample plant with $G = I = 2$ is presented in Figure 4.1.

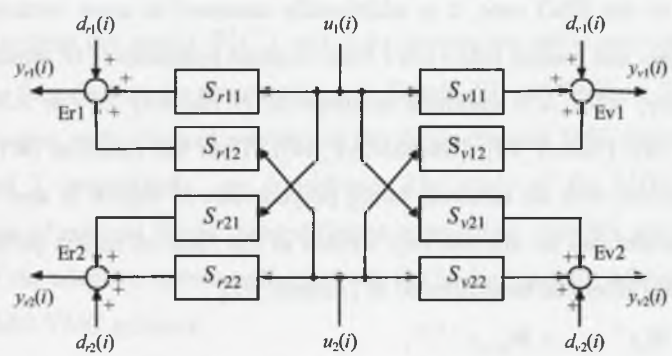

Figure 4.1 A plant with two inputs, and two real and two virtual outputs.

Rational transfer functions of the real and virtual paths can be grouped together in polynomial matrices, $\mathbf{S}_r(z^{-1})$ and $\mathbf{S}_v(z^{-1})$, respectively, of dimension G x I:

$$\mathbf{S}_r(z^{-1})=\begin{bmatrix} S_{r11}(z^{-1}) & S_{r12}(z^{-1}) & \cdots & S_{r1I}(z^{-1}) \\ S_{r21}(z^{-1}) & S_{r22}(z^{-1}) & \cdots & S_{r2I}(z^{-1}) \\ \vdots & \vdots & \ddots & \vdots \\ S_{rG1}(z^{-1}) & S_{rG2}(z^{-1}) & \cdots & S_{rGI}(z^{-1}) \end{bmatrix},$$

$$\mathbf{S}_v(z^{-1})=\begin{bmatrix} S_{v11}(z^{-1}) & S_{v12}(z^{-1}) & \cdots & S_{v1I}(z^{-1}) \\ S_{v21}(z^{-1}) & S_{v22}(z^{-1}) & \cdots & S_{v2I}(z^{-1}) \\ \vdots & \vdots & \ddots & \vdots \\ S_{vG1}(z^{-1}) & S_{vG2}(z^{-1}) & \cdots & S_{vGI}(z^{-1}) \end{bmatrix}. \tag{4.1}$$

Model matrices of corresponding paths are indicated by hats. Theoretically, a more general case could be considered where the number of real microphones were different than the number of virtual microphones. This would, however, complicate description of the MIMO systems. Particularly for the VMC systems application-specific transform matrices should be developed to map signals measured by the real microphones to signals at the virtual microphones (Chapter 3). On the other hand, practical importance of such considerations is rather moderate.

Control filters are grouped together in matrix $\mathbf{W}(z^{-1})$ of dimension I x G, built in a similar way to the plant matrices, so that

$$\mathbf{W}(z^{-1})=\begin{bmatrix} W_{11}(z^{-1}) & W_{12}(z^{-1}) & \cdots & W_{1G}(z^{-1}) \\ W_{21}(z^{-1}) & W_{22}(z^{-1}) & \cdots & W_{2G}(z^{-1}) \\ \vdots & \vdots & \ddots & \vdots \\ W_{I1}(z^{-1}) & W_{I2}(z^{-1}) & \cdots & W_{IG}(z^{-1}) \end{bmatrix}. \tag{4.2}$$

Similarly to the SISO case, it is additionally assumed in some sections that both the paths, their models and control filters have finite impulse responses (FIR structure), even very long if necessary, what is a common assumption in majority of the ANC publications (e.g. [SnyderH_94], [SaitoS_96], [Michalczyk_04]). Then the matrices (4.1) and (4.2) are polynomial matrices with all elements being polynomials of degree M and N, respectively. Polynomial matrices can be alternatively written in the form of matrix polynomials which, e.g. for the control filter can be expressed as [AhlenS_91]

$$\mathbf{W}(z^{-1})=\mathbf{W}_0+\mathbf{W}_1 z^{-1}+\ ...+\mathbf{W}_{N-1}z^{-(N-1)}, \tag{4.3}$$

where $\mathbf{W}_j$ are constant matrices of filter parameters

$$\mathbf{W}_j=\begin{bmatrix} w_{11j} & w_{12j} & \cdots & w_{1Gj} \\ w_{21j} & w_{22j} & \cdots & w_{2Gj} \\ \vdots & \vdots & \ddots & \vdots \\ w_{I1j} & w_{I2j} & \cdots & w_{IGj} \end{bmatrix}. \tag{4.4}$$

Summarising, the matrix $\mathbf{W}(z^{-1})$ contains $I\cdot G\cdot N$ parameters, and matrices $\mathbf{S}_r(z^{-1})$, $\mathbf{S}_v(z^{-1})$, $\hat{\mathbf{S}}_r(z^{-1})$ and $\hat{\mathbf{S}}_v(z^{-1})$ contain $I\cdot G\cdot M$ parameters. A general plant characterised by the matrix $\mathbf{S}$ will also be used. As in single-channel systems the explicit dependence on the complex variable z^{-1} will be dropped, where it will not lead to confusion.

Depending on the number of sensors and actuators a MIMO system is [Elliott_01]:

- overdetermined (more sensors than actuators – $G > I$),
- fully-determined (the same number of sensors and actuators – $G = I$),
- underdetermined (less sensors than actuators – $G < I$).

The disturbances, if they are stochastic and wide-sense stationary, can be modelled as uncorrelated wide-sense stationary white noise sequences with unity variances filtered by a matrix of shaping filters, [Elliott_01], i.e.

$$\mathbf{d}(i)=\mathbf{F}(z^{-1})\mathbf{e}(i). \tag{4.5}$$

The matrix $\mathbf{F}(z^{-1})$ can be found by performing spectral factorisation on the PSD matrix of the disturbance [GrimbleJ_88], [NiederlinskiKF_97] (Appendix A.3)

$$\mathbf{S}_{dd}(z^{-1})=\mathbf{F}(z^{-1})\mathbf{F}^T(z)\big|_{z^{-1}=e^{-j\omega T_S}}, \tag{4.6}$$

where

$$\dim\left(\mathbf{F}(z^{-1})\right)=G\ \times\ G, \tag{4.7}$$

provided $\mathbf{S}_{dd}(e^{-j\omega T_S})$ is analytic and positive definite for all ωT_S [KailathSH_00]. The shaping filters in both the matrix $\mathbf{F}(z^{-1})$ and in its inverse are stable and causal [Elliott_01]. Methods for the factorisation are presented, e.g. in [Davis_63] and [Wilson_72].

In this chapter multi-channel versions of the single-channel IMC and VMC systems of Chapters 2 and 3, respectively, are considered. The study of the MIMO IMC system, including design of optimal filters using different approaches, stability analysis, and design and analysis of the adaptive system will constitute the background for subsequent design and analysis of MIMO VMC systems.

All the assumptions defined in Section 1.5 remain valid, accordingly.

4.2 Internal Model Control System

Multi-channel realisation of the IMC system is presented in Figure 4.2, where $\mathbf{x}(i)$, $\mathbf{u}(i)$, $\mathbf{y}_r(i), \mathbf{y}_v(i), \mathbf{d}(i)$ are vectors composed of respective signals from all the channels at time instant i, e.g.

$$\mathbf{x}(i) = [x_1(i), x_2(i), ..., x_G(i)]^T . \tag{4.8}$$

Optimal IMC system is considered in Section 4.2.1, whereas adaptive control is dealt with in Section 4.2.2.

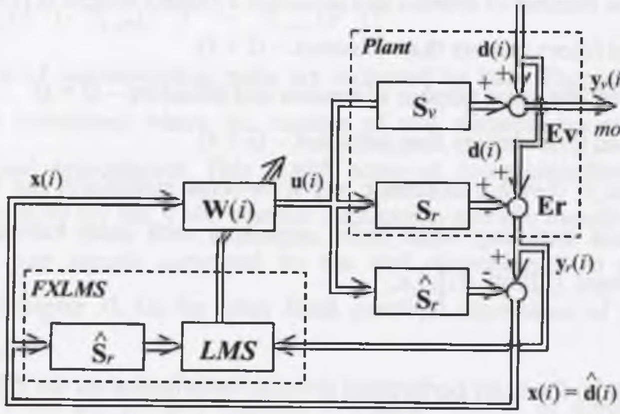

Figure 4.2 The MIMO IMC system.

4.2.1 Optimal control

It follows from Figure 4.2 that

$$\mathbf{u}(i) = \mathbf{W}\mathbf{x}(i), \tag{4.9}$$

$$\mathbf{x}(i) = \mathbf{y}_r(i) - \hat{\mathbf{S}}_r \mathbf{u}(i). \tag{4.10}$$

Substituting for $\mathbf{u}(i)$ from (4.9) and rearranging gives

$$\mathbf{x}(i) = \left[\mathbf{I}_G + \hat{\mathbf{S}}_r \mathbf{W}\right]^{-1} \mathbf{y}_r(i). \tag{4.11}$$

Combining again with (4.9) yields

$$\mathbf{u}(i) = \mathbf{W}\left[\mathbf{I}_G + \hat{\mathbf{S}}_r \mathbf{W}\right]^{-1} \mathbf{y}_r(i) = -\mathbf{H}\mathbf{y}_r(i), \tag{4.12}$$

where $\mathbf{H}$ is the I x G matrix of the overall MIMO IMC controller in the negative feedback notation and $\mathbf{I}_G$ denotes squared unity matrix of dimension G.

The residual signal at the real microphone is

$$\mathbf{y}_r(i) = \mathbf{d}(i) + \mathbf{S}_r \mathbf{u}(i). \tag{4.13}$$

Combining (4.12) and (4.13) results in

$$\mathbf{y}_r(i) = \left[\mathbf{I}_G - \mathbf{S}_r \mathbf{W}\left(\mathbf{I}_G + \hat{\mathbf{S}}_r \mathbf{W}\right)^{-1}\right]^{-1} \mathbf{d}(i). \tag{4.14}$$

Assuming the square matrix $\mathbf{I}_G + \hat{\mathbf{S}}_r \mathbf{W}$ is non-singular the following matrix algebra can be applied to (4.14):

$$\begin{aligned}\mathbf{y}_r(i) &= \left[\left(\mathbf{I}_G + \hat{\mathbf{S}}_r \mathbf{W}\right)\left(\mathbf{I}_G + \hat{\mathbf{S}}_r \mathbf{W}\right)^{-1} - \mathbf{S}_r \mathbf{W}\left(\mathbf{I}_G + \hat{\mathbf{S}}_r \mathbf{W}\right)^{-1}\right]^{-1} \mathbf{d}(i) = \\ &= \left\{\left[\mathbf{I}_G + \left(\hat{\mathbf{S}}_r - \mathbf{S}_r\right)\mathbf{W}\right]\left[\mathbf{I}_G + \hat{\mathbf{S}}_r \mathbf{W}\right]^{-1}\right\}^{-1} \mathbf{d}(i).\end{aligned} \tag{4.15}$$

Hence, finally

$$\mathbf{y}_r(i) = \left[\mathbf{I}_G + \hat{\mathbf{S}}_r \mathbf{W}\right]\left[\mathbf{I}_G + \left(\hat{\mathbf{S}}_r - \mathbf{S}_r\right)\mathbf{W}\right]^{-1} \mathbf{d}(i) = \mathbf{V}_r \mathbf{d}(i), \tag{4.16}$$

where $\mathbf{V}_r$ is the matrix Real-Output Sensitivity Function. Taking the 'complementarity constraint' into account (e.g. [MorariZ_89], [SeronBG_97]) and using similar matrix algebra the matrix Real-Output Complementary Sensitivity Function is then

$$\mathbf{T}_r = -\mathbf{S}_r \mathbf{W}\left[\mathbf{I}_G + \left(\hat{\mathbf{S}}_r - \mathbf{S}_r\right)\mathbf{W}\right]^{-1} . \tag{4.17}$$

It is convenient for further analysis to write (4.16) in the general notation as

$$\mathbf{y}(i) = (\mathbf{I}_G + \mathbf{S}_1\mathbf{W})(\mathbf{I}_G + \mathbf{S}_2\mathbf{W})^{-1}\mathbf{F}\mathbf{e}(i), \tag{4.18}$$

where

$$\begin{cases}\mathbf{S}_1 = \hat{\mathbf{S}}_r \\ \mathbf{S}_2 = \hat{\mathbf{S}}_r - \mathbf{S}_r . \\ \mathbf{y} = \mathbf{y}_r\end{cases} \tag{4.19}$$

Let the cost function be defined as

$$L = \operatorname{trace} E\left\{\mathbf{y}(i)\mathbf{y}^T(i)\right\} . \tag{4.20}$$

In the frequency domain this corresponds to

$$L_\omega = \operatorname{trace}\mathbf{S}_{yy}(e^{-j\omega T_S}) = \operatorname{trace} E\left\{\mathbf{y}(e^{-j\omega T_S})\mathbf{y}^H(e^{-j\omega T_S})\right\}, \tag{4.21}$$

where $\{.\}^H$ denotes Hermitian, i.e. complex conjugate transpose. It should be mentioned that the cost functions address a trade-off among control of the different system outputs.

4.2.1.1 Polynomial-based approach

The matrix of optimal causal control filters in the MIMO IMC system minimising (4.20) can be immediately written by taking into account results of the general analysis of the SISO IMC system presented in Chapter 2 and applying the analysis from [Elliott_01] and [MorariZ_89] (made there for a simplified MIMO system with perfect plant model):

$$\mathbf{W}_{opt+}(z^{-1}) = -\left[\mathbf{S}_1^{(o)}(z^{-1})\right]^{-1}\left\{\left[\mathbf{S}_1^{(i)}(z)\right]^T \mathbf{F}(z^{-1})\right\}_+ \mathbf{F}^{-1}(z^{-1}). \tag{4.22}$$

To calculate this matrix the following inner-outer factorisation must be performed (Appendix A.7)

$$\mathbf{S}_1(z^{-1}) = \mathbf{S}_1^{(i)}(z^{-1})\mathbf{S}_1^{(o)}(z^{-1}), \tag{4.23}$$

where, for $G \geq I$:

- $\mathbf{S}_1^{(i)}(z^{-1})$, $\mathbf{S}_1^{(o)}(z^{-1})$ and $[\mathbf{S}_1^{(o)}(z^{-1})]^{-1}$ are stable, i.e. elements of the matrices are stable polynomials,
- $$\begin{cases}\dim\left(\mathbf{S}_1^{(i)}(z^{-1})\right) = \dim\left(\mathbf{S}_1(z^{-1})\right) = G \times I, \\ \dim\left(\mathbf{S}_1^{(o)}(z^{-1})\right) = I \times I,\end{cases} \tag{4.24}$$
- $$\left[\mathbf{S}_1^{(i)}(z)\right]^T \mathbf{S}_1^{(i)}(z^{-1}) = \mathbf{I}_I, \tag{4.25}$$
- $$\left[\mathbf{S}_1^{(o)}(z)\right]^T \mathbf{S}_1^{(o)}(z^{-1}) = \mathbf{S}_1^T(z)\mathbf{S}_1(z^{-1}). \tag{4.26}$$

Relation (4.26) can be interpreted as spectral factorisation of $\mathbf{S}_1^T(z)\mathbf{S}_1(z^{-1})$ giving minimum phase causal factor $\mathbf{S}_1^{(o)}(z^{-1})$. After such factorisation has been performed, e.g. using the methods described in [Davis_63], [Wilson_72] or [MorariZ_89], the inner matrix can be easily found from (4.23) since the outer matrix is square and can be inverted if it is non-singular.

Similarly to the SISO systems (Chapter 2) the equivalent polynomial-based method of designing optimal Wiener filters with the aid of Diophantine equations and co-inner-outer factorisation of the matrix $\mathbf{S}_1$, developed by Ahlén and Sternad, can also be applied to the MIMO systems [AhlenS_91].

The residual signal at the virtual microphone of primary interest to the user is (Figure 4.2)

$$\mathbf{y}_v(i) = \mathbf{d}(i) + \mathbf{S}_v\mathbf{u}(i). \tag{4.27}$$

Taking (4.12) and (4.14) together gives

$$\mathbf{y}_v(i) = \left[\mathbf{I}_G + \left(\hat{\mathbf{S}}_r - \mathbf{S}_r + \mathbf{S}_v\right)\mathbf{W}\right]\left[\mathbf{I}_G + \left(\hat{\mathbf{S}}_r - \mathbf{S}_r\right)\mathbf{W}\right]^{-1}\mathbf{d}(i) = \mathbf{V}_v\mathbf{d}(i), \tag{4.28}$$

where $\mathbf{V}_v$ is the matrix Virtual-Output Sensitivity Function.

4.2.1.2 Frequency-domain approach

In this approach the cost function (4.21) is minimised. Similarly to the SISO system (Chapter 2) the matrices of discrete frequency responses of the shaping filters, inner and outer parts of the transfer functions, and finally causal control filters need to be calculated. The problem of spectral factorisation in the discrete frequency domain in MIMO systems based on eigenvalue / eigenvector decomposition has been considered, e.g. in [CookE_99].

4.2.1.3 Correlation-based approach

It is very difficult to express the optimal MIMO solution to the problem defined by the cost function (4.20) in terms of the matrix form using the correlation-based approach. An easier way is to present the cost function in an equivalent form as [Elliott_01]

$$L = E\left\{\mathbf{y}^T(i)\mathbf{y}(i)\right\}. \tag{4.29}$$

Similarly to the SISO case, it is assumed for the purpose of this approach that all the elements of the matrix of general transfer functions $\mathbf{S}_1$ are of FIR structure of order M. The vector of parameters of optimal causal and constrained FIR feedforward control filters has been first obtained by Whittle [Whittle_63]. For the control of general outputs given by (4.18) and (4.19), and including modelling errors, it can be expressed as

$$\mathbf{w}_{opt+} = -\left[E\left\{\hat{\mathbf{R}}^T(i)\hat{\mathbf{R}}(i)\right\}\right]^{-1} E\left\{\hat{\mathbf{R}}^T(i)\mathbf{d}(i)\right\}. \tag{4.30}$$

In this equation:

- $\mathbf{w}$ is a concatenated vector of parameters of the control filters, of length $I \cdot G \cdot N$, given by
$$\mathbf{w} = \left[\mathbf{w}_0^T\,\mathbf{w}_1^T \ldots \mathbf{w}_{N-1}^T\right]^T, \tag{4.31}$$
$$\mathbf{w}_j = \left[w_{11j}\; w_{12j} \ldots w_{1Gj}\; w_{21j} \ldots w_{IGj}\right]^T, \tag{4.32}$$
- $\mathbf{d}(i)$ is a vector of disturbances at time instant i, defined according to (4.8),

- $\mathbf{R}(i)$ is a block Toeplitz matrix, of dimension $G \,\mathrm{x}\, (I \cdot G \cdot N)$, defined as

$$\hat{\mathbf{R}}(i) = \begin{bmatrix} \hat{\mathbf{r}}_1^T(i) & \hat{\mathbf{r}}_1^T(i-1) & \cdots & \hat{\mathbf{r}}_1^T(i-N+1) \\ \hat{\mathbf{r}}_2^T(i) & \hat{\mathbf{r}}_2^T(i-1) & \cdots & \hat{\mathbf{r}}_2^T(i-N+1) \\ \vdots & \vdots & \ddots & \vdots \\ \hat{\mathbf{r}}_G^T(i) & \hat{\mathbf{r}}_G^T(i-1) & \cdots & \hat{\mathbf{r}}_G^T(i-N+1) \end{bmatrix}, \tag{4.33}$$

where

- $$\hat{\mathbf{r}}_l(i) = \left[\hat{r}_{l11}(i)\hat{r}_{l12}(i)\ldots\hat{r}_{l1G}(i)\hat{r}_{l21}(i)\ldots\hat{r}_{lIG}(i) \right]^T, \tag{4.34}$$
- $$\hat{r}_{lmj}(i) = \underline{s}_{l,lm}^T \, \underline{d}_j(i) , \tag{4.35}$$
- $$\underline{d}_j(i) = \left[d_j(i), d_j(i-1), \ldots, d_j(i-M+1) \right]^T . \tag{4.36}$$

Because of the inverse operation in (4.30) none of the filtered-disturbance signals can be perfectly correlated with another or a linear combination of other signals [Elliott_01]. Since in the considered group of acousto-electric plants the disturbances at different microphones differ practically only slightly the paths and consequently their models must differ enough. However, in this group of plants the difference can also be small. Therefore, some precautions as briefly quoted in the following subsection should be considered.

4.2.1.4 Stability and robustness of feedback MIMO systems

Let all elements of the matrix of the general plant responses $\mathbf{S}$ (G x I) and matrix of the overall negative feedback controllers $\mathbf{H}$ (I x G; for IMC see (4.12)) be assumed stable. Then, the overall MIMO control system is stable provided all roots of the determinant of the so-called 'return difference matrix', i.e.

$$\det\left[\mathbf{I}_G + \mathbf{S}\,\mathbf{H}\right] = 0 \tag{4.37}$$

lie in the unit circle [Maciejowski_89], [MorariZ_89]. Under the same assumptions the generalised Nyquist criterion requires the locus of the function

$$\det\left[\mathbf{I}_G + \mathbf{S}(e^{-j\omega T_S})\mathbf{H}(e^{-j\omega T_S})\right] \tag{4.38}$$

not to encircle the origin for ωT_S changing from $-\pi$ to π or, equivalently, locus of all the eigenvalues

$$\mathrm{eig}\left[\mathbf{S}(e^{-j\omega T_S})\mathbf{H}(e^{-j\omega T_S})\right] \tag{4.39}$$

not to encircle the Nyquist point. However, for MIMO systems there is no simple relation between the above frequency responses and gains or phases of components of the matrices. Therefore, geometrical analysis is generally impossible [Elliott_01].

Following the last interpretation of the generalised Nyquist criterion a conservative sufficient condition for stability can be drawn. It claims that the modulus of the largest eigenvalue (4.39), known as the 'spectral radius', should be less than one. This directly leads to the 'small-gain theorem':

$$\underset{\omega T_S}{\forall}\, \bar{\sigma}\left\{ \mathbf{S}(e^{-j\omega T_S})\right\}\bar{\sigma}\left\{\mathbf{H}(e^{-j\omega T_S})\right\} < 1, \tag{4.40}$$

where $\bar{\sigma}\{.\}$ stands for the largest singular value of a respective matrix [MorariZ_89], [Elliott_01].

It is convenient for stability analysis in case of changes of a general MIMO plant, $\mathbf{S}$, to express the changes in terms of the structured (parametric) uncertainty (perturbations) or, more conservatively, multiplicative unstructured output uncertainty of the nominal plant, $\mathbf{S}_0$, or the plant model, $\hat{\mathbf{S}}$, [MorariZ_89], [Elliott_01], i.e.

$$\mathbf{S}(e^{-j\omega T_S}) = \left[\mathbf{I}_G + \boldsymbol{\delta}\mathbf{S}(e^{-j\omega T_S})\right]\, \mathbf{S}_0(e^{-j\omega T_S}) . \tag{4.41}$$

Then, the sufficient and necessary condition for robust stability is given by

$$\left\| \mathbf{T}_0(e^{-j\omega T_S})\overline{\delta S}(e^{\omega T_S}) \right\|_\infty < 1, \tag{4.42}$$

where

$$\mathbf{T}_0(e^{-j\omega T_S}) = -\left[\mathbf{I}_G + \mathbf{S}_0(e^{-j\omega T_S})\mathbf{H}(e^{-j\omega T_S})\right]^{-1} \mathbf{S}_0(e^{-j\omega T_S})\mathbf{H}(e^{-j\omega T_S}) \tag{4.43}$$

is the matrix Complementary Sensitivity Function for the nominal plant, and $\overline{\delta S}(e^{\omega T_S})$ is the upper bound of the uncertainties (strictly, it is the upper bound of the largest singular value of the matrix of uncertainties, $\boldsymbol{\delta}\mathbf{S}(e^{-j\omega T_S})$). The symbol $\|\|_\infty$ denotes the H_∞ matrix norm equal to the largest of all singular values for any frequency (Appendix A.5) [MorariZ_89], [Elliott_01]. The matrix of uncertainties is a full matrix with the same dimension as $\mathbf{S}$ for unstructured uncertainty or it has a specific structure for structured uncertainties. For the IMC system, taking (4.17) into account, the condition (4.42) receives the simple form

$$\left\| \hat{\mathbf{S}}_r(e^{-j\omega T_S})\mathbf{W}(e^{-j\omega T_S})\overline{\delta S}_r(e^{\omega T_S}) \right\|_\infty < 1. \tag{4.44}$$

The robust stability condition can also be written in terms of the 'structured singular value – SSV' of the 'interconnection matrix', i.e. the matrix nominal transfer function from the output of the perturbations to their inputs [MorariZ_89]. This leads to the 'generalised small-gain theorem'. Such description gives the tightest possible bound for stability due to plant perturbations [BaiZ_04]. However, the resulting so-called μ-synthesis problem is more difficult than the above formulation.

In order to improve robustness of MIMO control system the cost function ((4.20), (4.21), (4.29)) can be modified by including a weighting on control filter parameters, e.g. [Elliott_01]

$$L = E\{\mathbf{y}^T(i)\mathbf{y}(i)\} + \beta \mathbf{w}^T\mathbf{w}. \tag{4.45}$$

In the polynomial-based approach this modifies the spectral factorisation of the disturbance, (4.6), to

$$\mathbf{F}(z^{-1})\mathbf{F}^T(z) = \mathbf{S}_{dd}(z^{-1}) + \beta \mathbf{I}_G\Big|_{z^{-1}=e^{-j\omega T_S}}, \tag{4.46}$$

and similarly in the discrete-frequency domain. In turn, in the correlation-based approach (4.30) is changed to

$$\mathbf{w}_{opt+} = -\left[E\left\{\hat{\mathbf{R}}^T(i)\hat{\mathbf{R}}(i) + \beta \mathbf{I}_{IGN}\right\}\right]^{-1} E\left\{\hat{\mathbf{R}}^T(i)\mathbf{d}(i)\right\}. \tag{4.47}$$

This solution is equivalent to adding uncorrelated white noise signals of variance β to the reference signals being the disturbances for the case considered [Orfanidis_88]. A less conservative way than (4.45) is to include control signal weighting to the cost function.

Stability of the control system can also be improved by applying additional low-pass filters to the H_2 controllers designed for perfect plant model [MorariZ_89]. Another methodology, not addressed here, is to directly design a robust controller that minimises H_∞ norm of the controlled outputs or matrix Sensitivity Function and maintains the robust constraints [SkogestadP_96]. It has been argued in [MorariZ_89] that such approach protects against large disturbance amplification at some frequencies that are possible for the H_2 controllers.

4.2.1.5 Decentralised control

From the point of view of implementation purposes and control system analysis it is sometimes convenient to perform decentralised control, in which each secondary source is individually adjusted to control noise at a given individual microphone. In this case the matrix model $\hat{\mathbf{S}}_r$ is diagonal, whereas the system matrix $\mathbf{S}_r$ can still be full. It has been shown in [ElliottB_94] and [Elliott_01] that for a simplified case of a symmetrical plant with two inputs

and two outputs ($S_{11} = S_{22}$ and $S_{12} = S_{21}$) belonging to the considered group of acousto-electric plants, and tonal disturbances such control system is stable "provided a microphone is closer to the loudspeaker controlling it than it is to the other loudspeaker". In case of multiple tones the control system can also be decoupled to independently operate on different harmonics. This is justified if the measured (feedforward system) or estimated (feedback system) reference signals are orthogonal [Elliott_01]. An extensive analysis of decentralised control systems has been provided in [MorariZ_89]. It includes conditions for stability and controllability as well as benefits of this approach, e.g. design and hardware simplicity, and higher failure tolerance.

4.2.2 ADAPTIVE CONTROL

Multi-channel version of the FXLMS algorithm presented in Chapter 2 has been developed by Elliott and co-workers in 1987 [ElliottSN_87] in a simplified form for one reference signal and a number of secondary sources. It has been named the 'Multiple error LMS algorithm'. Since that time it has been extended for a more general case of many inputs and outputs for both feedforward and feedback architectures, and some useful analyses of its properties have been performed. There have also been several practical implementations of this algorithm, e.g. to control noise in aircraft cabins [DorlingEMRS_89], [ElliottNSB_90], in 3-D enclosures [Michalczyk_04] or in the group of plants under consideration [Pawelczyk_02c, 02e, 03a, 03d, 03e, 04a], [DiegoGFP_04].

Multi-Channel FXLMS called MIMO FXLMS has the form [ElliottN_85]

$$\mathbf{w}(i+1) = \mathbf{w}(i) - \mu \hat{\mathbf{R}}^T(i)\mathbf{y}(i). \tag{4.48}$$

In this expression $\mathbf{w}(i)$ is the time-dependent concatenated vector of control filter parameters ((4.31), (4.32)). In turn, $\hat{\mathbf{R}}(i)$ is the matrix ((4.33), (4.34)) of reference signals filtered by models of plant paths

$$\hat{r}_{lmj}(i) = \hat{s}_{lm}^T \underline{x}_j(i), \tag{4.49}$$

since impulse responses of the plant paths are unknown in practice (see (2.67) for a SISO case). Under assumptions J.1-J.5 defined in Section 1.5 the sufficient condition for convergence 'of the mean' has the form

$$\mu < \frac{2\,\mathrm{Re}\left(\mathrm{eig}\, E\left\{\hat{\mathbf{R}}^T(i)\mathbf{R}(i)\right\}\right)}{\left|\mathrm{eig}\, E\left\{\hat{\mathbf{R}}^T(i)\mathbf{R}(i)\right\}\right|^2}, \tag{4.50}$$

where 'eig' denotes eigenvalues of respective matrix and $\mathbf{R}(i)$ is the matrix of reference signals filtered by plant paths [Elliott_01]. Similarly to the SISO case, if for an excited mode of the algorithm corresponding eigenvalue has negative real part, then the algorithm can diverge. So it is important to provide a reliable convergence condition addressing the modelling problem. Assuming that J.1-J.5 are satisfied, then the sufficient condition for convergence 'with probability one' of the Multi-Channel FXLMS algorithm is [WangR_99b], [Elliott_01]

$$\underset{\omega T_s}{\forall}\ \mathrm{eig}\left[\hat{\mathbf{S}}^H(e^{-j\omega T_s})\mathbf{S}(e^{-j\omega T_s}) + \mathbf{S}^H(e^{-j\omega T_s})\hat{\mathbf{S}}(e^{-j\omega T_s})\right] > 0. \tag{4.51}$$

To the author knowledge, no corresponding condition for feedback systems has been derived yet. Following the discussion from Chapter 2 the condition (4.51) can constitute only a rough approximate of actual condition for feedback systems.

To improve convergence properties in face of modelling errors and complicated dynamics of the plant a modification analogous to that of a SISO system is possible by using the cost function (4.45). Then, Multi-Channel LFXLMS (Leaky FXLMS) is obtained [KuoM_96], [Elliott_01]:

$$\mathbf{w}(i+1) = (1-\beta\mu)\mathbf{w}(i) - \mu\hat{\mathbf{R}}^T(i)\mathbf{y}(i). \tag{4.52}$$

The sufficient condition for convergence, (4.51), takes the form now

$$\underset{\omega T_s}{\forall}\ \mathrm{eig}\left[\hat{\mathbf{S}}^H(e^{-j\omega T_s})\mathbf{S}(e^{-j\omega T_s}) + \mathbf{S}^H(e^{-j\omega T_s})\hat{\mathbf{S}}(e^{-j\omega T_s}) + 2\beta\mathbf{I}_G\right] > 0, \tag{4.53}$$

under the assumptions J.1-J.3, J.5. Also the upper bound on the convergence coefficient is modified accordingly.

Convergence rate of the adaptive algorithm can be considered in terms of time constants of the algorithm modes. Similarly to the SISO system they depend on the eigenvalue spread of $E\{\hat{\mathbf{R}}^T(i)\mathbf{R}(i)\}$. In case of the MIMO system this spread can be much larger than for SISO because it has more contributors [Elliott_01], [ChenM_04]:

- spectral properties of the reference signals,
- correlation between the reference signals,

- properties of matrices of the plant and its model including dynamics of different paths and their mutual dependence.

For the considered group of acousto-electric plants the reference signals are highly correlated, e.g. they are estimates of the disturbances for IMC. Moreover, differences between responses of the plant paths are not significant. Therefore, some of the eigenvalues can be close to zero whereas some of the others are large. By introducing the regularisation (4.45) and choosing β correctly the eigenvalue spread of the regularised matrix can be substantially reduced allowing for faster response of the slow modes. Obviously, the filter weighting term in the cost function (4.45) affects the performance. However, experiments have demonstrated that the attenuation is not meaningfully degraded [KuoM_96]. Another way of speeding up the algorithm is, e.g. by distinguishing different convergence coefficients for different modes or even for different frequency components, what is particularly efficient when performing the control filter update in the frequency domain [Haykin_96], [KuoM_96].

It has been found convenient for interpretation, implementation and tuning purposes to express the Multi-Channel LFXLMS algorithm in another form using the polynomial matrices [Pawelczyk_03a, 04a]

$$\mathbf{W}(i+1) = (1-\beta\mu)\mathbf{W}(i) - \mu\left(\mathbf{Q}_{IxG} \otimes \hat{\mathbf{S}} \otimes \mathbf{Y}(i)\right)\mathbf{X}(i), \tag{4.54}$$

where

- $$\mathbf{X}(i) = [\underbrace{\mathbf{x}(i), \mathbf{x}(i), \ldots, \mathbf{x}(i)}_{G}]^T, \tag{4.55}$$
- $$\mathbf{Y}(i) = [\underbrace{\mathbf{y}(i),\ \mathbf{y}(i),\ \ldots,\ \mathbf{y}(i)}_{I}]^T, \tag{4.56}$$
- $\mathbf{Q}_{IxG}$ – is a matrix weighting models of the cross paths by coefficient q; models of the main paths are not weighted (e.g., $\mathbf{Q}_{GxG} = q\mathbf{I}_G$ for $I = G$),
- $\otimes$ – denotes a product of corresponding matrix elements or blocks,
- $\mathbf{W}(i)$ (strictly, $\mathbf{W}(z^{-1}, i)$) is the time-dependent polynomial matrix defined by (4.2),
- $\hat{\mathbf{S}}$ is the polynomial matrix of the models of general paths defined similarly to (4.1).

The weighting by $\mathbf{Q}$ has been introduced to reduce a hazardous effect that arise during simultaneous adaptation of all control filters in the MIMO control system. The leakage guarantees robustness. Additionally, convergence coefficient, μ, can be updated as in the Correlation FXLMS algorithm given by (2.84) [KuoM_96], [ShanK_98].

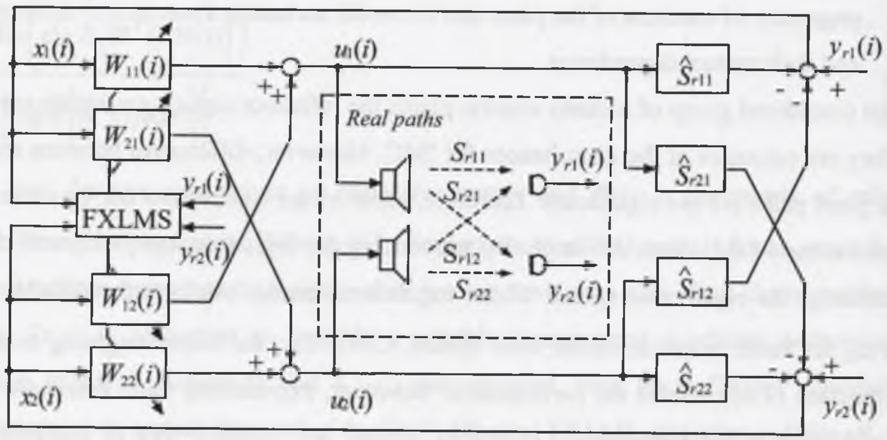

Figure 4.3 The DIDO IMC system.

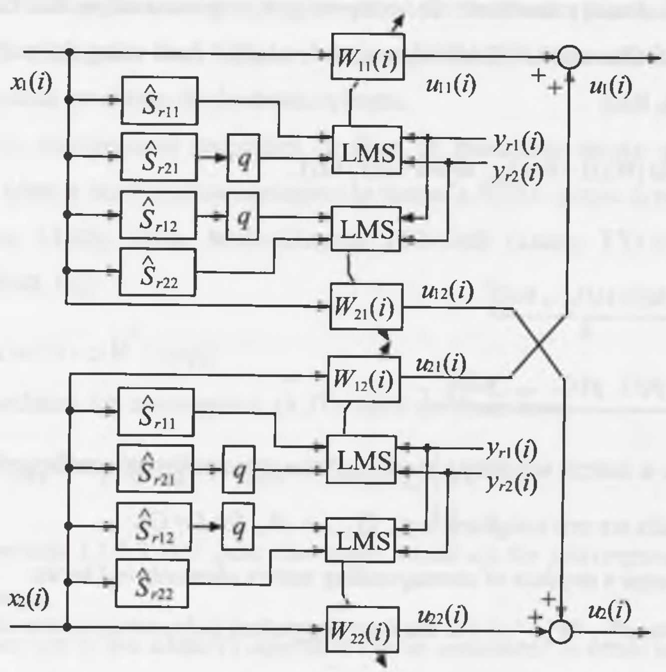

Figure 4.4 The DIDO FXLMS algorithm.

With the above notation the control law takes the form

$$\mathbf{u}(i) = \mathbf{W}(i)\mathbf{x}(i)\,, \tag{4.57}$$

and the reference signals are estimated dependent on the control system structure.

In the adaptive IMC system parameters of the control filters are updated according to (4.54), where $\hat{\mathbf{S}} = \hat{\mathbf{S}}_r$, $\mathbf{y}(i) = \mathbf{y}_r(i)$ and the reference signals are estimated as

$$\mathbf{x}(i) = \mathbf{y}_r(i) - \hat{\mathbf{S}}_r\,\mathbf{u}(i)\,. \tag{4.58}$$

For illustration, a double input – double output (DIDO) adaptive IMC system can be schematically presented as in Figure 4.3 and Figure 4.4 by adopting the diagrams from [KuoM_96].

4.3 Multi-channel Virtual Microphone Control systems

In this section multi-channel versions of the single-channel VMC systems considered in Chapter 3 are designed. All the VMC systems aim at attenuating noise at a number of positions of virtual microphones using available measurements from respective real microphones.

4.3.1 Structure 1

In the MIMO VMC1 system estimated residual signals at virtual microphones are minimised in the mean-square sense. The signals are also control filter inputs – Figure 4.5.

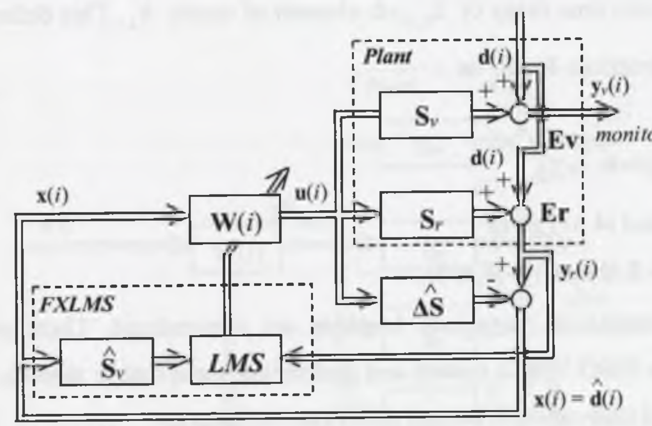

Figure 4.5 The MIMO VMC1 system.

4.3.1.1 Optimal control

For the MIMO VMC1 system the following relation can be derived

$$\mathbf{y}(i) = -\mathbf{S}_2\mathbf{W}\mathbf{y}(i) + \mathbf{F}\mathbf{e}(i)\,, \tag{4.59}$$

where

$$\begin{cases} \mathbf{S}_2 = \Delta\hat{\mathbf{S}} - \mathbf{S}_r = \Delta\hat{\mathbf{S}} - \Delta\mathbf{S} - \mathbf{S}_v \\ \mathbf{y}(i) = \hat{\mathbf{y}}_v(i) \end{cases}. \tag{4.60}$$

Applying the methodology used for SISO VMC1 the purpose is to split the matrix of disturbance-shaping filters into two matrices to obtain uncorrelated components on the RHS of (4.59). Similarly to Section 3.2.1, it is assumed that for notational convenience, without loss of generality, the disturbance-shaping filters are of FIR structure. Because control filters in matrix $\mathbf{W}$ are without delay, to the delay in each $\{j, l\}$-th element of $\mathbf{S}_2\mathbf{W}$ contribute exactly all elements of the j-th row of matrix $\mathbf{S}_2$. Therefore, let the following Diophantine equation be applied

$$\mathbf{F}(z^{-1}) = \mathbf{F}_1(z^{-1}) + \mathbf{Z} \otimes \mathbf{F}_2(z^{-1}), \tag{4.61}$$

where $\mathbf{Z}$ is the matrix of backward-shift operators:

$$\mathbf{Z} = \begin{bmatrix} z^{-k_1} & z^{-k_1} & \cdots & z^{-k_1} \\ z^{-k_2} & z^{-k_2} & \cdots & z^{-k_2} \\ \vdots & \vdots & \ddots & \vdots \\ z^{-k_G} & z^{-k_G} & \cdots & z^{-k_G} \end{bmatrix}, \tag{4.62}$$

$$k_j = \min_l k_{jl}, \tag{4.63}$$

and k_{jl} is the discrete time delay of $S_{2,jl}$-th element of matrix $\mathbf{S}_2$. This defines dimensions of elements of the matrices $\mathbf{F}_1$, $\mathbf{F}_2$ as

$$\begin{cases} \dim F_{1,jl} = k_j - 1 \\ \dim F_{2,jl} = \dim F_{jl} - k_j \end{cases}. \tag{4.64}$$

Combining (4.59) and (4.61) gives

$$\mathbf{y}(i) = [-\mathbf{S}_2\mathbf{W}\mathbf{y}(i) + \mathbf{Z} \otimes \mathbf{F}_2\mathbf{e}(i)] + [\mathbf{F}_1\mathbf{e}(i)], \tag{4.65}$$

where the two components in square brackets are uncorrelated. Then, continuing the methodology of the SISO VMC1 system and performing some matrix algebra, the matrix of optimal single-sided (sub-optimal) control filters can be found as

$$\mathbf{W}_{opt+}(z^{-1}) = \left[\mathbf{S}_2^{(o)}(z^{-1})\right]^{-1} \left\{ \left[\mathbf{S}_2^{(i)}(z)\right]^T \left[\mathbf{F}(z^{-1}) - \mathbf{F}_1(z^{-1})\right] \right\}_+ \mathbf{F}_1^{-1}(z^{-1}), \tag{4.66}$$

where the following inner-outer factorisation is used

$$\mathbf{S}_2(z^{-1}) = \mathbf{S}_2^{(i)}(z^{-1})\mathbf{S}_2^{(o)}(z^{-1}). \tag{4.67}$$

The residual signal at the virtual microphone takes the form

$$\mathbf{y}_v(i) = [\mathbf{I}_G + (\mathbf{S}_2 + \mathbf{S}_v)\mathbf{W}][\mathbf{I}_G + \mathbf{S}_2\mathbf{W}]^{-1}\mathbf{d}(i) = \mathbf{V}_v\mathbf{d}(i). \tag{4.68}$$

Stability of the MIMO VMC1 system is determined by properties of the polynomial matrix $\mathbf{I}_G + \mathbf{S}_2\mathbf{W}$ (Section 4.2.1.4).

4.3.1.2 Adaptive control

In the adaptive MIMO VMC1 system, parameters of the control filters are updated according to (4.54), where $\hat{\mathbf{S}} = \hat{\mathbf{S}}_v$,

$$\mathbf{y}(i) = \mathbf{y}_v(i) = \mathbf{y}_r(i) - \Delta\hat{\mathbf{S}}\,\mathbf{u}(i), \tag{4.69}$$

and the reference signals are estimated as the residual signals at the virtual microphones, i.e. $\mathbf{x}(i) = \mathbf{y}(i)$. For properties of the adaptive system, required assumptions and related comments see Section 4.2.2.

4.3.2 STRUCTURE 2

In the MIMO VMC2 system, estimated residual signals at virtual microphones are minimised in the mean-square sense, whereas estimates of the disturbances are the control filter inputs (Figure 4.6).

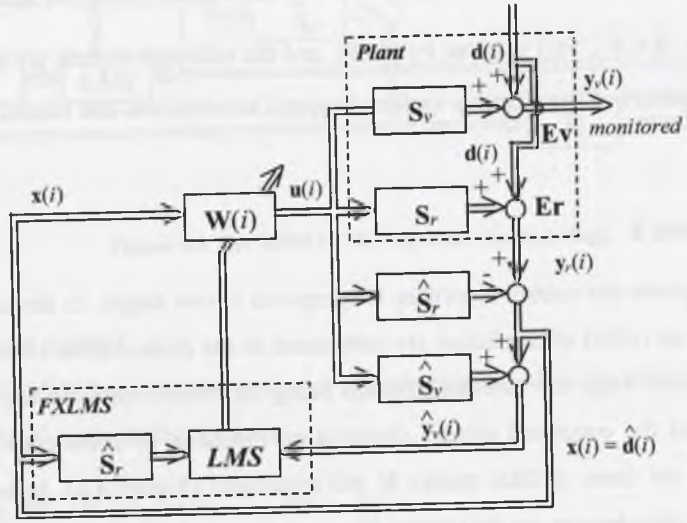

Figure 4.6 The MIMO VMC2 system.

4.3.2.1 Optimal control

For the MIMO VMC2 system the following relation can be derived:

$$\mathbf{y}(i)=\left[\mathbf{I}_G+\mathbf{S}_1\mathbf{W}\right]\left[\mathbf{I}_G+\mathbf{S}_2\mathbf{W}\right]^{-1}\mathbf{d}(i), \tag{4.70}$$

where

$$\begin{cases}\mathbf{S}_1=\hat{\mathbf{S}}_v\\ \mathbf{S}_2=\hat{\mathbf{S}}_r-\mathbf{S}_r\\ \mathbf{y}=\mathbf{y}_v\end{cases} \tag{4.71}$$

Applying the methodology used for the SISO VMC2 system and the general notation the matrix of optimal single-sided control filters, $\mathbf{W}_{opt+}$ is given by (4.22) with the inner-outer factorisation defined by (4.23). The design can also be performed using the frequency-domain or correlation-based approach as for the MIMO IMC system. The residual signal at the virtual microphone takes the form

$$\mathbf{y}_v(i)=\left[\mathbf{I}_G+(\mathbf{S}_2+\mathbf{S}_v)\mathbf{W}\right]\left[\mathbf{I}_G+\mathbf{S}_2\mathbf{W}\right]^{-1}\mathbf{d}(i)=\mathbf{V}_v\mathbf{d}(i). \tag{4.72}$$

Due to similarity of the structures, stability of MIMO VMC2 is subject to the same constraints as for MIMO IMC (Section 4.2.1.4).

4.3.2.2 Adaptive control

In the adaptive MIMO VMC2 system parameters of the control filters are updated according to (4.54), where $\hat{\mathbf{S}}=\hat{\mathbf{S}}_v$, $\mathbf{y}(i)$ is given by (4.69), and the reference signals are estimated using (4.58). For properties of the adaptive system, required assumptions and related comments see Section 4.2.2.

4.3.3 STRUCTURE 3

In the VMC3 system the control algorithm is composed of two stages. In the tuning stage the residual signals at virtual microphones are minimised in the mean-square sense (Figure 4.7). Then, in the control stage the estimated signals being differences between the signals at real microphones and the command signals obtained on the basis of knowledge gained in the tuning stage in the form of filter matrix **K** are minimised (Figure 4.8). In both stages the estimates of the disturbances are the control filter inputs.

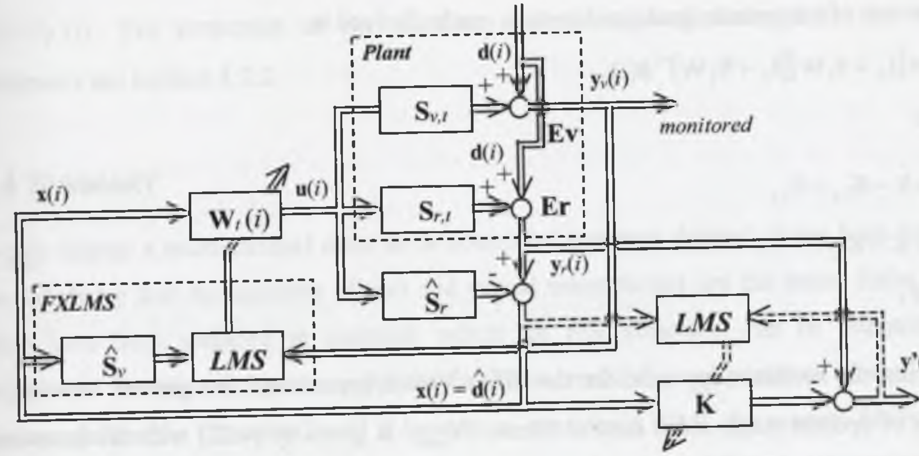

Figure 4.7 The MIMO VMC3 system – tuning stage.

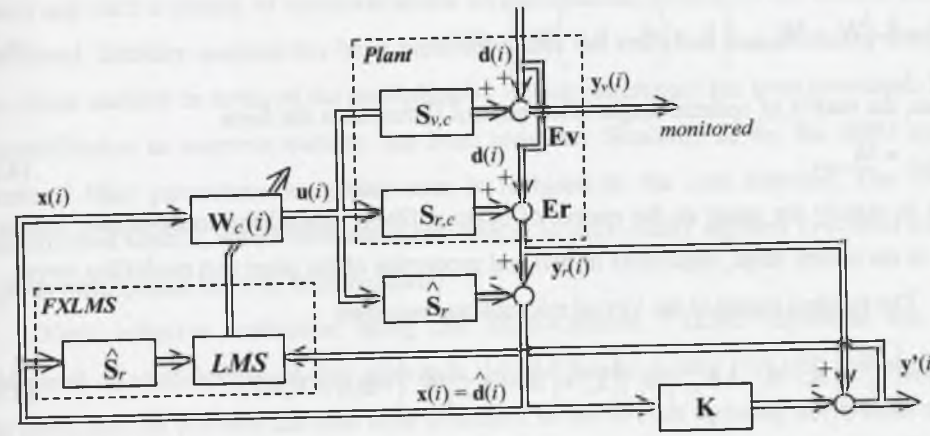

Figure 4.8 The MIMO VMC3 system – control stage.

4.3.3.1 Optimal control

For the MIMO VMC3 system the vector of signals minimised in the mean-square sense by filters in matrix **K** in the tuning stage is

$$\mathbf{y}'(i)=\left[\mathbf{I}_G+\hat{\mathbf{S}}_r\mathbf{W}_t-\mathbf{K}\right]\left[\mathbf{I}_G+\left(\hat{\mathbf{S}}_r-\mathbf{S}_{r,t}\right)\mathbf{W}_t\right]^{-1}\mathbf{d}(i). \tag{4.73}$$

Hence, assuming that the control filters in matrix $\mathbf{W}_t$ are optimal and causal

$$\mathbf{K}_{opt}=\mathbf{I}_G+\hat{\mathbf{S}}_r\mathbf{W}_{t,opt+}.$$

The vector of controlled signals in this stage can be derived as

$$\mathbf{y}(i) = [\mathbf{I}_G + \mathbf{S}_1\mathbf{W}][\mathbf{I}_G + \mathbf{S}_2\mathbf{W}]^{-1}\mathbf{d}(i), \tag{4.74}$$

where

$$\begin{cases} \mathbf{S}_1 = \hat{\mathbf{S}}_r - \mathbf{S}_{r,t} + \mathbf{S}_{v,t} \\ \mathbf{S}_2 = \hat{\mathbf{S}}_r - \mathbf{S}_{r,t} \\ \mathbf{y} = \mathbf{y}_v \end{cases} . \tag{4.75}$$

Applying the methodology used for the SISO VMC3 system and the general notation the matrix of optimal single-sided control filters, $\mathbf{W}_{t,opt+}$ is given by (4.22) with the inner-outer factorisation defined by (4.23). The design can also be performed using the frequency-domain or correlation-based approaches as presented for the MIMO IMC system.

In the control stage the following signals are controlled

$$\mathbf{y}'(i) = \hat{\mathbf{S}}_r(\mathbf{W}_c - \mathbf{W}_{t,opt+})\left[\mathbf{I}_G + \left(\hat{\mathbf{S}}_r - \mathbf{S}_{r,c}\right)\mathbf{W}_c\right]^{-1}\mathbf{d}(i). \tag{4.76}$$

Hence, the matrix of optimal single-sided control filters takes the form

$$\mathbf{W}_{c,opt+} = \mathbf{W}_{t,opt+}. \tag{4.77}$$

So it is exactly the same as the matrix of optimal filters minimising mean-square values of $\mathbf{y}_v(i)$ in the tuning stage, regardless of $\mathbf{d}(i)$ and properties of the plant and modelling errors.

The residual signal at the virtual microphone becomes

$$\mathbf{y}_v(i) = \left[\mathbf{I}_G + \left(\hat{\mathbf{S}}_r - \mathbf{S}_{r,c} + \mathbf{S}_{v,c}\right)\mathbf{W}_c\right]\left[\mathbf{I}_G + \left(\hat{\mathbf{S}}_r - \mathbf{S}_{r,c}\right)\mathbf{W}_c\right]^{-1}\mathbf{d}(i) = \mathbf{V}_v\mathbf{d}(i). \tag{4.78}$$

Due to similarity of the structures, stability of MIMO VMC3 is subject to the same constraints as for MIMO IMC (Section 4.2.1.4).

4.3.3.2 Adaptive control

In the tuning stage of the MIMO VMC3 system parameters of the control filters are updated according to (4.54), where $\hat{\mathbf{S}} = \hat{\mathbf{S}}_v$, $\mathbf{y}(i) = \mathbf{y}_v(i)$ and the reference signals are estimated using (4.58). Filters in matrix $\mathbf{K}$ can also be updated using additional Multi-Channel LMS algorithm. In the control stage, similarly, parameters of the control filters are updated according to (4.54) and the reference signals are estimated using (4.58), whereas $\hat{\mathbf{S}} = \hat{\mathbf{S}}_r$ and $\mathbf{y}(i) = \mathbf{y}'(i)$. For properties of the adaptive system, required assumptions and related comments see Section 4.2.2.

4.4 SUMMARY

In this chapter a multi-channel plant to be controlled has been defined. It has been assumed for simplicity that the numbers of real and virtual microphones are the same. Paths of the plant have been gathered in matrices, which for FIR structures can be interpreted as polynomial matrices or matrix polynomials. Then, multi-channel versions of the control systems defined in Chapters 2 and 3 have been considered. First, the control filters in the Internal Model Control system have been designed using different approaches. The polynomial and frequency-domain approaches require factorisation of the disturbance matrix PSD and inner-outer factorisation of the matrix of real path models. In turn, in the correlation-based approach a matrix of autocorrelations of disturbances filtered by the models must be calculated. Stability analysis has been performed, and the sufficient and necessary condition for robust stability in terms of the multiplicative output uncertainty has been presented. Then, a modification to improve stability has been provided. Similarly as for the SISO system, a control filter parameters weighting term is included to the cost function. The idea of decentralised control, where each secondary source is individually adjusted to control noise at a given microphone has also been recalled.

Next, adaptive realisation using the Multi-Channel FXLMS algorithm has been addressed. A modification of this algorithm, Multi-Channel Leaky FXLMS, followed from the modified cost function has also been presented in the form of updating polynomial matrix of control filters. It has been supported by weighting models of the cross paths and the Correlation modification. In case of the multi-channel systems this modification is particularly useful because no full analysis of convergence of the FXLMS algorithm operating in a feedback structure for a non-minimum phase MIMO plant including delay is available so far. Only a necessary condition for convergence and an evaluation of the upper bound of the convergence coefficient are known. It should be stressed that the conditions are stronger for the MIMO system than for the SISO system.

A general notation has been applied in the design and analysis of the IMC system to allow for application of the results to the multi-channel Virtual Microphone Control systems, mainly VMC2 and VMC3. In turn, for VMC1, similarly to its SISO version, the matrix of disturbance-shaping filters is split using a Diophantine equation including a matrix of backward-shift operators due to plant delays. Adaptive realisations of the VMC systems have also been addressed. Formal analysis of convergence requires tedious research using, e.g. the martingale method [ChenG_91]. However, as for the SISO case, convergence properties of the algorithm in the VMC1 structure are expected to be poorer than those in the VMC2 and VMC3 structures.

CHAPTER 5

LABORATORY EXPERIMENTS

5.1 ACTIVE HEADREST SYSTEM

An active headrest system is a good representative of the considered group of acousto-electric plants (Chapter 1). A prototype available for experiments consists of a frame supporting the head with four loudspeakers, G1 through G4, accompanied by two electret real microphones, Er1 and Er2. The microphones belong to the same horizontal surface as the user ears and are located between two loudspeakers for each channel [FigwerOP_02]. Figure 5.1 adopted from [Kociolek_02] shows details on geometrical arrangement of the loudspeakers and microphones. Before designing the current fixed structure preliminary experience was gained with a structure allowing easy change of position and angle of the loudspeakers and microphones [Pawelczyk_02f, 04a]. Two primary goals have been formulated during the design. First, the user cannot be annoyed at all. Therefore, the real microphones must be 'hidden' within the headrest, what additionally protects against direct contact of the user skin with the electric components. Second, the shape of the active headrest should mimic the shape of a real headrest. Therefore, the loudspeakers cannot be turned more towards the ears since in many working environments such as assembly lines or control rooms the user needs to see a wide surrounding area for safety. Obviously, such arrangement is not optimal from the control point of view and may significantly deteriorate attenuation results. Hence, similar designs are rarely met in literature (see, e.g. [HolmbergRS_02], [BrothanekJ_02]). Fortunately, a larger distance between secondary sources and microphones can contribute to obtaining larger zones of quiet [JosephEN_94]. A DS1104 board with MPC8240 processor of PowerPC 603 architecture and converters, a computer, power and voltage amplifiers, and a set of analogue anti-aliasing and reconstruction filters are also embedded in the circuit (Figure 1.2). The sampling frequency used to excite the plant inputs and measure its outputs is 2 kHz. It suffices to control most of the industrial noise components covering frequencies up to 700 Hz and guarantees sufficiently long sampling period even for advanced algorithms with high computational load. The analogue filters are 4th order Butterworth filters with cut-off frequencies set to 650 Hz. This provides sufficient signal reduction at the Nyquist frequency being half of the sampling frequency and does not introduce excessive phase lags and hence large discrete time delays. The cut-off frequencies could be higher resulting in a smaller overall discrete-time delay for considered frequencies, if the sampling frequency were higher. However, the number of control filter parameters should be then larger to allow the parameters to decay. This, together with a shorter sampling period, could make it difficult to perform calculations for some algorithms. Virtual microphones, Ev1 and Ev2, are placed during the laboratory experiments in locations where the attenuation is desired, i.e. at the user ears. For the system considered they are generally in the distance of about 150 mm from respective real microphones, whereas in most references they are much closer than 100 mm. They are used for performance monitoring or in the tuning stage of some algorithms and are not employed by control systems during actual operation. The loudspeaker generating the primary noise is located about 2100 mm in front of the headrest. Recorded sounds or generated signals have been used as the primary noise.

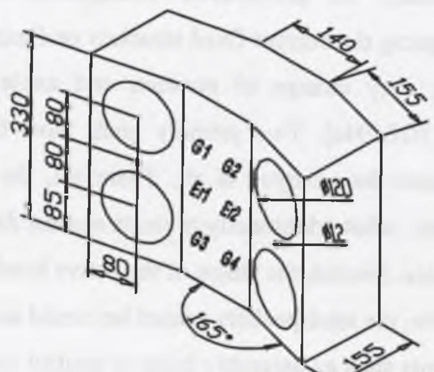

Figure 5.1 Geometrical arrangement of main components of the active headrest system used for experiments (dimensions in [mm]).

It is spectacular for this device that frequency responses of the real and virtual paths are subject to variations mainly due to a change of the head position. Positions as presented in Figure 5.2 are considered. This figure refers to the horizontal surface crossing the real microphones and the ears, which will also be called as the basic surface. The nominal position of the centre of the head is '0b'.

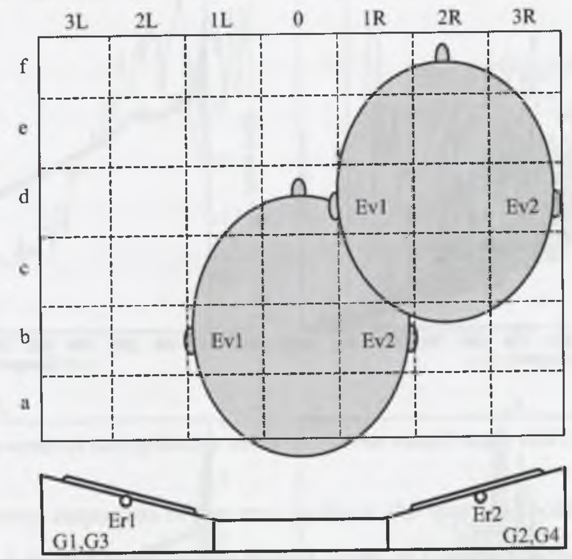

Figure 5.2 Measurement scheme; each box, of dimensions 60 x 60 mm, represents the position of the centre of the head.

Families of magnitudes and phases of frequency responses of sample paths (real main path S_{r11}, real cross path S_{r21}, and virtual main path S_{v11},) obtained for all positions on the basic surface and a surface parallel to that but located 60 mm above are presented in Figure 5.3. It is seen that the magnitude can change significantly, whereas change of phase does not exceed 2 rad for the virtual paths and 1.5 rad for the real paths, for considered frequencies. In case of optimal (fixed) control increase of the magnitude can result in violation of the stability condition, whereas decrease of the magnitude can yield poor performance. In turn, in adaptive control increase of the magnitude with a fixed convergence coefficient or phase error can make the system divergent.

Upper bounds of multiplicative uncertainties for sample main real and virtual paths are presented in Figure 5.4. It follows from this figure that large uncertainties are at frequencies below 150 Hz, where the secondary loudspeakers used operate poorly, and at frequencies above 550 Hz, fortunately less contributing to the industrial noise.

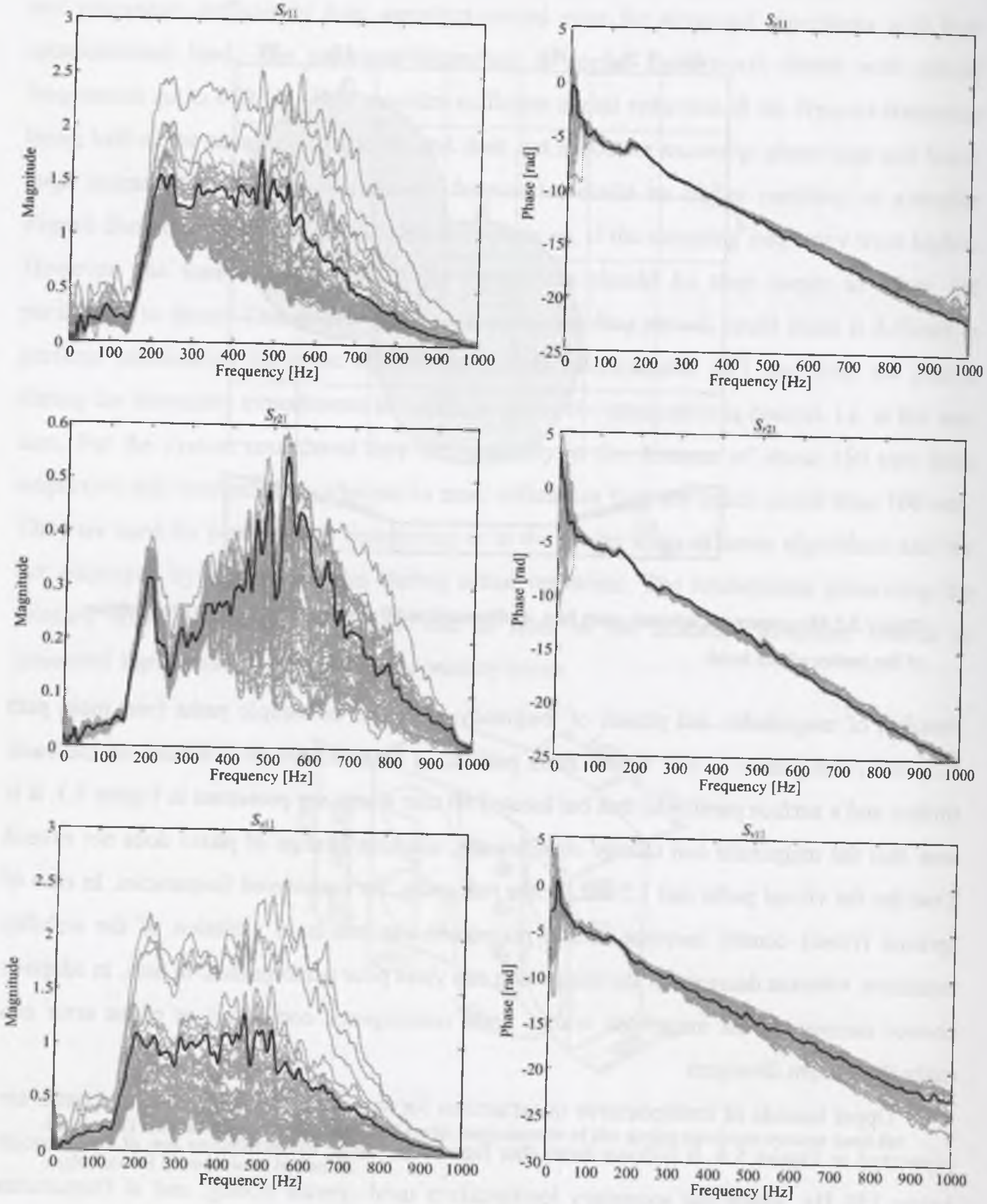

Figure 5.3 Families of frequency responses of sample paths obtained for different head positions (thick lines represent the nominal position '0b').

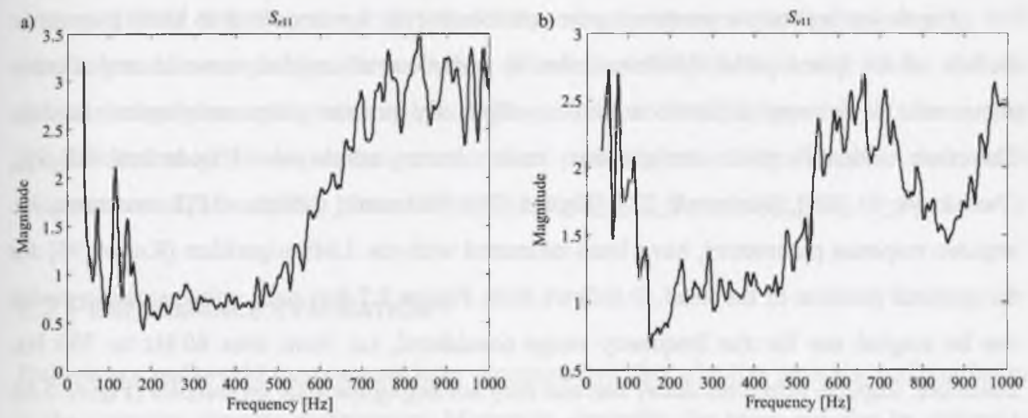

Figure 5.4 Upper bounds of multiplicative uncertainties for sample main real (a) and virtual (b) paths.

Typical frequency responses of the real paths at the nominal position of the head are presented in Figure 5.5a and those of the virtual paths in Figure 5.5b (see also Figure 5.1). Comparing the responses of the real main and cross paths (Figure 5.5a) it is seen that contribution of the cross paths to the system can be noticeable because the magnitude is approximately three-four times lower under the same settings in the electronic circuit.

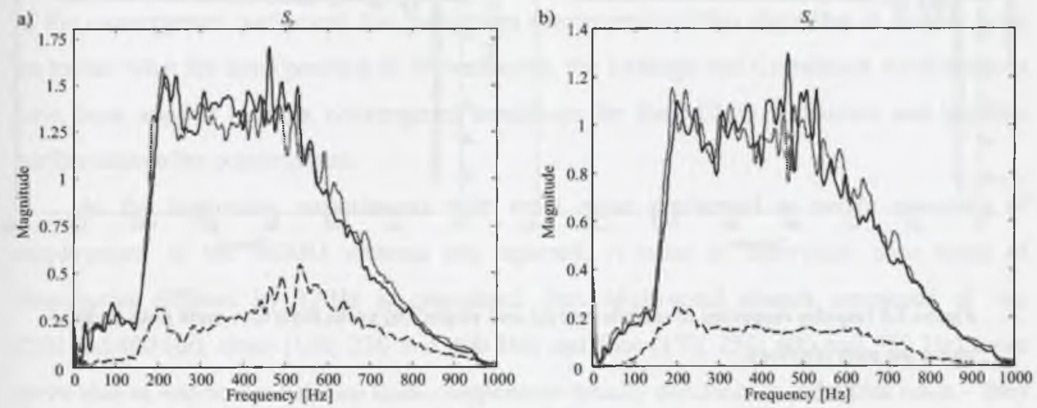

Figure 5.5 Frequency responses of sample real (a) and virtual (b) paths: main path from the upper loudspeaker (solid), main path from the lower loudspeaker (dotted), and cross path from the upper loudspeaker (dashed).

In case of virtual paths (Figure 5.5b) the cross paths damp the acoustic wave more, i.e. about five times, than the main paths due to presence of the head recognised as an acoustic barrier. The responses from two loudspeakers for the same headrest channel differ mainly due to presence of the user torso (solid and dotted lines in Figure 5.5).

For designing and parameterising the control systems it is important to know parametric models of the plant paths. However, due to complicated coupled acoustic and electric phenomena it is very difficult to build sufficiently precise phenomenological models. Therefore, identification techniques have been employed [NiederlinskiKF_93], [Pawelczyk_01, 02i], [Kasprzyk_03], [Figwer_04]. Parametric models of FIR structures, i.e. impulse response parameters, have been estimated with the LMS algorithm [KuoM_96] for the nominal position of the head. It follows from Figure 5.5 that only a few acoustic modes can be singled out for the frequency range considered, i.e. from over 60 Hz to 700 Hz. Therefore, impulse responses decay fast and they are negligible after 64 samples (Figure 5.6). Hence, 64 parameters are found enough for the path models. Lower structures do not allow for successful control at low frequencies in that band. Larger structures are not necessary. It follows from the obtained models that the real main paths have delay of 3 samples, the virtual main paths – 4 samples, and both the real and virtual cross paths – 5 samples.

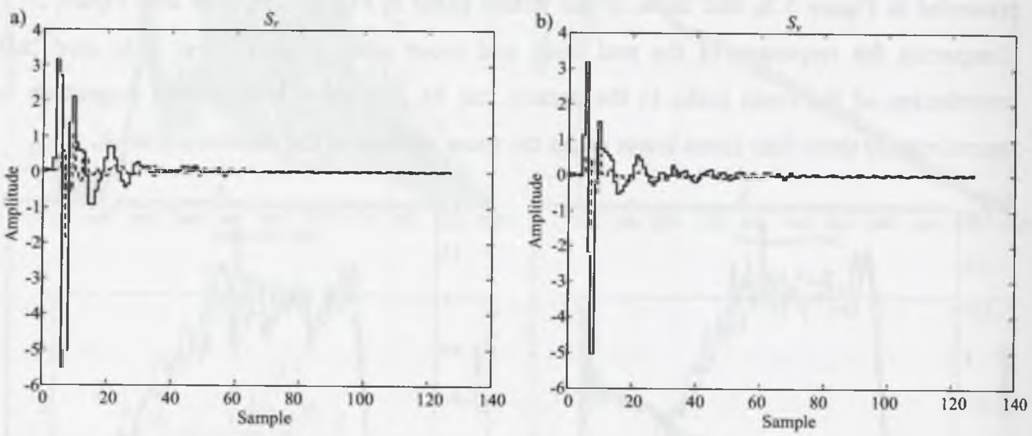

Figure 5.6 Impulse responses of sample real (a) and virtual (b) paths from G1: main path (solid), and cross path (dashed).

Analysis of distribution of zeros of the models leads to conclusion that they are non-minimum phase. In fact, two premises contribute to this phenomenon – the zeros outside the unit circle are located both on the right and left-half planes, e.g. for $\hat{S}_{11}$: {-1.75 ± j1.89, 1.85 ± j2.23}, for $\hat{S}_{21}$: {-1.97 ± j0.44, 1.84 ± j1.64}, for $\hat{S}v_{11}$: {-2.17, 1.96 ± j1.95}, for $\hat{S}v_{21}$: {-2.10 ± j1.89, 2.53} [Pawelczyk_03c]. Thus firstly, the physical system itself is non-minimum phase due to multiple path interference in the reverberant three-dimensional enclosure as well as due to presence of the microphones in acoustic near-fields of secondary

sources [Elliott_01], [Pawelczyk_01]. Secondly, non-minimum phase features emerge with sampling and, consequently, the modelling [NiederlinskiKF_93]. It is well known that the non-minimum phase phenomenon has negative influence on performance of the control systems due to problems to design controllers perfectly cancelling the noise over entire frequency band [Morari_89], [SeronBG_97], [Rafaely_97], [Pawelczyk_99a].

5.2 Performance Evaluation

Preliminary real-world experiments have demonstrated that adaptive systems perform better in the changing acoustic environment. Moreover, generally, the noise can also be subject to change due to, e.g. switching on and off some of noisy devices. Therefore, results of adaptive systems are presented in this chapter. Results obtained by means of simulations with Matlab and Simulink for both optimal and adaptive control systems are presented in Appendix C. The laboratory measurements have been performed with SVAN 912AE sound analyser and Solartron-Schlumberger spectral analyser, after the adaptive systems converged. Control filter parameters have been updated using the Multi-Channel FXLMS algorithm. According to conclusions drawn from the analysis performed in Appendix B.8 there is a large set of values of the convergence coefficient that guarantees convergence of this algorithm in similar time, no matter what the head position is. Nevertheless, the Leakage and Correlation modifications have been applied to relax convergence conditions for the MIMO realisation and improve performance after convergence.

At the beginning, experiments with tonal noise performed to verify necessity of employment of the MIMO systems are reported. A series of individual pure tones of frequencies differed by 10 Hz is considered first. Multi-tonal sounds composed of two (250 and 400 Hz), three (170, 250 and 400 Hz) and four (170, 250, 400 and 550 Hz) tones serve also as test-noises because tonal components usually dominate in industrial noise – they are generated by any rotating or reciprocating machines.

As the work reported concentrates mainly on generation of well located zones of high attenuation, their surfacial distributions are presented in the sequel for two types of noise. A 250 Hz tone is considered first, since tones of similar frequencies belong to the highly audible noise components in vehicles [Park_02], [RamosSLM_02]. Another noise is a real-world industrial recording (Figure 5.7). For the purpose of this presentation, measurements have been performed with the sound analyser at about 300 points on the basic surface around the head staying at the same position (in the midpoints the results are interpolated).

Then, similarly acquired results of noise control at the right ear in face of changes of plant response due to head movements are provided. This type of experiments has also been recently reported for a different plant in [DiegoGFP_04]).

All results except distribution of zones of quiet are presented for one channel (real – virtual microphones pair). They are similar for the other channel, which has been put into operation at the same time. During all experiments the chair has been occupied by a test-user because presence of the body, not only the head, reveals to significantly influence the results. Unfortunately, the author have not had any appropriate standardised head and torso mannequin, e.g. the 4100-type Brüel & Kjær to his disposal and employment of an artificial head does not suffice.

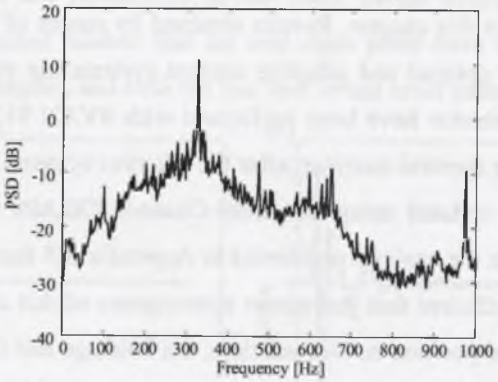

Figure 5.7 PSD estimate of the real industrial noise used for experiments.

Wavelength of the 250 Hz tone is about 1360 mm, whereas the smallest wavelength contributing to the real noise is about 480 mm and the dominating one – about 1000 mm. The smallest wavelength contributing to the multi-tonal noise is 620 mm. Hence, all the wavelengths are significantly larger than the distance between the real and virtual microphones, reaching 150 mm. Therefore, the basic assumption qualifying the headrest system to the considered group of acousto-electric plants can be considered satisfied.

5.3 Experimental results

It is claimed in the literature that influence of the cross paths is negligible for the active headrest system and two independent control systems operating on the two headrest channels suffice [RafaelyE_99], [HolmbergRS_02], [TsengRE_02]. Therefore, to the author knowledge, SISO systems have only been tested. However, in the system considered

(Figure 5.1) the loudspeakers are not directly turned towards the respective ears and operate also for the other ear (Figure 5.5). Therefore, to verify necessity of employment of MIMO systems including cross paths instead of simpler independent SISO systems (decentralised control) appropriate experiments have been performed [FigwerOP_03]. The IMC systems in different configurations have been employed to attenuate a series of tonal noises of frequencies from 60 to 700 Hz. They are: the SISO system operating for the right channel only, two SISO systems operating independently for the two channels, and the MIMO system operating for both channels. Results measured by the real and virtual microphones for the right channel are presented in Figure 5.8. It is seen that attenuation obtained with the MIMO system is higher of about 4 dB, in average, compared to that for two independent SISO systems. Moreover, the MIMO system behaves better in a long time horizon being tuned to converge with high rate (the tests have been performed for five hours for selected tones). Such setting provides higher acoustic comfort when changes in the noise spectrum or in the plant appear. Results of the MIMO system for the right ear are, however, close to the results obtained for a single SISO system operating for the right channel. Summarising the analysis one can say that the cross-coupling between the headrest channels is too large for the decentralised control to yield performance comparable to the MIMO system. The full structure compensates for influence of the cross paths and produces results similar, or with little additional benefit, to those obtained when only one channel operates. Analogous conclusions are drawn from experiments performed with other control systems considered here [Pawelczyk_03a, 04a]. Hence, in the reminder of this chapter results of noise control with MIMO systems are reported.

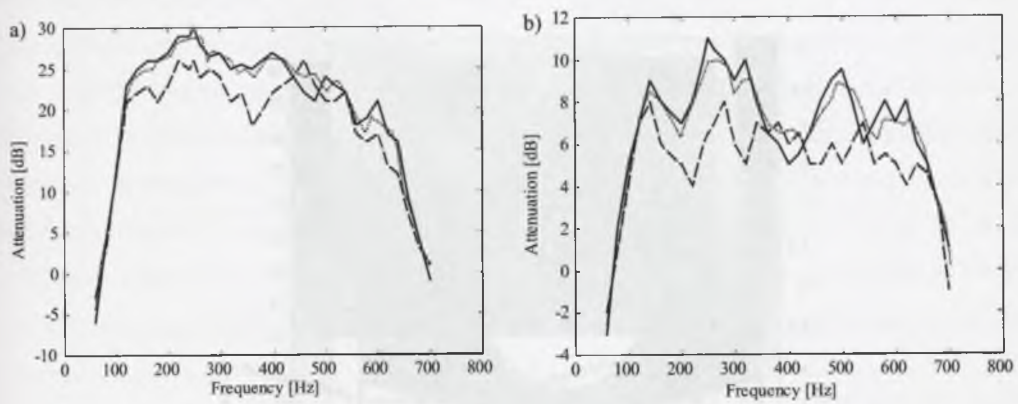

Figure 5.8 Attenuation at the real microphone (a) and at the user ear (b) for a sequence of pure tone excitations: SISO (dotted), two independent SISO (dashed), and MIMO (solid) IMC systems.

It also follows from the experiments that attenuation measured for the individual frequency corresponding to a tone is much smaller compared to the overall attenuation reported above [Pawelczyk_02f, 04a]. This is a consequence of presence of significant broadband acoustic floor, additional noise components generated due to plant non-linearities and remainings of inter-sample effects, as well as noise reinforcement at some other frequencies.

Dependent on impulse response of the plant and noise to be controlled appropriate filter order should be used. Whereas low order suffices for the tonal noise, it should be higher for the multi-tonal or real noise. On the basis of analysis of impulse response of the optimal filters designed for the real noise 128 parameters have been chosen for each of the control filters. However, there are ANC applications where hundreds or thousands parameters are necessary [Michalczyk_04]

5.3.1 Double input – double output IMC system

Distribution of zones of quiet for a 250 Hz tone, obtained with a double input – double output (DIDO) IMC system ($q = 0.9$ in (4.54)) under the time-invariance condition (head in position '0b') is presented in Figure 5.9. It confirms the expectations that the zones are irregular, [TokhiL_92] and [Pawelczyk_02c], and the highest attenuation is observed at the real microphones. In fact, little noise reinforcement appears at the diaphragms of the loudspeakers. However, it is not clearly evident from this figure as the diaphragms belong to a different horizontal surface than the one considered. Although the highest possible attenuation reaches 30 dB, the ears are covered by the 11 dB zone only. Such attenuation also extends sidewards.

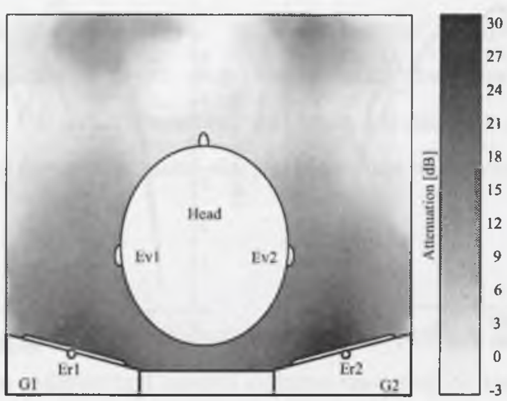

Figure 5.9 Distribution of zones of quiet for a 250 Hz tone and a DIDO IMC system.

The attenuation decreases rapidly in front and at the distance of scarcely 50 mm a 7 dB zone is present. The results remain in agreement with results of acoustical analysis presented in [Garcia_96]. However, it is impossible to conclude from Figure 5.9 what can be the attenuation at the ear for different head positions because the acoustic field distribution changes then also. To answer this question additional experiments have been performed.

Figure 5.10 and Figure 5.11 present results of tonal and real noise control, respectively, at the right ear for different positions of the head. A point in the figures corresponds to geometrical position of the centre of the head (with respect to the headrest), for which measurement has been done at the right ear. This way of presentation implies the shift in the figures and lack of the head contour.

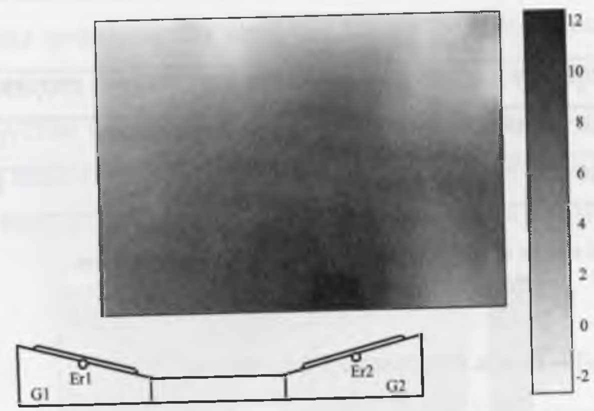

Figure 5.10 Control results of a 250 Hz tone with a DIDO IMC system under head movements.

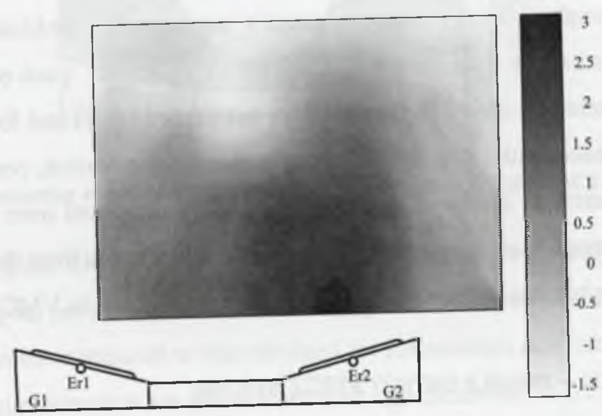

Figure 5.11 Control results of the real noise with a DIDO IMC system under head movements.

It is seen that the surfacial gradient of attenuation is lower than in case of the results reported in Figure 5.9. The tonal noise is attenuated by 11 dB for the nominal position of the head. In case of lateral movements to the left it drops down slowly. The gradient is much higher when approaching the right loudspeaker because the magnitude of the main path response increases (Figure 5.3) and the system must retune to guarantee stable operation. The attenuation suffers at the same time. In case of the real noise the conclusions are generally similar. The attenuation is, however, much lower but also the user perceives small change when moving the head.

Results of multi-tonal noise attenuation are collected in Table 1. It is seen that this type of noise is well suppressed at the real microphone, although the more tones the poorer the performance.

Noise / Frequency [Hz]	250, 400	170, 250, 400	170, 250, 400, 550
J [dB] at the real micr.	27.7	24.2	19.0
J [dB] at the ear	9.6	8.1	6.4

Table 5.1 Control results of multi-tonal noise with a DIDO IMC system.

5.3.2 Double input – double output VMC1 system

Analysis of the VMC1 system (Chapters 3 and 4) leads to conclusion that its properties are similar to properties of a classical feedback system. Such a system with the FXLMS algorithm operates unsatisfactorily for the application considered here and other similar applications. Although it works stably it reveals convergence problems, particularly for deterministic disturbances (see comments in Chapter 3), or quasi-periodic bursts are generated. The attenuation for a 250 Hz tone does not exceed 10 dB and for the real noise it is less than 2 dB. Consequently, it is less suitable for the test-application, compared to the other VMC systems. Therefore, results of its operation are not presented here. Simulation results obtained with this system are reported in Appendix C.3. It follows from the experiments that, contrary to adaptive realisation, optimal VMC1 performs similarly to VMC2 and VMC3.

5.3.3 Double input – double output VMC2 system

It follows from the identification results for the virtual paths (Figure 5.5b) that the contribution of cross paths to the secondary sound at the virtual microphones is much less

than that of the main paths. Therefore, models $\hat{S}_{v12}$ and $\hat{S}_{v21}$ could be omitted in estimating $\hat{y}_{v1}(i)$ and $\hat{y}_{v2}(i)$ without significant loss in performance. However, rejecting the models neither improves convergence nor saves much computational time. Therefore, if the signal processor permits, it is recommended to take the virtual cross paths into account to guarantee proper behaviour over a long-time horizon.

Distribution of zones of quiet for a 250 Hz tone, obtained with a double input – double output VMC2 system ($q = 0.9$ in (4.54)) is presented in Figure 5.12. It is seen that the areas of highest attenuation are well located although the attenuation reaching 18 dB is significantly lower than at the real microphones for the IMC system (Figure 5.9). This can be explained by the modelling errors and the fact that the assumption about the same disturbance at the virtual and real microphones underlying this algorithm has not been fully met in the laboratory configuration. However, in this case presence of the head imposes zero pressure gradient at its surface where the virtual microphones are located, what flattens the secondary field and thereby extends the zones close to the head [GarciaEB_97], [RafaelyEG_99], [RafaelyE_99]. Attenuation higher than 13 dB is guaranteed for 150 mm sidewards and 100 mm in front.

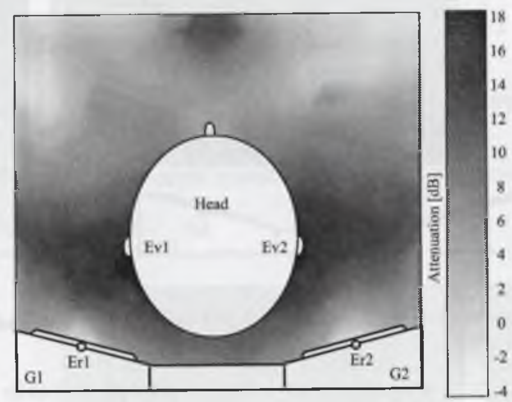

Figure 5.12 Distribution of zones of quiet for a 250 Hz tone and a DIDO VMC2 system.

Figure 5.13 and Figure 5.14 present results of tonal and real noise control, respectively, at the right ear changing its position. It is seen that changes of the head position result in gradual decrease of attenuation compared to that obtained for the nominal position. Nevertheless, both lateral and forward movements are possible without significant loss in performance. In case of the real noise the ear is covered by a 3 dB zone over a large area. The attenuation at different positions in Figure 5.13 is generally higher than in case of the steady conditions reported in Figure 5.12. This is due to movements of the head, at which the secondary field is flattened.

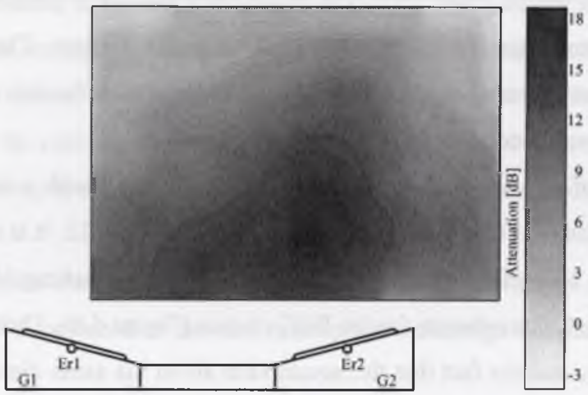

Figure 5.13 Control results of a 250 Hz tone with a DIDO VMC2 system under head movements.

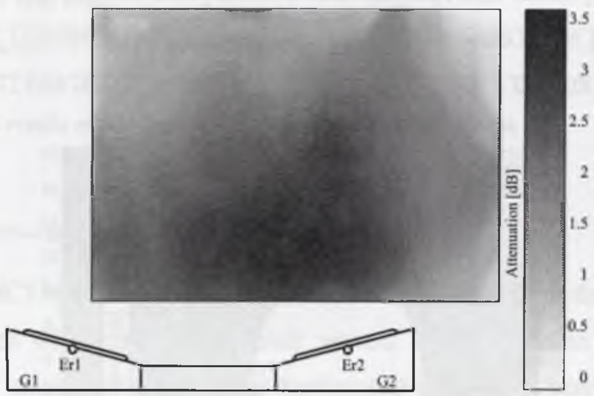

Figure 5.14 Control results of the real noise with a DIDO VMC2 system under head movements.

Results of multi-tonal noise attenuation are collected in Table 5.2. It is seen that this type of noise is well attenuated mainly at the assumed location, i.e. at the ear, although the attenuation at the real microphone is also significant. However, similarly to the IMC system, the more tones the poorer the performance.

Noise / Frequency [Hz]	250, 400	170, 250, 400	170, 250, 400, 550
J [dB] at the real micr.	10.1	8.2	6.9
J [dB] at the ear	17.2	15.6	13.1

Table 5.2 Control results of multi-tonal noise with a DIDO VMC2 system.

5.3.4 Double input – double output VMC3 system

Distribution of zones of quiet for a 250 Hz tone, obtained with a double input – double output VMC3 system (q = 0.9 in (4.54)) is presented in Figure 5.15. The figure confirms that the areas of highest attenuation are at desired locations. The attenuation reaches about 27 dB directly at the ears and gradually decreases leaving subsequent zones. However, the 15 dB zone covers the distance of about 110 mm to the left and 150 mm to the right. In front of the ears the zones change more rapidly, i.e. the attenuation drops down faster until reaching a 5 dB zone, which extends widely.

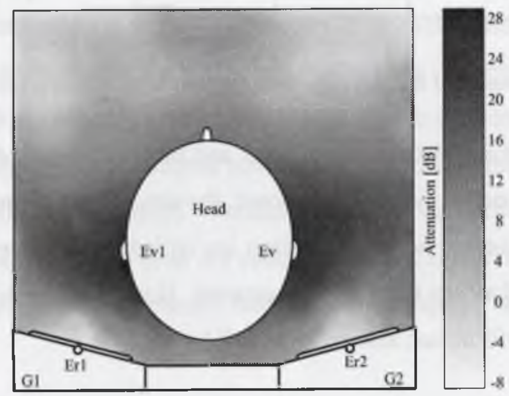

Figure 5.15 Distribution of zones of quiet for a 250 Hz tone and a DIDO VMC3 system.

Figure 5.16 and Figure 5.17 present results of tonal and real noise control, respectively, at the right ear changing its position.

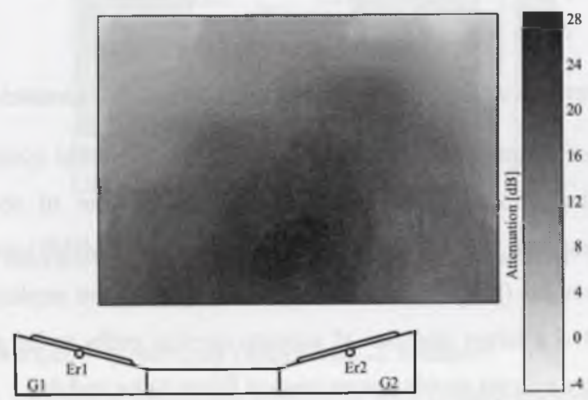

Figure 5.16 Control results of a 250 Hz tone with a DIDO VMC3 system under head movements.

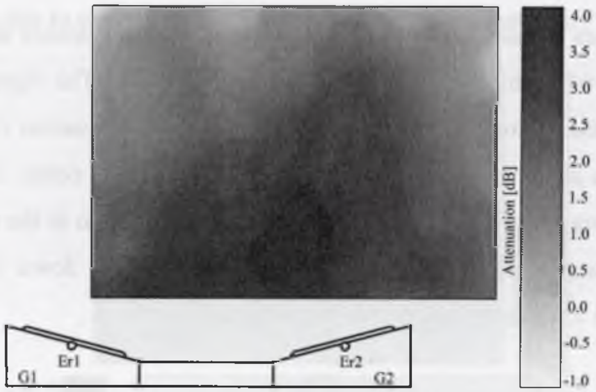

Figure 5.17 Control results of the real noise with a DIDO VMC3 system under head movements.

It can be inferred that the zones are much larger and more uniformly distributed, compared to those for the previous control systems. Moreover, the attenuation at the ears is higher.

Results of multi-tonal noise attenuation are collected in Table 5.3. It is seen that the results are still better than for the previous systems. However, the conclusion that the more tones the poorer the performance also remains valid.

Noise / Frequency [Hz]	250, 400	170, 250, 400	170, 250, 400, 550
J [dB] at the real micr.	8.3	7.0	5.6
J [dB] at the ear	25.5	22.1	17.6

Table 5.3 Control results of multi-tonal noise with a DIDO VMC3 system.

5.3.5 Control systems with more microphones or loudspeakers

In this section, zones of quiet obtained with some extended control systems are considered. Increase of both the number of microphones and the number of secondary sources is examined. Overdetermined, fully-determined and undetermined MIMO systems are presented in subsequent subsections (properties of these types of systems are explained in [Elliott_01]). Such systems involve a larger number of acousto-electric paths to be identified and these using more secondary sources involve more control filters to be updated.

5.3.5.1 Quadruple input – double output VMC2 system

The prototype of the active headrest system is provided with additional real microphones. They are located at the edges of the headrest. Also two additional virtual microphones are applied. Arrangement of the microphones is presented in Figure 5.18. Appropriate models have been identified. The full structure including all possible real and virtual paths as well as control filters has been implemented.

Distribution of the zones of quiet for a 250 Hz tone, obtained with a quadruple input – double output (QIDO) VMC2 system (q = 0.8 in (4.54)) is presented in Figure 5.18. Compared to the DIDO VMC2 system (Figure 5.12) the zones of quiet are significantly larger, although the attenuation is barely 2 dB lower. The enlargement is a result of the fact that presence of more microphones for a headrest channel has the potential to reduce both the acoustic pressure and its gradient, as theoretically analysed in [GarciaEB_97]. The zones are shifted a little with respect to the assumed positions, due to modelling errors caused, e.g. by changes in the acoustic environment. Results of further experiments demonstrate that substantial position changes of the head are possible without significant loss in performance. The system being overdetermined operates stably and the adaptive algorithm converges with a high rate.

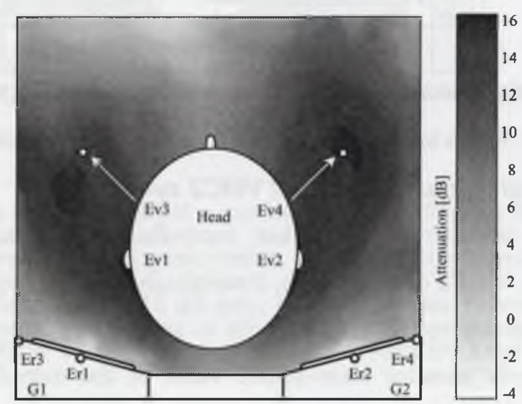

Figure 5.18 Distribution of zones of quiet for a 250 Hz tone and a QIDO VMC2 system.

5.3.5.2 Quadruple input – quadruple output VMC2 system

An increase of the number of secondary sources to four loudspeakers in the VMC2 system with four real and virtual microphones makes the system fully-determined. After performing a number of experiments it has been decided to simplify this algorithm by omitting contribution of the estimate of the reference signal in one path to control signals in the other path. Consequently, only the control filters on the diagonal of **W** are considered, although models of all cross paths are still used for estimating the reference signals. This modification reduces convergence time from over 6 s to less than 3 s without significant change of attenuation.

Distribution of the zones of quiet for a 250 Hz tone, obtained with a quadruple input – quadruple output (QIQO) VMC2 system (q = 0.7 in (4.54)) is presented in Figure 5.19. Both the zones are larger and the attenuation is higher compared to those for the respective system with two loudspeakers (Figure 5.12).

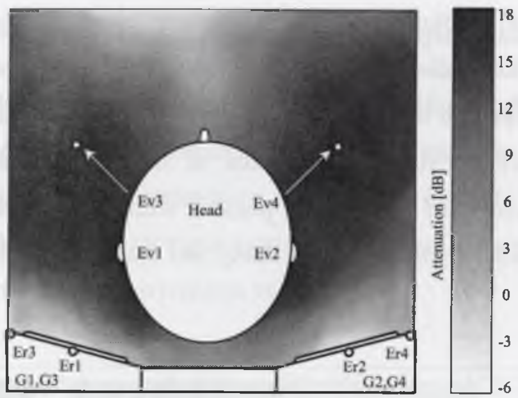

Figure 5.19 Distribution of zones of quiet for a 250 Hz tone and a QIQO VMC2 system.

5.3.5.3 Double input – quadruple output VMC2 system

If there are more secondary sources than controlled signals the system is said to be undetermined. Then, VMC2 does not have, theoretically, a unique solution [Elliott_01]. It has been, therefore, experimentally verified with a supervisory algorithm. The aim of this algorithm is to simply monitor mean-square value of the output signal over a 1 s time window, i.e. 2000 samples, and reset the adaptation in case of increase of this value for several windows or rapid increase within a window. This protects against unpleasant acoustic effects if the adaptive system diverges. Slow and temporary increase is interpreted as a local burst.

Similarly as in case of the DIDO VMC2 system all real and virtual paths are taken into account to estimate the residual signals, $\hat{y}_{v1}(i)$ and $\hat{y}_{v2}(i)$, although the contribution of cross paths to the secondary sound at the virtual microphones is much less than that of the main

paths (Figure 5.5). However, the system is simplified by neglecting the filters W_{12}, W_{21}, W_{32}, and W_{41} [Pawelczyk_03c]. During laboratory experiments the adaptive system with the LFXLMS algorithm including the Correlation modification has converged fast to similar values in terms of control filter parameters when run several times for the same noise.

Distribution of zones of quiet for a 250 Hz tone, obtained with a double input – quadruple output (DIQO) VMC2 system (q = 0.7 in (4.54)) is presented in Figure 5.20. The areas of highest attenuation reaching 20 dB are located directly at the user ears as for the DIDO VMC2 system (Figure 5.12). However, due to additional secondary sources the zones are slightly larger. Also the attenuation gradient is lower. It is, however, much higher compared to the systems employing more virtual microphones.

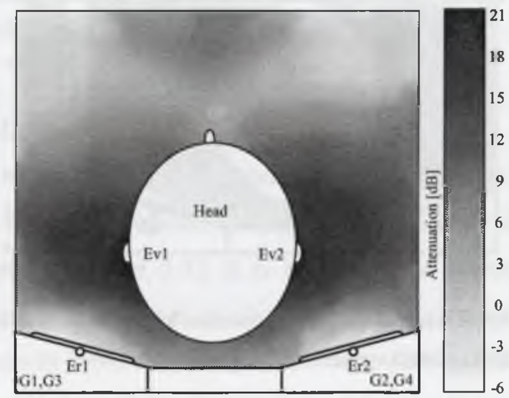

Figure 5.20 Distribution of zones of quiet for a 250 Hz tone and a DIQO VMC2 system.

The IMC system in the double input – quadruple output structure has also been verified to check whether the zones of quiet generated at the real microphones reach the user ears. They become larger, indeed, and an 18 dB zone touches the ears. However, even very small head movements imply large attenuation gradient. This system has been reported in details in [Pawelczyk_03a, 03c].

5.3.6 OTHER EXPERIMENTS

Additional experiments under different conditions than those considered hitherto have also been performed. The results are reported in following subsections.

5.3.6.1 Attenuation above the basic surface

Results of attenuation of a 250 Hz tone obtained with an adaptive DIDO VMC2 system, measured 60 mm above the basic surface are presented in Figure 5.21. Comparing to Figure 5.12 some conclusions about propagation of the zones of quiet in the vertical direction can be drawn. It is seen that the attenuation decreases by 4 dB, in average, and the zones of highest attenuation extend less sidewards than on the basic surface. Nevertheless, they are sill concentrated close to the ears. Areas of a little higher reinforcement are present.

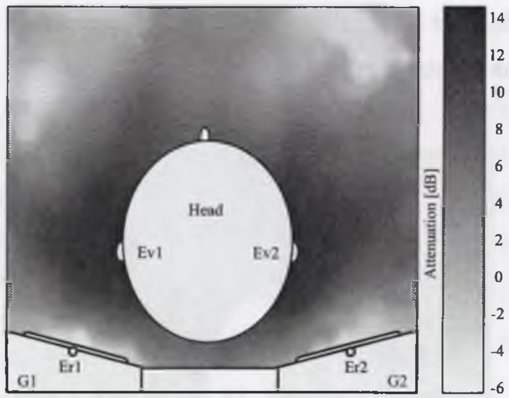

Figure 5.21 Distribution of zones of quiet on the surface located 60 mm above the basic surface for a 250 Hz tone and a DIDO VMC2 system.

5.3.6.2 Attenuation with lower sampling frequency

Results of attenuation of a 250 Hz tone obtained with an adaptive DIDO VMC2 system operating with 1 kHz sampling frequency, measured on the basic surface are presented in Figure 5.22. This experiment has required a new setting of the cut-off frequency of the analogue filters (to 300 Hz) and identification of new models of the plant paths. It is seen, comparing to Figure 5.12, that the results differ a little. At some areas the attenuation is higher by about 1 dB, which can be due to the analogue filters that in this case suppress influence of harmonics of the fundamental frequency.

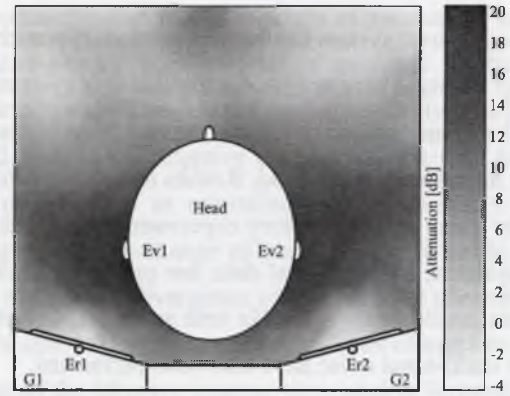

Figure 5.22 Distribution of zones of quiet on the basic surface for a 250 Hz tone and a DIDO VMC2 system operating with 1 kHz sampling frequency.

5.3.6.3 Attenuation of a lower frequency tone

Results of attenuation of a 170 Hz tone obtained with an adaptive DIDO VMC2 system operating with 2 kHz sampling frequency, measured on the basic surface are presented in Figure 5.23. Comparing to Figure 5.12 it is seen that the attenuation areas are larger. However, the attenuation itself is lower by about 6 dB. Enlargement of the areas is a direct consequence of significantly lower frequency of the tone, whereas the decrease of attenuation can be due to poor propagation of this frequency by the secondary sources (Figure 5.3) and associated non-linear effects.

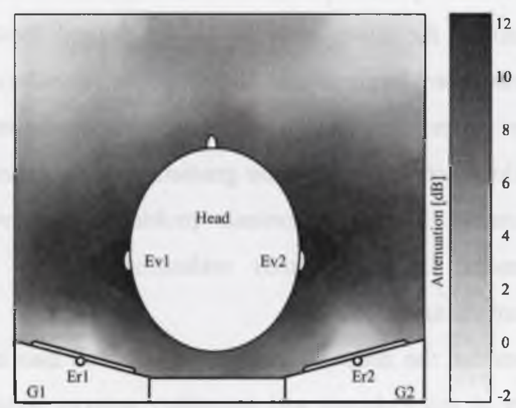

Figure 5.23 Distribution of zones of quiet on the basic surface for a 170 Hz tone and a DIDO VMC2 system.

5.4 Summary

In this chapter an active headrest system has been presented. It constitutes a good example of the considered group of plants. There are no doubts that this system requires two channels, each equipped with at least one secondary source and real microphone to overcome problems of the acoustic shadow introduced by the head. Results of noise control with adaptive systems discussed in this chapter come from laboratory experiments. Simulation results obtained with optimal and adaptive systems, based on real data, are presented in Appendix C. Two main types of noise have been considered – a 250 Hz tone and a real industrial recording, although some experiments with multi-tonal noise have also been performed.

At the beginning it has been experimentally shown that two independent SISO control systems operating for each channel degrade performance mutually. Hence, MIMO structures have been considered. Improvement of the acoustic comfort of the user becomes a challenging problem. It can be considered from the point of view of two comparably important counterparts – the attenuation level and dimensions of the zones of quiet (the problem of residual noise shaping has not been addressed in the experiments). Therefore, the results have been presented graphically as distribution of the zones and attenuation at the ear when changing position of the head. The conclusions are that the adaptive IMC system (Chapters 2 and 4) provides high noise attenuation but only at the real microphones. At the user ears the attenuation is much lower. Moreover, head movements imply perceiving high attenuation gradient what annoys the user. To guarantee higher attenuation at the ears and allow the user to move much more freely without rapidly leaving areas of high attenuation the adaptive VMC2 and VMC3 systems (Chapters 3 and 4), can be employed. The proposed algorithms generate indeed the zones of quiet at the desired locations, i.e. at the ears. Moreover, their dimensions are larger due to flattening the secondary field at the head. The adaptive VMC3 system performs better, i.e. it converges faster, the attenuation is higher and the zones are larger. However, the attenuation gradient is also higher. The adaptive VMC1 system yields poor results because it reveals problems to converge, particularly for deterministic disturbances. Optimal (fixed) realisation of this algorithm verified in Appendix C operates satisfactorily.

It has been shown that the zones of quiet propagate well also in the vertical direction. Increase of the number of microphones and secondary sources significantly extends them. Moreover, the attenuation itself may be higher. Decrease of the sampling frequency does not improve the results noticeably. It could, however, allow for employment of a slower, and

therefore cheaper, processing unit. Contrary to expectations, a trial to attenuate a lower-frequency have not produced better results in terms of attenuation and dimensions of zones of quiet. The explanation comes from analysis of response of the acousto-electric plant, namely the secondary loudspeakers used in the prototype poorly pass low frequencies.

The IMC, VMC2 and VMC3 adaptive control systems with Multi-Channel LFXLMS including Correlation modification or normalisation operate stably. Even quite significant head movements, or, moreover, exchange of persons occupying the chair during operation of the algorithms does not lead to divergence of control filter parameters. This confirms that the adaptive systems are able to compensate for significant changes in this particular plant.

Simulation results of the adaptive systems presented in Appendix C well coincide with results of the laboratory experiments. The zones of quiet are distributed generally in the same way. Also the attenuation is similar. The little differences are due to the fact that simulations refer to a 'closed world'. For instance, plant modelling errors for the nominal position of the head are neglected and no changes of the plant during the experiment are considered, acoustic floor is stationary, etc. Moreover, in the laboratory experiments a measurement (virtual) microphone is placed in subsequent locations on the surface to monitor the performance, what additionally changes the acoustic field to some extend.

In Appendix C simulation results obtained with optimal systems are also provided. All of them, except VMC1 produce results comparable to their adaptive realisations. They are, however, slightly worse in case of modelling errors and hence the zones of quiet are smaller. The optimal VMC1 system operates much better than performed as adaptive. Its results are close to results of the other optimal VMC systems for the data considered.

CHAPTER 6

SUMMARY

The purpose of this research has been to design and verify feedback control algorithms capable to attenuate acoustic noise at desired locations in a group of acousto-electric plants. This group has been characterised by small distances between these locations and locations of corresponding real microphones compared to the smallest acoustic wavelength significantly contributing to the noise. Because the plants considered are non-minimum phase including time delays complete noise cancellation is impossible with causal and stable controllers. Among feedback structures, the Internal Model Control approach has been found particularly useful. Although optimal control in this structure has been well examined in the literature, it has been systematised here for active control and originally applied for the rarely mentioned case of imperfect plant modelling. Design of the optimal H_2 control filter has been performed using the polynomial, frequency-domain and correlation-based approaches. It has been confirmed by means of simulations that all the design methods lead to equivalent solutions, although their complexity and convenience of usage is different. In case of the polynomial-based approach inner-outer factorisation of the model of the non-minimum phase path with delay and spectral factorisation of the disturbance PSD estimate are required. Also the causal part of the optimal filter should be extracted or a Diophantine equation should be solved. These operations are simpler when performed in the discrete-frequency domain. However, such approach involves finally designing a time-domain control filter that well matches the obtained frequency response. The alternative correlation-based approach requires, in turn, calculating an autocorrelation matrix and a vector of cross correlation, what in fact is more computationally efficient when performed in the frequency domain. The problem of optimal control of deterministic disturbances has been considered separately. It has been shown that it always has a solution, which is not unique, provided the filter length is sufficiently large. In this case perfect, i.e. to the acoustic floor level, cancellation is possible regardless of properties of the plant provided it does not have deep valleys in the response for the frequencies being controlled. A simplified stability analysis of the optimal control system has been briefly addressed. It follows from the analysis that a solution, more robust to imperfect modelling due to changes in the plant or insufficient excitation, can be obtained by modifying the H_2 cost function to include a parameter weighting term.

Adaptive control has been considered next. The FXLMS algorithm has been chosen for updating parameters of the control filter of FIR structure. Different representations and modifications of this algorithm have also been briefly reported. Sufficient conditions for convergence defined in different sense of feedforward and IMC adaptive systems have been provided. The latter involve assumptions not applicable for the acousto-electric plants. Therefore, to take advantage of the results available for feedforward systems, the control path is linearised allowing to obtain a convergence phase condition convenient for analysis. It has been shown that this condition differs as compared to that for feedforward systems and is dependent on the control filter. Moreover, it demonstrates a significant coupling between stability of the structural feedback loop and convergence of the parameter-update algorithm. The coupling is reduced if the real path model well matches the real path or magnitude of the control filter is small. Then, the IMC system can be considered as a purely feedforward system. A more reliable analysis of stability of such adaptive feedback systems is still an open problem for research. It has been shown that modification of the cost function as for the optimal algorithm can improve stability and convergence. The resulting Leaky FXLMS algorithm has been found particularly useful.

Stability, convergence, convergence time (and rate), tracking and noise attenuation are crucially influenced by the convergence coefficient in the FXLMS algorithm. It has been shown that for small convergence coefficient there is a reciprocal dependence between this coefficient and convergence time, regardless of plant modelling error. Then, there is an optimal value of the coefficient, which depends on the plant delay and the control filter length. Further increase of the convergence coefficient increases the convergence time due to fluctuations of the residual signal, and finally the adaptive system suddenly diverges.

The IMC system has also been considered for multi-channel plants. The design methodology similar to that for single-channel systems has been applied. Both optimal and adaptive solutions have been presented and discussed. The sufficient and necessary condition for robust stability in terms of the output uncertainty has been quoted. Sufficient conditions for convergence of the Multi-Channel FXLMS algorithm in an adaptive feedforward system have been presented. However, there is no reliable analysis of convergence of this algorithm operating in the feedback system for a non-minimum phase plant including a delay. Stability of such overall adaptive system is also not fully addressed. Then, a modification appropriate for improving stability has been provided. This is the Multi-Channel Leaky FXLMS algorithm supported by weighting models of the cross paths and Correlation update of the convergence coefficient.

The IMC system has been experimentally verified for generating zones of quiet in a prototype of the active headrest system. The active headrest is a good example of the group of acousto-electric plants under consideration. Due to geometrical arrangement of its components a significant coupling exists between the channels that can lead to instability when performing a decentralised control. Moreover, it has been shown that the attenuation is meaningfully degraded for this strategy, compared to fully multi-channel implementation. Therefore, the latter has been chosen. Nevertheless, such a simplification has been used in the literature. It has been demonstrated here by means of simulations of the optimal and adaptive systems as well as real-world experiments with the adaptive system that, according to expectations, the IMC system generates areas of the highest attenuation at the real microphones mounted in the headrest. The attenuation at the user ears is significantly lower and the attenuation gradient directly at the ears is high. As a result unpleasant effects are heard even in case of little head movements.

It has been found on the basis of the above experiments that it is necessary to design control systems capable to efficiently shift the zones of quiet to desired locations. The properties of the considered group of plants allow for easy estimation of the residual signal at the virtual microphone representing position of the user ear. In the first of the proposed systems, VMC1, this signal is minimised in a classical feedback structure, i.e. it provides the control filter input. Design of the optimal system requires solving a Diophantine equation to split the disturbance-shaping filter. The inner-outer factorisation of a transfer function, spectral factorisation of PSD estimate of the disturbance and extraction of the causal part are also necessary. Adaptive realisation of the VMC1 system performed with the FXLMS algorithm has turned out to require a strong convergence condition. Moreover, since the correlation between the control filter input and the disturbance deteriorates when the system tends to converge, the condition for good performance of this algorithm is ruined. This has been confirmed by experiments. Therefore, results of the adaptive realisation are poor, particularly for tonal signals, whereas the optimal system operates satisfactorily. The control filter has also been designed alternatively as a solution to an optimisation problem. It has been defined by a performance index related to noise attenuation over required frequency band subject to constraints due to stability margin and acceptable noise reinforcement beyond that band.

To overcome convergence problems of the adaptive realisation the structure has been modified. In the VMC2 system the estimated residual signal at the virtual microphone is minimised again, but an estimate of the disturbance is the control filter input. The optimal solution has been found taking advantage of the derivations performed for the IMC system and the general notation. The adaptive realisation requires much weaker conditions for convergence compared to those for the VMC1 system. Experimental verification has confirmed the expectations. For both optimal and adaptive control the zones of quiet are generated at desired locations. Moreover, the attenuation gradient is much smaller compared to that for the IMC system. Even for significant head movements the attenuation at the ears is high. At the same time the attenuation at the real microphones is much smaller or noise reinforcement is observed.

There are a number of ANC applications where the noise can be considered stationary over a long time horizon and the plant changes are not crucial. Then, it is reasonable to include knowledge about the noise and plant to the adaptive system and respond to the small changes. Applying this idea, the VMC3 system has been proposed. It is composed of two stages. In the tuning stage the signal at the virtual microphone is directly minimised. At the same time the knowledge is gained in an additional filter. This filter is then used in the actual operation, where the virtual microphone cannot be used, to produce a command signal to that measured by the real microphone. This system has proven itself to operate successfully in both optimal and adaptive realisations. The attenuation at the user ears is higher than in case of the other systems and convergence conditions for the adaptive system are weaker.

For all presented control systems expressions for the spatial attenuation gradient due to change of the virtual path have been derived. It has also been shown that higher attenuation and larger zones of quiet can be obtained by increasing the number of microphones and loudspeakers. However, such a solution makes the system complicated, increases computational load and is less robust to plant perturbations. To minimise these difficulties the algorithm can be simplified by omitting contribution of the estimate of the reference signal in one path to control signals in the other path. However, models of all cross paths are still used for estimating the reference signals.

The problem of noise control at locations larger than assumed at the very beginning has also been addressed. In this case a filter mapping the noise reaching the real microphone to noise at the position of the virtual microphone should be used in the design of both optimal

and adaptive control systems. However, generally such a filter is difficult to find. It depends strongly on location of the primary source with respect to the microphones, and acoustic environment. Application of an array of real microphones does not solve the problem. Therefore, if the zones are expected far from the secondary source, it is advised to use a wireless real microphone and then employ the VMC systems to shift the zones by a shorter distance compared to the acoustic wavelength.

It has been assumed for the entire analysis that the plant is linear. This assumption is generally satisfied. However, there are some applications where plant non-linearities can be severe, particularly at very low frequencies and for very small distances between the secondary source and real microphone [Pawelczyk_01]. Then, performance of the ANC systems can be deteriorated when applying the linear approach to control. Non-linear control techniques can be used to cope with this problem. In recent years, some researchers have tried to employ neural networks. The major problem of the ANC systems with multilayer perceptron neural networks is slow convergence (learning) rate. The algorithms can be speeded up by adopting several strategies [Bouchard_01]. The fuzzy neural networks and fuzzy modelling techniques can also be used [ZhangG_04b], [BottoSC_05]. In addition, they allow including linguistic information to support the numerical processing.

APPENDIX A

DEFINITIONS AND THEOREMS

A.1 INTERNAL STABILITY

A control system is internally stable if bounded signals injected at any point of the control system generate bounded responses at any other point. A linear time-invariant control system is internally stable if the transfer functions between any two points of the control system are stable [MorariZ_89].

A.2 PROPER AND CAUSAL SYSTEM

A SISO system $S(z^{-1})$ is proper (causal) if $\lim_{z\to\infty} S(z^{-1})$ is finite. A proper system is strictly proper if $\lim_{z\to\infty} S(z^{-1}) = 0$ and semi-proper if $\lim_{z\to\infty} \left|S(z^{-1})\right| > 0$. All SISO systems which are not proper are called improper (non-causal) [MorariZ_89].

A MIMO system $\mathbf{S}(z^{-1})$ is proper (causal) if all its elements $S_{jl}(z^{-1})$ are proper (causal). All MIMO systems which are not proper are called improper (non-causal).

A.3 SPECTRAL DENSITY MATRIX

The (auto) spectral density matrix between elements of an I-length vector of ergodic discrete-time random sequences of duration N samples is

$$\mathbf{S}_{xx}(e^{-j\omega T_s}) = \lim_{N\to\infty} \frac{1}{N} E\left[\mathbf{X}(e^{-j\omega T_s})\mathbf{X}^H(e^{-j\omega T_s})\right],$$

where

$$\mathbf{X}(e^{-j\omega T_s}) = \left[X_1(e^{-j\omega T_s}), X_2(e^{-j\omega T_s}), \ldots, X_I(e^{-j\omega T_s})\right]^T$$

is the vector of spectra of the sequences for an individual l-th set $\mathbf{x}(i)$ (or strictly $\mathbf{x}_l(i)$) and the expectation is taken over the sets of data [GrimbleJ_88], [Elliott_01]. For notational convenience the spectral density matrix is often written as

$$\mathbf{S}_{xx}(e^{-j\omega T_s}) = E\left[\mathbf{X}(e^{-j\omega T_s})\mathbf{X}^H(e^{-j\omega T_s})\right].$$

Elements on the diagonal of this matrix are real-valued (auto) spectral densities of signals being elements of $\mathbf{X}(e^{-j\omega T_s})$. The cross-spectral density matrix is then defined as

$$\mathbf{S}_{xy}(e^{-j\omega T_s}) = E\left[\mathbf{Y}(e^{-j\omega T_s})\mathbf{X}^H(e^{-j\omega T_s})\right].$$

These definitions are slightly different than those in [BendatP_93] but are used for convenience in algebraic manipulation.

If the Z-transform of $\mathbf{x}(i)$ exists (see [Jury_70], [OppenheimS_75], [BendatP_93]) and is $\mathbf{X}(z^{-1})$ then the spectral density matrix can also be written in terms of the expectation over the Z-transforms of individual data samples of lengths tending to infinity [GrimbleJ_88]

$$\mathbf{S}_{xx}(z^{-1}) = E\left\{\mathbf{X}(z^{-1})\mathbf{X}^T(z)\right\}.$$

$\mathbf{S}_{xx}(z^{-1})$ is also the Z-transform of a matrix of autocorrelation function

$$\mathbf{R}_{xx}(m) = E\left\{\mathbf{x}(i+m)\mathbf{x}^T(i)\right\}.$$

A.4 Strictly positive real transfer function

A rational stable SISO transfer function $S(z^{-1})$ is called strictly positive real (SPR) if [FraanjeVD_03]

$$\mathrm{Re}\left\{S(e^{-j\omega T_s})\right\} > 0 \qquad 0 \le \omega T_S \le 2\pi.$$

A matrix $\mathbf{S}(z^{-1})$ of rational functions with real coefficients is called SPR, if $\mathbf{S}(z^{-1})$ has no poles in $|z^{-1}| \le 1$ and [ChenG_91]

$$\mathbf{S}(e^{-j\omega T_s}) + \mathbf{S}^H(e^{-j\omega T_s}) > 0 \qquad 0 \le \omega T_S \le 2\pi.$$

A.5 Vector and matrix norms

Any vector norm must obey the following conditions [SkogestadP_96]:

- $\|\mathbf{x}\| \ge 0$,
- $\|\mathbf{x}\| = 0$ if and only if all elements of $\mathbf{x}$ are zero,

- $\|a\mathbf{x}\| = |a|\|\mathbf{x}\|$ for any complex a,
- $\|\mathbf{x}+\mathbf{y}\| \le \|\mathbf{x}\| + \|\mathbf{y}\|$

Any matrix norm must obey, in addition to the above conditions,

- $\|\mathbf{xy}\| \le \|\mathbf{x}\|\|\mathbf{y}\|$.

If $X(z^{-1})$ is the Z-transform of a signal $x(i)$ or describes a system with impulse response x_i, then the squared H_2 norm is:

$$\|X(z^{-1})\|_2^2 = \sum_{i=1}^{N} |x(i)|^2$$

or, by Parseval's theorem (subject to constraints in [MorariZ_89]),

$$\|X(z^{-1})\|_2^2 = \frac{1}{2\pi}\int_{-\pi}^{\pi} \left|X(e^{-j\omega T_s})\right|^2 d\omega T_S.$$

In turn, the H_∞ norm is

$$\|X(z^{-1})\|_\infty = \max |x(i)|,$$

$$\|X(z^{-1})\|_\infty = \sup_\omega \left|X(e^{-j\omega T_s})\right|,$$

where 'sup' stands for supremum or least upper bound.

If $\mathbf{X}(z^{-1})$ is a system matrix then the respective norms are [SkogestadP_96], [Elliott_01]:

$$\|\mathbf{X}(z^{-1})\|_2^2 = \frac{1}{2\pi}\int_{-\pi}^{\pi}\sum_{l=1}^{N} \sigma_l^2\left\{\mathbf{X}\left(e^{-j\omega T_s}\right)\right\} d\omega T_S,$$

$$\|\mathbf{X}(z^{-1})\|_\infty = \sup_\omega \bar{\sigma}\left\{\mathbf{X}\left(e^{-j\omega T_s}\right)\right\}.$$

A.6 Causal/non-causal decomposition

Let a rational stable transfer function $S(z^{-1})$ be written as a Laurent series

$$S(z^{-1}) = \sum_{i=-\infty}^{\infty} s_i z^{-i}.$$

Then it can be decomposed into causal and non-causal parts [FraanjeVD_03]

$$S(z^{-1}) = \left\{S(z^{-1})\right\}_+ + \left\{S(z^{-1})\right\}_-,$$

where

$$\left\{S(z^{-1})\right\}_+ = \sum_{i=0}^{\infty} s_i z^{-i} \text{ is stable,}$$

$$\{S(z^{-1})\}_{-} = \sum_{i=-\infty}^{-1} s_i z^{-i}.$$

A.7 INNER – OUTER FACTORISATION

SISO SYSTEM

A rational stable transfer function $S(z^{-1})$ (or briefly S) can be factorised into inner and outer parts, i.e. [FraanjeVD_03]

$S = S^{(i)} S^{(o)}$,

where the inner part $S^{(i)}$ is stable and unitary, so that

$S^{(i)}(z^{-1}) S^{(i)}(z) = 1$.

The outer part $S^{(o)}$ and its inverse $[S^{(o)}]^{-1}$ are stable. The inverse outer part is causal if and only if $S^{(o)}(0) \neq 0$ [AhlenS_92]. The following are also valid:

$S^{(o)}(z^{-1}) S^{(o)}(z) = S(z^{-1}) S(z)$,

$\left|S^{(i)}(e^{-j\omega T_s})\right|^2 = 1$.

MIMO SYSTEM

Let now a polynomial matrix $\mathbf{S}(z^{-1})$ (or briefly $\mathbf{S}$) of dimension G x I and elements being stable discrete-time rational transfer functions be considered. Then (see [Vidyasagar_85], [AhlenS_92], [IonescuO_96], [OaraV_99])

- The matrix $\mathbf{S}$, where $G \geq I$, is 'inner' if $\mathbf{S}^H\mathbf{S} = \mathbf{I}_I$ for almost all $|z| = 1$. It is 'co-inner', where $G \leq I$ and $\mathbf{S}^H\mathbf{S} = \mathbf{I}_G$ for almost all $|z| = 1$.
- The matrix $\mathbf{S}$ for $G \leq I$ is 'outer' if and only if it has full row rank G for all $|z| \geq 1$. This means that it has no zeros in $|z| \geq 1$. It is 'co-outer', where $G \geq I$, if and only if it has full column rank I for all $|z| \geq 1$.
- The matrix $\mathbf{S}$ with full rank $N = \min\{G, I\}$ for all $z = e^{j\omega T_s}$ (no zeros on the unit circle) has an 'inner-outer factorisation'

  $\mathbf{S}_{GxI} = \mathbf{S}^{(i)}_{GxN} \mathbf{S}^{(o)}_{NxI}$,

  with the 'outer' factor $\mathbf{S}^{(o)}$ having a stable right inverse. It has a 'co-inner-outer factorisation'

  $\mathbf{S}_{GxI} = \mathbf{S}^{(co)}_{GxN} \mathbf{S}^{(ci)}_{NxI}$,

  with the 'co-outer' factor $\mathbf{S}^{(co)}$ having a stable left inverse. If $G \leq I$ the co-outer matrix is square and its inverse is unique.

The matrix $\mathbf{S}$ is co-inner (co-outer) if $\mathbf{S}^T$ is inner (outer). The outer and co-outer matrices are stably invertible. The inverses are causal if the instantaneous gain matrices $\mathbf{S}^{(o)}(0)$ and $\mathbf{S}^{(co)}(0)$ have full rank N. Multiplication by a (co)inner matrix does not modify PSD of as signal vector.

A.8 CONVERGENCE

Let

- P be a probability measure on a σ-algebra of sets in the basic space of samples ϖ,
- ξ and ξ_i, $i = 1, 2, \ldots$ be random variables,
- $F_\xi(x) \triangleq P(\varpi : \xi(\varpi) < x)$, $\forall x \in \mathbb{R}$ be the distribution function for random variable ξ
- $E\{\xi\}$ be the expectation of the random variable ξ.

Then (see [ChenG_91] and [Macchi_95]):

1. ξ_i converges to ξ 'with probability one' or 'almost surely – a.s.', i.e. $\xi_i \xrightarrow[i\to\infty]{} \xi$ *a.s.* if

   $P(\xi_i \to \xi) = 1$
2. ξ_i converges to ξ 'in probability', i.e. $\xi_i \xrightarrow{P} \xi$ if for any $\varepsilon > 0$

   $P(|\xi_i - \xi| > \varepsilon) \xrightarrow[i\to\infty]{} 0$
3. ξ_i 'converges weakly' to ξ if for any x and continuous $F_\xi(x)$

   $F_{\xi_i}(x) \xrightarrow[i\to\infty]{} F_\xi(x)$
4. ξ_i converges to ξ 'in the mean-square sense' if

   $E\{|\xi_i - \xi|^2\} \xrightarrow[i\to\infty]{} 0$
5. ξ_i converges to ξ 'in the mean' if

   $E\{|\xi_i - \xi|\} \xrightarrow[i\to\infty]{} 0$
6. ξ_i converges to ξ 'of the mean' if

   $E\{\xi_i - \xi\} \xrightarrow[i\to\infty]{} 0$

Both convergence 'with probability one' as well as convergence 'in the mean-square sense' imply convergence 'in probability', which implies, in turn, 'weak convergence' [ChenG_91]. Convergence 'in the mean' follows from convergence 'in the mean-square sense' due to Schwartz inequality. Convergence 'of the mean' is the poorest convergence, because it only guarantees that expected value of the difference between the random variables "oscillates in the vicinity of zero" [Macchi_95]. Convergence 'of the mean' and convergence 'in the mean' follow from convergence 'with probability' if there exists an integrable random variable η such that $|\xi_i| \leq \eta$.

APPENDIX B

SIMULATION ANALYSIS

In this appendix results of simulation analysis are presented. The data come from the prototype of the active headrest system discussed in Chapter 5. Spectral factorisation of the disturbance and inner-outer factorisation of the path model are addressed, all the design approaches are briefly verified, properties of the adaptive systems are analysed and the VMC systems are compared.

B.1 SPECTRAL FACTORISATION OF THE DISTURBANCE

Figure B.1 presents PSD estimate of the real noise used for experiments and squared magnitude of the frequency response of a time-domain minimum phase causal FIR disturbance-shaping filter obtained by factorisation of this PSD estimate.

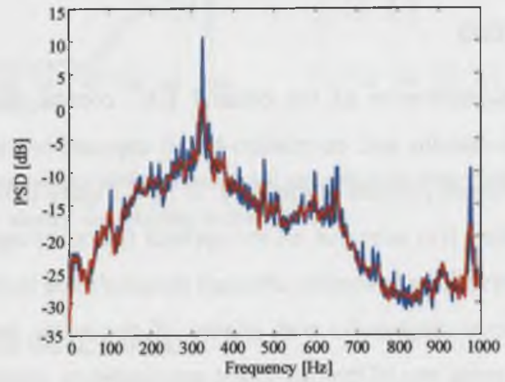

Figure B.1 Results of spectral factorisation of the real noise: PSD estimate of the real noise (blue), and squared magnitude of the frequency response of a causal FIR disturbance-shaping filter (red).

B.2 Inner-outer factorisation of real path model

Figure B.2 presents magnitudes of frequency response of 64 parameter real path model obtained for the nominal position of the head and frequency response of its time-domain outer factor (minimum phase causal filter). It is seen that magnitudes of the responses well match each other, whereas phase of the outer factor is much smaller. Magnitude of the inner part is constant.

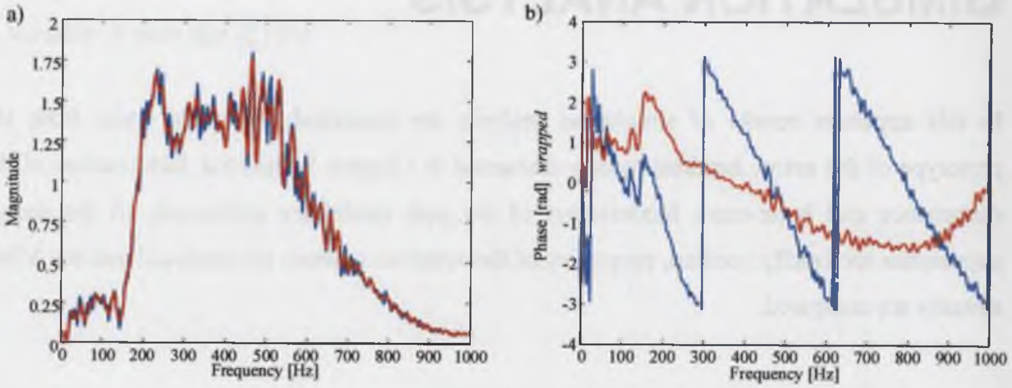

Figure B.2 Results of inner-outer factorisation of the real path model: frequency response of the real path model (blue), and frequency response of the causal FIR filter modelling the outer part (red).

B.3 Control filters

Figure B.3a illustrates parameters of the optimal IMC control filters designed using the polynomial, frequency-domain and correlation-based approaches to control the real noise (Figure B.1) for the nominal position of the head. In turn, Figure B.3b presents parameters of the adaptive control filter. It is seen that all the optimal filters are equivalent. Distribution of parameters of the adaptive filter is similar, although the amplitude is different.

Figure B.4 presents magnitudes and phases of frequency responses of the optimal control filter designed using one of the equivalent approaches to control the real noise (Figure B.1), and the adaptive filter. It is seen that the adaptive filter well matches the optimal filter at the contributing frequencies. The differences are mainly below 150 Hz and above 750 Hz, where the plant responses a little due to quality of the loudspeaker and signal reduction by the analogue filters, respectively.

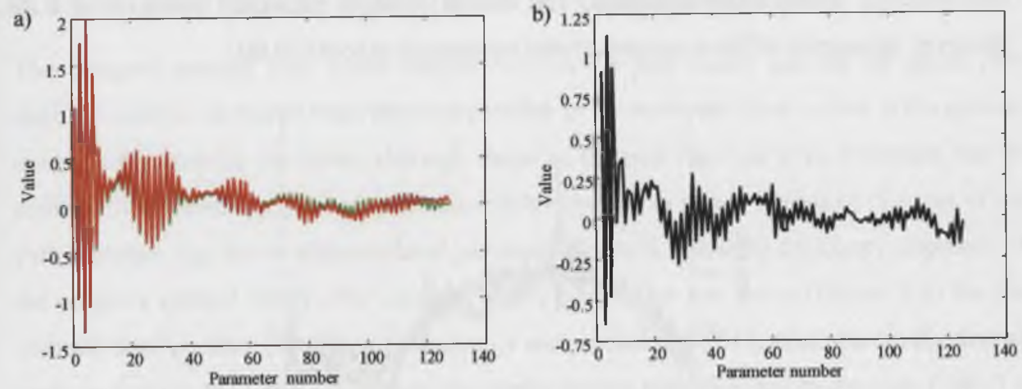

Figure B.3 Parameters of the optimal (a) and adaptive (b) control filters; in figure (a) the parameters have been obtained using: polynomial (red), frequency-domain (blue), and correlation-based approaches (green).

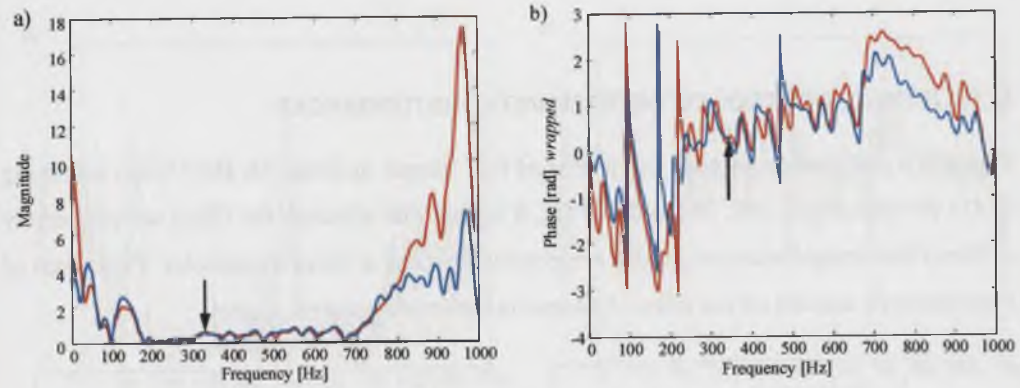

Figure B.4 Frequency responses of the optimal (red) and adaptive (blue) control filters; the arrow points to the frequency mostly contributing to the real noise.

B.4 Control of the real noise

Figure B.5 presents PSD estimates of the primary real noise and residual noise obtained with a sample optimal (all the designs are equivalent) and adaptive IMC control systems for the nominal position of the head. It is seen that results for the optimal and adaptive systems are very similar. The little differences are noticeable at very low frequencies and at frequencies above 750 Hz, i.e. where the noise components are negligible and analogue anti-aliasing and reconstruction filters suppress signals. The overall noise is attenuated barely by 2.7 dB. However, attenuation of the dominating tonal component exceeds 30 dB.

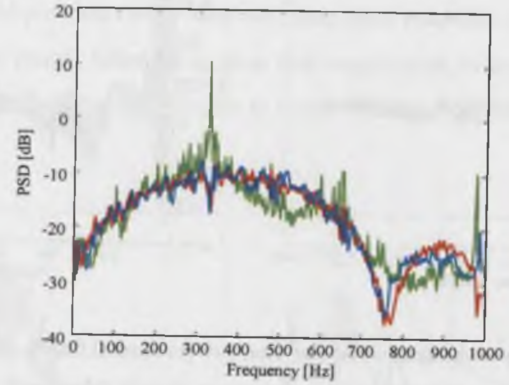

Figure B.5 Results of the real noise control at the right real microphone: PSD estimate of the primary noise (green), and PSD estimate of residual noise obtained with optimal (red) and adaptive (blue) IMC systems.

B.5 OPTIMAL CONTROL OF DETERMINISTIC DISTURBANCES

Figure B.6 presents magnitudes and phases of four sample optimal FIR IMC filters satisfying (2.41) for frequencies 200, 300 and 500 Hz. It is seen that although the filters are completely different their magnitudes and phases are exactly the same at these frequencies. Thus, each of them perfectly cancels all the tones of interest in the active headrest system.

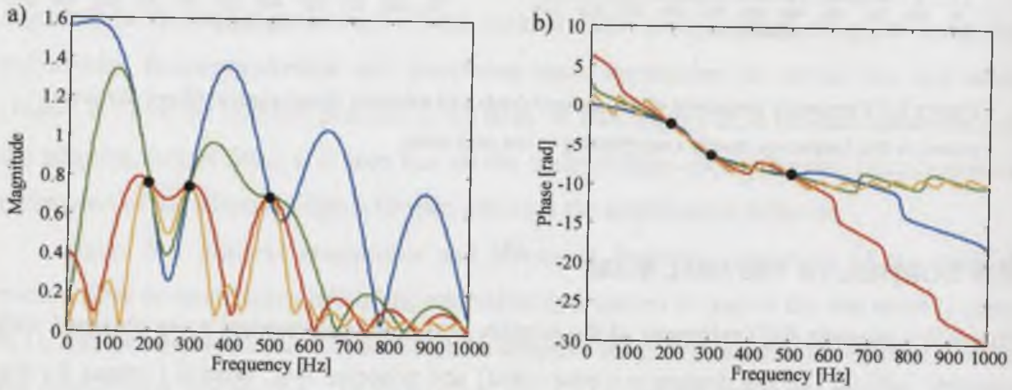

Figure B.6 Frequency responses of four different optimal control filters cancelling three tones (dots).

B.6 INFLUENCE OF PATH RESPONSE ON THE CONTROL FILTER

The designed optimal IMC filters depend only on the path model and not the actual path itself. Therefore, no matter what the head position in the active headrest system is the optimal control filter remains the same, although shape of the cost function at its minimum can be completely different. In turn, adaptive control is expected to retune in case of changes of the path response, e.g. due to different head positions. Figure B.7 presents frequency responses of the adaptive control filters after convergence to control the real noise (Figure B.1) for the nominal head position ('0b'), head maximally moved forward ('0f'), head maximally moved backward and to the left ('3La'), head maximally moved backward and to the right ('3Ra') – see Figure 5.2 for the notation. It is seen that, generally, the adaptive filter responses differ and the further the head from the right loudspeaker (consequently the smaller the path gain) the larger the control filter gain. As expected, the best matching of the responses appears for the most contributing frequencies of the noise, i.e. 170 – 350 Hz.

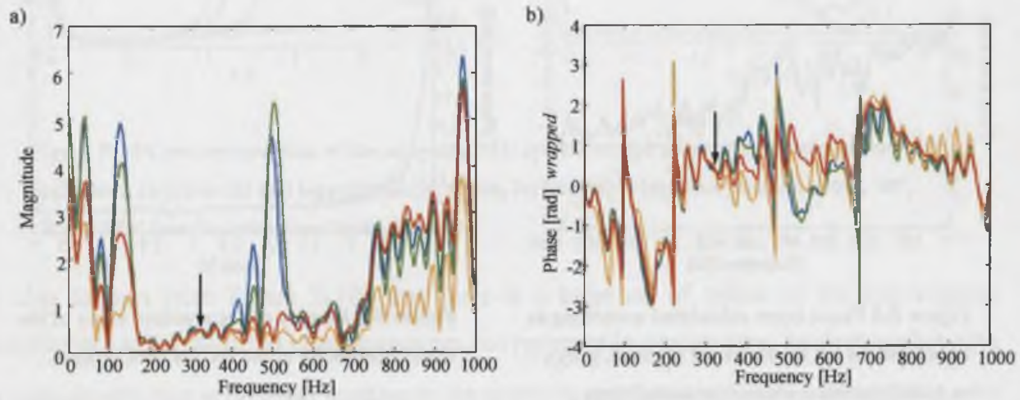

Figure B.7 Frequency responses of adaptive control filters in the IMC system updated for the following head positions: '0b' – red, '0f' – blue, '3La' – green, '3Ra' – yellow; the arrow points to the frequency mostly contributing to the real noise.

B.7 INFLUENCE OF FEEDBACK LOOP ON THE PHASE ERROR

Figure B.8 presents the phase error evaluated according to the condition for feedforward system (dashed, see (2.77)) and according to the condition for the IMC system (solid, see (2.105)). They have been obtained after convergence of the adaptive filter controlling the real noise (Figure B.1) for '0f' head position (Figure 5.2), i.e. a path significantly different in phase compared to the assumed model (identified for '0b' head position). It is seen that the first condition is violated at low and high frequencies and adaptive feedforward system would diverge. However, the second condition is satisfied and the adaptive IMC system works stably provided it is updated slowly. Figure B.9 presents, in turn, change in time of the absolute value of the maximal phase error for the adaptive IMC system. At the beginning of adaptation, when the control filter starts from its zero initial value, the phase error in IMC is equal to that of the feedforward system (compare (2.77) and (2.105)). Hence, the phase error in Figure B.9 at $t = 0$ equals the maximal phase error from Figure B.8 for the feedforward filter. After convergence the phase error from Figure B.9 tends to maximal phase error in Figure B.8 for the IMC system. However, that error appears for frequencies not contributing to the signal, i.e. below 50 Hz and above 950 Hz. For the contributing frequencies the error is lower.

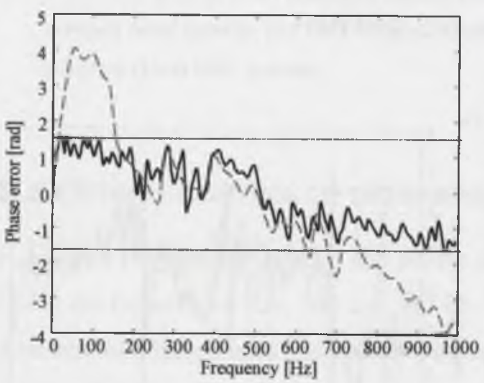

Figure B.8 Phase error calculated according to the condition for feedforward (dashed, grey), and IMC (solid) systems; the dotted lines represent phase error of $+\pi/2$ and $-\pi/2$.

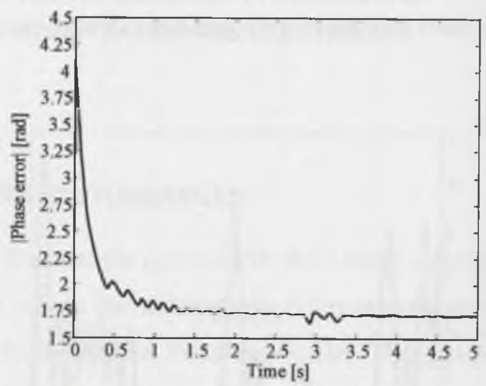

Figure B.9 History of the absolute value of the maximum phase error for the IMC system.

B.8 Influence of modelling errors on the optimal convergence coefficient and convergence time

It is obvious that convergence time of an adaptive LMS-based algorithm depends on the convergence coefficient μ. This dependence has been verified by means of simulations for different paths corresponding to: nominal head position ('0b'), head maximally moved forward ('0f'), head maximally moved backward and to the left ('3La'), and head maximally moved backward and to the right ('3Ra') (Figure 5.2). It follows from Figure B.10 generated

for a 250 Hz tone that the dependence is not monotonic. For a small convergence coefficient, μ, increase of its value decreases the convergence time, t_C, defined as a time for which the residual signal is attenuated by 20 dB. The curves plotted in logarithmic scale (Figure B.10b) for different head positions are parallel for those values. Then, there is an optimal value of the convergence coefficient in terms of the fastest convergence. Its further increase increases the convergence time due to fluctuations of the residual signal, i.e. the so-called excess mean-square error. After crossing the critical value (last point on each curve) the adaptive system becomes suddenly divergent.

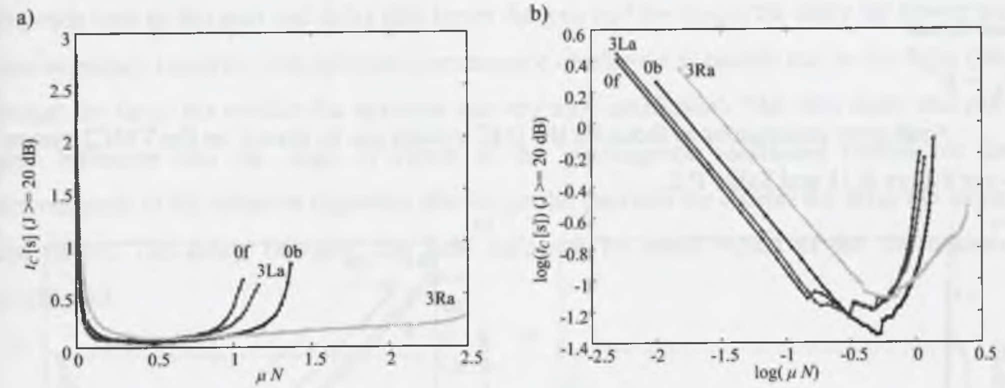

Figure B.10 Convergence time of the adaptive IMC system vs. the normalised convergence coefficient, in linear (a) and logarithmic (b) scales, for the following head positions: '0b', '0f', '3La', '3Ra' (see the references in the figures).

It also follows from Figure B.10a that there is a large set of values of the convergence coefficient ($\mu N \in (0.4;0.8)$) that guarantees convergence in similar time, no matter what path is considered (what is the head position in the active headrest system). This conclusion is very promising because it says that the convergence coefficient does not need to be updated for changes of the head position.

The logarithmic dependence of the convergence time and normalised convergence coefficient (Figure B.10b) can be modelled for small values of the convergence coefficient with a first-order polynomial

$$\log(t_C) = p_1 \log(\mu N) + p_0 .$$

Parameters of the polynomials for different head positions are gathered in Table B.1.

Head position	0b	0f	3La	3Ra
p_1	-1.02	-1.03	-1.02	-1.00
p_0	-1.78	-1.97	-1.91	-1.47

Table B.1 Parameters of the first order polynomial modelling logarithmic dependence of the convergence time and normalised convergence coefficient for different head positions; IMC system.

Because for all paths the parameter p_1 is close to unity, the following relation can be written

$\log(t_C) \approx -\log(\mu) - \log N + p_0$,

and hence

$t_C \sim \mu^{-1}$

Analogous conclusions to those for the IMC system can be drawn for the VMC2 system – see Figure B.11 and Table B.2.

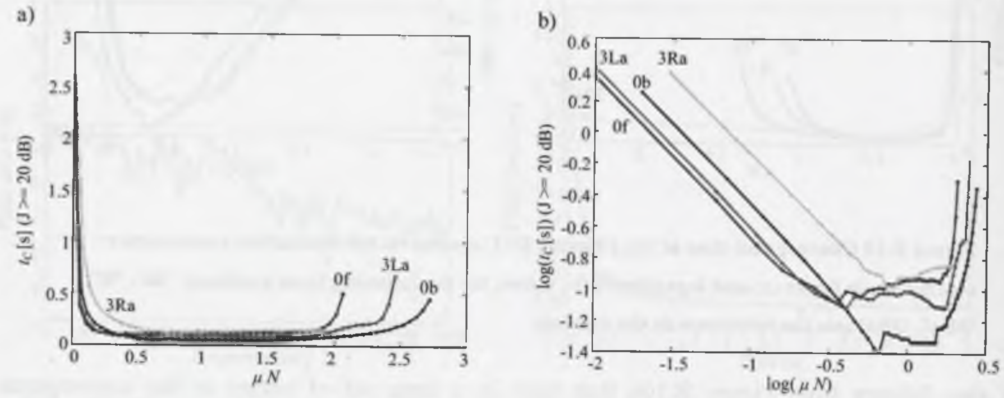

Figure B.11 Convergence time of the adaptive VMC2 system vs. the normalised convergence coefficient, in linear (a) and logarithmic (b) scales, for the following head positions: '0b', '0f', '3La', '3Ra' (see the references in the figures).

Head position	0b	0f	3La	3Ra
p_1	-1.01	-1.03	-1.02	-1.00
p_0	-1.47	-1.71	-1.63	-1.13

Table B.2 Parameters of the first order polynomial modelling logarithmic dependence of the convergence time and normalised convergence coefficient for different head positions;VMC2 system.

It follows from the above analysis that the closer the head to the operating loudspeaker is the larger convergence coefficient is required to provide the same convergence time. To tell if this is due to the larger gain or shorter delay an additional experiment with the IMC system has been performed. In simulations the same path '0b' has been artificially modified by including additional one-sample delay, and separately by doubling the gain (Figure B.12). The model has been the same every time and it has matched the original path. It is seen that the larger the gain compared to the gain of the path model the larger the convergence coefficient required to converge with the same rate. Minimum value of the convergence time depends both on the gain and delay (the larger the gain and the longer the delay the slower the convergence). However, the optimum convergence coefficient is mainly due to the delay (the longer the delay the smaller the optimum convergence coefficient). The time delay and path gain influence also the range of values of the convergence coefficient responsible for convergence of the adaptive algorithm (the larger the gain and the shorter the delay the larger the range). The delay, however, has little influence for small values of the convergence coefficient.

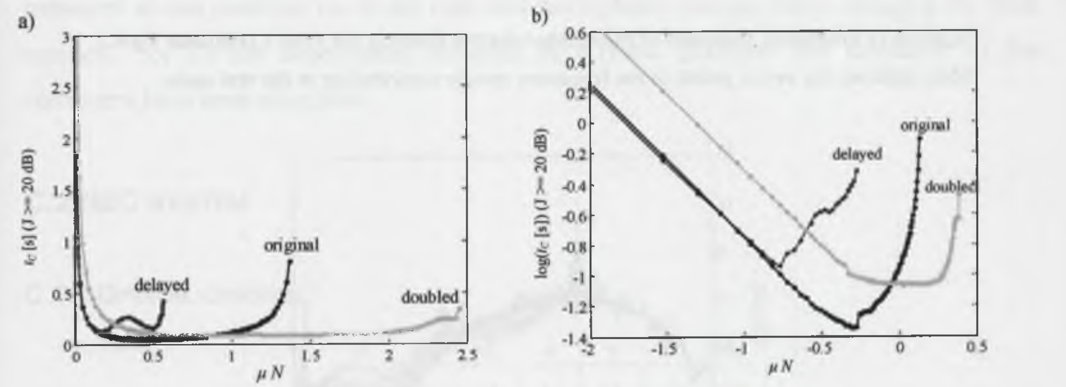

Figure B.12 Convergence time vs. normalised convergence coefficient in linear (a) and logarithmic (b) scales, for the path under the nominal head position: original, with additional one-sample delay, with doubled gain (see the references in the figures).

B.9 Comparison of the optimal VMC systems

Figure B.13 presents frequency responses of the optimal control filter in the VMC1 and VMC2 structures designed to control the real noise (Figure B.1). Results of the control at the right ear for the nominal head position are illustrated in the form of PSD estimates in Figure B.14. Although the structures are substantially different the results are comparable. The main differences are noticeable at frequencies above 750 Hz, i.e. where the noise components are negligible and analogue anti-aliasing and reconstruction filters suppress signals. The overall attenuation is about 2.5 dB for both cases.

The optimal control filter in the VMC3 structure is the same as that in the VMC2 structure, when neglecting modelling errors. Therefore, control results are also the same.

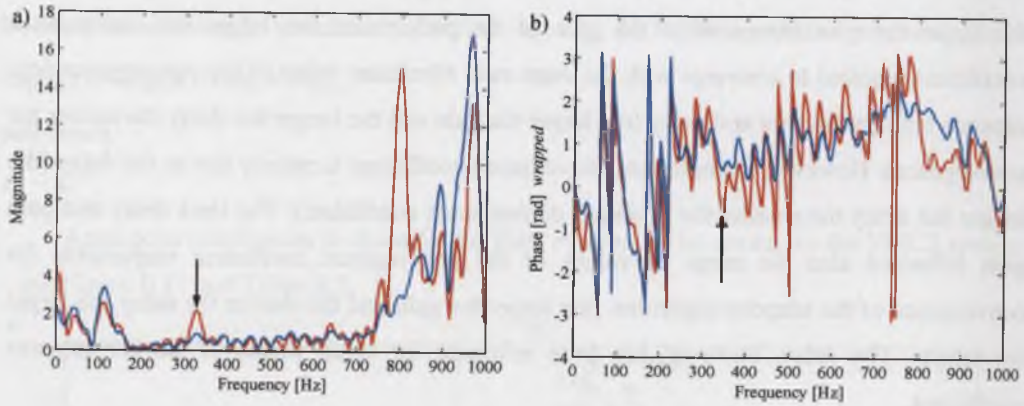

Figure B.13 Frequency responses of the optimal control filters in the VMC1 (red) and VMC2 (blue) systems; the arrow points to the frequency mostly contributing to the real noise.

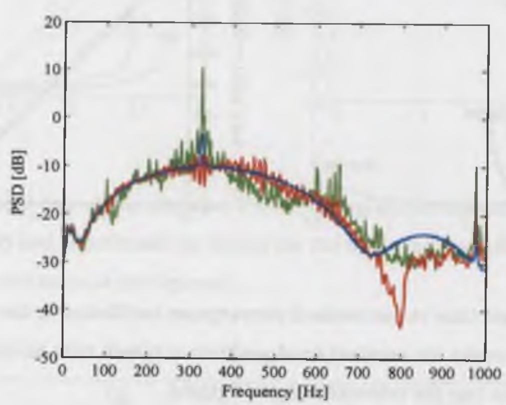

Figure B.14 Results of the real noise control: PSD estimate of the primary noise (green), and PSD estimates of the residual noise obtained with the optimal VMC1 (red) and VMC2 (blue) systems.

Appendix C

Simulation Results

C.1 Simulation

Attenuation results of a 250 Hz tone and the real noise (Figure 5.7) at the right ear, obtained by means of simulation of optimal and adaptive systems for different head positions are presented in this appendix. Sample results at the right real microphone are also reported to justify necessity of the effort to shift the zones of quiet. They demonstrate how the attenuation measured at one position, i.e. at the right real microphone changes when changing the head position. For all the experiments presence of a 16-bit quantiser and saturation of the converters have been simulated.

C.2 IMC system

C.2.1 Optimal control

	3L	2L	1L	0	1R	2R	3R
f	0.9	1.4	2.8	1.7	3.1	1.9	1.0
e	0.9	1.4	4.1	2.6	4.7	1.9	0.7
d	1.7	2.2	4.6	4.2	7.4	3.3	2.6
c	3.1	3.3	5.3	7.0	7.8	2.8	2.9
b	4.3	4.3	9.2	9.0	11.6	4.2	1.8
a	5.1	6.5	8.2	14.5	16.3	3.2	0.9

Figure C.1 Attenuation of a 250 Hz tone at the right ear obtained with optimal IMC system.

Attenuation at the right real microphone is the same for any registered head position and for a 250 Hz tone it is limited by the quantisation noise only.

a)

	3L	2L	1L	0	1R	2R	3R
f	-0.6	0.1	-0.6	-0.1	0.8	0.2	-1.2
e	-0.3	-0.1	-0.9	0.4	1.4	0.4	-0.3
d	0.0	0.4	1.2	1.0	1.6	0.8	0.0
c	0.7	0.9	1.3	1.6	1.9	0.8	0.3
b	0.8	1.3	2.0	2.1	2.1	1.3	0.4
a	1.0	1.4	1.9	2.3	2.5	1.4	1.1

b)

	3L	2L	1L	0	1R	2R	3R
f	2.4	2.5	2.1	2.5	2.6	2.6	2.4
e	2.3	2.5	2.1	2.3	2.7	2.7	2.7
d	2.6	2.6	2.8	2.6	2.7	2.7	2.6
c	2.5	2.6	2.7	2.8	2.8	2.8	2.6
b	2.5	2.7	2.8	2.7	2.3	1.8	1.7
a	2.6	2.7	2.8	2.5	2.0	1.6	1.5

Figure C.2 Attenuation of the real noise at the right ear (a) and at the right real microphone (b), obtained with optimal IMC system.

C.2.2 Adaptive control

	3L	2L	1L	0	1R	2R	3R
f	0.3	1.4	2.8	1.5	3.1	1.9	0.5
e	0.7	1.3	3.3	2.1	4.7	1.9	0.3
d	1.5	2.2	4.6	4.2	7.4	3.3	0.7
c	2.7	3.3	5.3	7.0	7.8	2.8	1.5
b	3.6	4.3	9.2	8.9	11.6	4.2	3.7
a	4.7	6.5	8.2	14.5	16.3	3.2	2.0

Figure C.3 Attenuation of a 250 Hz tone at the right ear obtained with adaptive IMC system.

	3L	2L	1L	0	1R	2R	3R
f	-0.2	0.4	0.0	0.3	0.9	0.3	-0.8
e	-0.1	0.1	-0.9	0.6	1.5	0.4	-0.1
d	0.2	0.6	1.4	1.1	2.0	1.0	0.3
c	0.7	1.0	1.4	1.9	2.1	0.7	0.6
b	1.0	1.3	2.1	2.1	2.5	1.4	1.4
a	1.2	1.6	1.9	2.6	2.8	1.1	1.5

Figure C.4 Attenuation of the real noise at the right ear obtained with adaptive IMC system.

Attenuation at the right real microphone is the same for any registered head position and for a 250 Hz tone it is limited by the quantisation noise only, whereas for the real noise it is 2.9 dB.

C.3 VMC1 system

C.3.1 Optimal control

a)

	3L	2L	1L	0	1R	2R	3R
f	1.4	3.5	6.2	4.8	7.5	5.8	1.9
e	1.0	2.7	7.0	6.4	11.6	5.9	2.3
d	2.6	4.7	10.2	9.6	22.6	8.2	4.1
c	5.0	7.1	12.3	18.5	22.6	6.4	3.3
b	8.1	9.4	30.4	30.1	23.0	7.2	3.1
a	12.8	17.8	28.7	6.7	7.5	4.3	2.6

a)

	3L	2L	1L	0	1R	2R	3R
f	2.2	2.8	3.6	3.4	3.8	3.5	3.3
e	1.8	3.0	4.0	3.5	4.3	3.6	3.1
d	1.9	3.3	4.4	4.2	5.2	4.1	3.7
c	2.3	3.4	4.9	4.9	5.7	4.6	4.2
b	3.1	3.8	5.5	6.0	7.0	7.1	5.9
a	3.3	4.5	5.5	7.7	8.5	10.7	8.4

Figure C.5 Attenuation of a 250 Hz tone at the right ear (a) and at the right real microphone (b) obtained with optimal VMC1 system.

a)

	3L	2L	1L	0	1R	2R	3R
f	-0.1	-0.4	0.5	-0.1	1.0	0.7	-0.3
e	0.1	-0.3	1.5	1.7	1.9	0.7	0.2
d	-0.5	-1.1	1.3	1.6	2.2	1.4	0.2
c	0.7	0.6	1.2	2.5	2.3	1.8	0.7
b	0.4	0.2	1.6	2.5	2.2	1.4	0.8
a	-0.2	-0.8	-2.8	1.4	1.2	1.1	0.5

b)

	3L	2L	1L	0	1R	2R	3R
f	-0.9	-3.0	-0.9	-3.2	-0.4	0.0	-0.1
e	-0.2	-2.3	-0.6	-1.4	-0.3	0.5	0.4
d	-0.1	-2.2	0.3	0.6	1.1	0.9	0.8
c	0.5	-1.0	-0.5	0.9	1.3	0.9	0.8
b	0.3	0.1	-0.8	1.3	1.1	0.2	0.3
a	-0.4	-1.0	-2.3	1.4	1.6	1.5	1.4

Figure C.6 Attenuation of the real noise at the right ear (a) and at the right real microphone (b) obtained with optimal VMC1 system.

C.3.2 Adaptive control

The VMC1 system with adaptation performed using the FXLMS algorithm reveals poor results compared to the other VMC systems and they are not presented here.

C.4 VMC2 SYSTEM

C.4.1 OPTIMAL CONTROL

a)

	3L	2L	1L	0	1R	2R	3R
f	1.5	4.5	7.7	4.4	6.8	4.4	0.9
e	3.0	4.2	8.9	6.5	12.0	4.6	1.8
d	5.3	6.8	12.3	10.1	26.7	7.5	4.2
c	8.3	9.9	15.3	23	27.6	5.7	4.5
b	11.9	13.7	20.1	93.1	18.7	7.5	3.8
a	15.1	25.1	19.8	5.7	6.8	4.7	3.6

a)

	3L	2L	1L	0	1R	2R	3R
f	1.7	2.6	3.5	3.6	4.2	3.2	3.1
e	2.2	3.0	3.7	3.8	4.3	3.4	3.2
d	2.5	3.2	4.1	4.3	5.3	3.7	3.6
c	2.7	3.4	5.0	4.8	5.6	4.6	3.6
b	2.7	3.8	5.3	6.3	7.1	6.9	4.9
a	3.3	4.2	4.9	7.6	8.8	10.6	8.7

Figure C.7 Attenuation of a 250 Hz tone at the right ear (a) and at the right real microphone (b) obtained with optimal VMC2 system.

a)

	3L	2L	1L	0	1R	2R	3R
f	0.5	1.0	1.7	0.9	1.5	1.0	0.2
e	0.5	1.3	1.9	1.4	2.3	1.0	0.4
d	1.3	1.5	2.3	2.0	2.6	1.4	1.2
c	1.4	2.0	2.3	2.5	2.6	1.4	1.4
b	2.0	2.3	2.5	2.6	2.5	1.9	1.6
a	1.5	2.4	2.6	1.4	1.1	1.5	0.6

b)

	3L	2L	1L	0	1R	2R	3R
f	0.4	0.7	1.0	1.0	1.3	1.3	1.1
e	0.6	0.9	1.3	1.2	1.4	1.4	1.2
d	0.9	1.2	1.4	1.4	1.4	1.1	1.1
c	1.2	1.2	1.5	1.5	1.4	1.4	1.2
b	1.2	1.3	1.5	1.5	1.1	1.5	1.3
a	1.3	1.3	1.5	1.6	1.1	0.9	0.8

Figure C.8 Attenuation of the real noise at the right ear (a) and at the right real microphone (b) obtained with optimal VMC2 system.

C.4.2 ADAPTIVE CONTROL

a)

	3L	2L	1L	0	1R	2R	3R
f	3.4	4.4	7.4	4.2	7.2	3.6	-1.0
e	3.9	4.1	8.6	6.3	12.0	4.5	-0.2
d	5.7	6.3	12.3	10.2	26.6	7.6	3.4
c	7.0	9.3	14.5	22.8	26.1	5.7	4.8
b	9.5	12.5	19.8	22.9	18.7	7.5	6.5
a	17.7	23.4	18.4	5.4	6.4	4.6	4.1

b)

	3L	2L	1L	0	1R	2R	3R
f	1.9	2.2	2.7	2.9	3.3	3.1	3.2
e	2.1	2.3	3.1	2.9	3.8	3.3	3.2
d	2.0	2.4	3.9	3.6	4.7	3.6	3.7
c	2.4	2.8	4.4	4.5	5.3	4.5	3.9
b	2.6	3.3	5.2	5.9	6.7	7.1	7.0
a	3.5	3.8	4.9	7.3	8.3	10.4	8.1

Figure C.9 Attenuation of a 250 Hz tone at the right ear (a) and at the right real microphone (b) obtained with adaptive VMC2 system.

a)

	3L	2L	1L	0	1R	2R	3R
f	0.7	1.3	1.7	1.2	1.9	0.6	0.2
e	0.9	1.4	1.6	1.8	2.4	1.2	0.8
d	1.4	1.9	2.4	2.3	2.7	1.9	1.1
c	1.8	2.3	2.4	2.7	2.7	1.5	1.3
b	2.2	2.5	2.5	2.7	2.7	2.0	1.8
a	1.6	2.4	2.5	1.6	1.8	1.5	1.0

b)

	3L	2L	1L	0	1R	2R	3R
f	0.2	0.3	0.7	0.6	1.0	0.9	0.8
e	0.3	0.4	0.9	0.8	1.2	1.0	1.0
d	0.3	0.5	1.0	1.1	1.4	1.2	1.1
c	0.4	0.6	0.9	1.4	1.6	1.3	1.2
b	0.7	0.8	1.6	1.7	1.7	2.0	1.7
a	0.5	1.0	1.4	2.0	2.1	2.5	1.4

Figure C.10 Attenuation of the real noise at the right ear (a) and at the right real microphone (b) obtained with adaptive VMC2 system.

C.5 VMC3 SYSTEM

C.5.1 OPTIMAL CONTROL

The optimal VMC3 system yields the same results as the optimal VMC2 system under assumption of lack of modelling errors for the nominal head position.

C.5.2 Adaptive control

a)

	3L	2L	1L	0	1R	2R	3R
f	0.9	4.3	7.4	4.8	8.2	3.4	-0.3
e	2.1	4.1	8.6	7.8	13.0	4.3	1.2
d	4.0	6.9	12.4	15.1	26.8	7.5	2.4
c	8.1	9.9	18.1	25.8	27.1	8.4	3.3
b	10.5	14.2	23.6	93.6	22.7	7.8	4.2
a	17.7	24.9	18.4	9.4	8.3	4.8	3.1

b)

	3L	2L	1L	0	1R	2R	3R
f	1.1	2.2	3.0	2.9	3.6	3.1	3.3
e	1.2	2.2	3.1	3.1	4.9	3.3	3.5
d	1.6	2.5	4.0	3.8	5.0	3.8	3.9
c	1.9	2.9	4.1	4.0	5.3	4.6	6.1
b	2.6	3.3	5.1	5.9	5.9	7.1	8.0
a	2.8	3.7	4.9	7.5	8.3	10.4	9.3

Figure C.11 Attenuation of a 250 Hz tone at the right ear (a) and at the right real microphone (b) obtained with adaptive VMC3 system.

a)

	3L	2L	1L	0	1R	2R	3R
f	0.7	1.1	1.9	1.1	1.8	0.91	0.5
e	0.7	1.1	2.1	1.9	2.3	1.1	0.1
d	1.6	1.7	2.3	2.2	2.7	1.9	0.8
c	1.9	2.1	2.4	2.5	2.7	1.4	0.6
b	1.9	2.5	2.5	2.7	2.7	2.0	1.5
a	2.0	2.3	2.5	1.5	1.6	1.6	1.3

b)

	3L	2L	1L	0	1R	2R	3R
f	0.5	0.7	1.2	1.1	1.3	1.3	1.0
e	0.8	1.0	1.3	1.3	1.4	1.3	1.4
d	1.0	1.1	1.4	1.4	1.5	1.4	1.4
c	0.9	1.1	1.5	1.5	1.6	1.5	1.6
b	1.1	1.0	1.6	1.7	1.7	2.0	1.9
a	1.1	1.2	1.6	1.8	1.8	2.1	2.0

Figure C.12 Attenuation of the real noise at the right ear (a) and at the right real microphone (b) obtained with adaptive VMC3 system.

References

[AhlenS_89] A. Ahlén, M. Sternad: "Optimal Deconvolution based on polynomial methods", *IEEE Trans. Acoustics, Speech and Signal Processing*, 37(2), 217-226, 1989.

[AhlenS_91] A. Ahlén, M. Sternad: "Wiener filter desing using polynomial equations", *IEEE Trans. Signal Processing*, 39(11), 2387-2389, Nov. 1991.

[AhlenS_94] A. Ahlén, M. Sternad: "Filter design via inner-outer factorization: comments on 'Optimal deconvolution filter design based on orthogonal principle'", *Signal Processing*, 35(1), 51-587, Jan. 1994.

[AhujaS_91] K.K. Ahuja, J.C. Stevens: "Recent advances in active noise control", *AiAA Journal*, 7, 1058-1066, 1991.

[AstromW_84] K.J Åström, B. Wittenmark: *Computer-Controlled Systems*, Englewood Cliffs, Prentice Hall, New Jersey, 1984.

[AstromW_95] K.J Åström, B. Wittenmark: *Adaptive Control*, Addison-Wesley, 1995.

[BaiZ_04] M.R. Bai, P. Zeung: "Design of a broadband active silencer using μ-synthesis", *Journal of Sound and Vibration*, 269, 113-133, 2004.

[BendatP_93] J.S. Bendat, A.G. Piersol: *Engineering Applications of Correlation and Spectral Analysis*, J. Wiley & Sons, 1993.

[BiesH_96] D.A. Bies, C.H. Hansen: *Engineering Noise Control: Theory and Practice*, 2nd edition, E & FN Spon, London, 1996.

[Bjarnason_95] E. Bjarnason: "Analysis of the Filtered-x LMS algorithm", *IEEE Trans. Speech and Audio Processing*, 3(6), 504-514, Nov., 1995.

[BodsonD_97] M. Bodson, S.C. Douglas: "Adaptive algorithms for the rejection of periodic disturbances with unknown frequencies", *Automatica*, 33, 2213–2221, 1997.

[BodsonJD_01] M. Bodson, J.S. Jensen, S.C. Douglas: "Active noise control for periodic disturbances", *IEEE Trans. Control Systems Technology*, 9(1), 200–205, 2001.

[BottoSC_05] M.A. Botto, J.M.C. Sousa, J.M.G. Sá da Costa: "Intelligent active noise control applied to a laboratory railway coach model", *Control Engineering Practice*, 13, 473–484, 2005.

[Bouchard_01] M. Bouchard: "New recursive-least-squares algorithms for non-linear active control of sound and vibrations using neural networks", *IEEE Trans. on Neural Networks*, 12, 135–147, 2001.

[BoucherEN_91] C.C. Boucher, S.J. Elliott, P.A. Nelson: "The effect of errors in the plant model on the performance of algorithms for adaptive feedforward control", Proc. IEE-F, 138, 313-319, 1991.

[BoxJ_70] G.P. Box, G.M. Jenkins: *Time Series Analysis, Forecasting and Control*, Holden-Day, New York, 1970.

[BrothanekJ_02] M. Brothánek, O. Jiříček: "Formating of zones of quiet around a head simulator", Proc. ACTIVE'02, Southampton, UK, 117-121, 2002.

[BrownZ_04] L.J. Brown, Qing Zhang: "Periodic disturbance cancellation with uncertain frequency", *Automatica,* 40, 631 – 637, 2004.

[BrüelKjær_01] Brüel and Kjær: *Sound & Vibration Measurements A/S: Environmental Noise*, Brüel & Kjær, 2001.

[Bruyne_03] F. De Bruyne: "Iterative feedback tuning for internal model controllers", *Control Engineering Practice*, 11, 1043-1048, 2003.

[Burgess_81] J.C. Burgess: "Active adaptive sound control in a duct: a computer simulation", *Journal of the Acoustical Society of America*, 70, 715-726, 1981.

[Cazzolato_02] B. Cazzolato: "An adaptive LMS virtual microphone", Proc. ACTIVE'02, Southampton, UK, 105-116, 2002.

[ChenG_91] H.F. Chen, L. Guo: *Identification and Stochastic Adaptive Control*, Birkhäuser, Boston, 1991.

[ChenM_04] G. Chen, K. Muto: "A theoretical study of convergence characteristics of a multiple channel ANC system", *Int. Journal of Acoustics and Vibration*, 9(4), 191-197, 2004.

[Coanda] H. Coanda: Procédé de protection contre les bruits. *French Patent*, FR 722.274, Oct. 1930.

[Conover_56] W.B. Conover: "Filtering noise with noise", *Noise Control*, 2, 78-82, 1956.

[CookE_99] J.G. Cook, S.J. Elliott: "Connection between multichannel prediction error filter and spectral factorisation", *Electronics Letters*, 35, 1218-1220, 1999.

[Crocker_97] M. Crocker Ed.: *Encyclopedia of Acoustics*, J. Wiley & Sons, 1997.

[Czyz_04] K. Czyż: "Nonuniformly sampled Active Noise Control system", Proc. IFAC Workshop on Programable Devices and Systems, Cracow, 351-355, 2004.

[Davis_63] M.C. Davis: "Factoring the spectral matrix", *IEEE Trans. Automatic Control*, 8, 296-305, 1963.

[DennisS_83] J.E. Dennis Jr., R.B. Schnabel: *Numerical Methods for Unconstrained Optimization and Nonlinear Equations*, Prentice-Hall, 1983.

[DiegoGFP_04] M. de Diego, A. Gonzales, M. Ferrer, G. Piñero: "Multichannel active noise control system for local spectral reshaping of multifrequency noise", *Journal of Sound and Vibration*, 274, 249-271, 2004.

[DorlingEMRS_89] C.M. Dorling, G.P. Eastwell, S.M. Mutchins, C.F. Ross, S.G.C. Sutcliffe: "A demonstration of active noise reduction in an aircraft cabin", *Journal of Sound and Vibration*, 128, 358-360, 1989.

[DoyleFT_92] J.C. Doyle, B.A. Francis, A.R. Tannenbaum: *Feedback Control Theory*, Maxwell MacMillan Int., 1992.

[Elliott_96] S.J. Elliott: "Active noise and vibration control" (Plenary paper), Proc. 3rd Int. Symp. on Methods and Models in Automation and Robotics MMAR'96, Międzyzdroje, Poland, 1996.

[Elliott_01] S.J. Elliott: *Signal Processing for Active Control*, Academic Press, London, 2001.

[ElliottB_94] S.J. Elliott, C.C. Boucher: "Interaction between multiple feedforward active control systems", *IEEE Trans. Speech and Audio Processing*, 2, 521-530, 1994.

[ElliottN_85] S.J. Elliott, P.A. Nelson: "Algorithm for multichannel LMS adaptive filtering", *Electronics Letters*, 21, 979-981, 1985.

[ElliottN_89] S.J. Elliott, P.A. Nelson: "Multiple point equalisation in a room using adaptive digital filters", *Journal of the Audio Engineering Society*, 37(11), 899-908, 1989.

[ElliottN_93] S.J. Elliott, P.A. Nelson: "Active noise control", *IEEE Signal Processing Magazine*, 12-35, Oct. 1993.

[ElliottNSB_90] S.J. Elliott, P.A Nelson, I.M. Stothers, C.C. Boucher: "In-flight experiments on the active control of propeller induced cabin noise", *Journal of Sound and Vibration*, 140, 219-238, 1990.

[ElliottR_97] S.J. Elliott, B. Rafaely: "Frequency-domain adaptation of feedforward and feedback controllers", Proc. ACTIVE'97, 771-788, 1997.

[ElliottR_00] S.J. Elliott, B. Rafaely: "Frequency-domain adaptation of causal digital fitlers", *IEEE Trans. Signal Processing*, 48, 1354-1364, 2000.

[ElliottS_96] S.J. Elliott, T.J. Sutton: "Performance of feedforward and feedback systems for active control", *IEEE Trans. Speech and Audio Processing*, 4, 214-223, 1996.

[ElliottSN_87] S.J. Elliott, I.M. Stothers, P.A. Nelson: "A multiple error LMS algorithm and its application to the active control of sound and vibration", *IEEE Trans. Acoustics Speech and Signal Processing*, ASSP-35, 1423-1434, 1987.

[Engel_84] Z. Engel: "Aktywna redukcja drgań i hałasu" (in Polish), Mat. XI Symp. Drgania w Układach Fizycznych, 124-125, Poznań, Poland, 1984.

[EngelK_95] Z. Engel, J. Kowal: *Sterowanie Procesami Wibroakustycznymi* (in Polish), Univesity of Mining and Metalurgy Press, Cracow, 1995.

[Eriksson_91] L.J. Eriksson: "Development of the Filtered-U algorithm for active noise control", *Journal of the Acousticl Society of America*, 89(1), 257-265, 1991.

[ErikssonA_89] L.J. Erikson, M.C. Allie: "Use of random noise for on-line transducer modeling in an adaptive active attenuation system," *Journal of the Acoustical Society of America*, 85(2), 797-802, 1989.

[ErikssonAG_87] L.J. Eriksson, M. Allie, R. Greiner: "The selection and application of an IIR adaptive filter for use in active sound control", *IEEE Trans. Acoustics, Speech and Signal Processing* ASSP-35(4), 433-437, Oct. 1987.

[Figwer_03] J. Figwer: "A new method of on-line model identification and update for multichannel active noise control systems", *Archives of Control Sciences*, 13(2), 11-155, 2003.

[FigwerB_03] J. Figwer , M. Blazej: "Chaos in active noise control", Proc. 10th Int. Congress on Sound and Vibration, Stockholm, Sweden, 203-209, 2003.

[FigwerOP_02] J. Figwer, Z. Ogonowski, M. Pawełczyk "Stanowiska laboratoryjne do badań algorytmów aktywnej redukcji hałasu" (in Polish), Mat. 49 Otwartego Seminarium z Akustyki, 169-174, Stare Jabłonki, 2002.

[FigwerOP_03] J. Figwer, Z. Ogonowski, M. Pawełczyk: "Adaptacja w układach aktywnego tłumienia hałasu" (in Polish), Mat. 50 Otwartego Seminarium z Akustyki, Szczyrk, 454-457, 2003.

[Figwer_04] J. Figwer: "Multisine transformation - properties and applications", *Nonlinear Dynamics*, 35(4), 331-346, March 2004.

[FilatovU_04] N.M. Filatov, H. Unbehauen: *Adaptive Dual Control. Theory and Applications*, Springer-Verlag, Berlin, 2004.

[Fletcher_87] R. Fletcher: *Practical Methods of Optimization*, J. Wiley & Sons, 1987.

[FonescaSB_01] P. De Fonesca, P. Sas, H. Van Brussel: "Robust design and robust stability analysis of active noise control systems", *Journal of Sound and Vibration*, 243(1), 23-42, 2001.

[FraanjeVD_03] R. Fraanje, M. Verhaegen, N. Doelman: "Convergence analysis of the Filtered-U LMS algorithm for active noise control in case perfect cancellation is not possible", *Signal Processing*, 83, 1239-1254, 2003.

[Francis_87] B.A. Francis: *A Course in H_∞ Control Theory*, Springer-Verlag, Berlin, 1987.

[Garcia_96] J. Garcia-Bonito: *Local active control in pure tone diffracted diffuse sound fields*, Ph.D. Dissertation, University of Southampton, U.K., 1996.

[GarciaEB_96] J. Garcia-Bonito, S.J. Elliott, C.C. Boucher: "A virtual microphone arrangement in a practical active headrest", Proc. Inter-Noise 96, 1115-1120, 1996.

[GarciaEB_97] J. Garcia-Bonito, S.J. Elliott, C.C. Boucher: "A novel secondary source for a local active noise control system", Proc. ACTIVE'97, Budapest, Hungary, 405-418, 1997.

[Gessing_96] R. Gessing: "Causal and noncausal discrete-time transfer functions and their applications", *Int. Journal on Control*, 65(1), 195-204, Sept. 1996.

[Grace_95] A. Grace: *Matlab Optimization Toolbox*, The MathWorks, 1995.

[Grimble_85] M.J. Grimble: "Polynomial systems approach to optimal linear filtering and prediction", *Int. Journal on Control*, 41, 1545-1564, June 1985.

[GrimbleJ_88] M.J. Grimble, M.A. Johnson: *Optimal Control of Stochastic Estimation: Theory and Applications*, Vol. 2, J. Wiley & Sons, Chichester, 1988.

[HansenS_97] C. Hansen, S.D. Snyder: *Active Control of Noise and Vibration*, E & FN Spon, Cambridge, 1997.

[Harazin_98] B. Harazin: "Wpływ jednczesnego działania hałasu i wibracji ogólnej na ostrość widzenia: badania własne" (in Polish), Mat. Zimowej Szkoły Zwalczania Zagrożeń Wibroakustycznych, Gliwice-Ustroń, Poland, 99-106, 1998.

[HassibiSK_96] B. Hassibi, A.H. Sayed, T. Kailath: "H_∞ optimality of the LMS algorithm", *IEEE Trans. Signal Processing*, 44(2), 267-280, Feb. 1996.

[Haykin_96] S. Haykin: *Adaptive Filter Theory*, 3rd edn., Prentice Hall, 1996.

[HaykinW_03] S. Haykin, B. Widrow: *Least-Mean-Square Adaptive Filters*, J. Wiley & Sons, New Jersey, 2003.

[HolmbergRS_02] U. Holmberg, N. Ramnér, R. Slovak: "Low complexity robust control of a headrest system based on virtual microphones and the Internal Model Principle", Proc. ACTIVE'02, Southampton, UK, 1243-1250, 2002.

[Horowitz_63] I. M. Horowitz: *Synthesis of Feedback Systems*, Academic Press, London, 1963.

[HorowitzLM_98] R. Horowitz, B. Li, J.W. McCormick: "Wiener-filter-based minimum variance self-tuning regulation", *Automatica*, 34(5), 531-545, 1998.

[IonescuO_96] V. Ionescu, C. Oară: "Spectral and inner-outer factorizations for discrete-time systems", *IEEE Trans. Automatic Control*, 41, 1840-1845, 1996.

[Ising_98] H. Ising: "Noise as a risk factor in myocardial infraction" (Plenary paper), Mat. XLV Otwartego Seminarium Akustyki, Poznań-Kiekrz, Poland, 1, 15-26, 1998.

[JacobsonJMS_01] C.A. Jacobson, C.R. Johnson, D.C. McCormick, W.A. Sethares: "Stability of active noise control", *IEEE Signal Processing Letters*, 8(3), 74-76, March 2001.

[JosephEN_94] P. Joseph, S.J. Elliott, P.A. Nelson: "Near field zones of quiet", *Journal of Sound and Vibration*, 172(5), 605-627, 1994.

[Jury_70] E.I. Jury: *Przekształcenie Z i jego zastosowania* (translated from *Theory and Application of the Z-transform Method*, Wiley), WNT, Warszawa, 1970.

[Kaczorek_93] T. Kaczorek: *Teoria sterowania i systemów* (in Polish), PWN, Warszawa, 1993.

[KailathSH_00] T. Kailath, A.M. Sayed, B. Hassibi: *Linear Estimation*, Prentice Hall, 2000.

[Kasprzyk_03] J. Kasprzyk: "MULTI-EDIP – an interactive software package for process identification, Proc. 13th IFAC Symp. System Identification – SYSID 2003", Rotterdam, 1484-1489, 2003.

[KestellCH_99] C. Kestell, B. Cazzolato, C. Hansen: "Active noise control in a free field with a virtual microphone and a virtual energy density sensor", *Journal of the Acoustical Society of America*, 48(4), 475–483, 1999.

[KestellCH_00] C. Kestell, B. Cazzolato, C. Hansen: "Virtual energy density sensing in active noise control systems". Proc. Int. Congress on Sound and Vibration, Adelaide, 2000.

[KestellHC_00] C. Kestell, C. Hansen, B. Cazzolato: "Active noise control with virtual sensors in a long narrow duct", *International Journal of Acoustics and Vibration*, 5(2), 63–76, 2000.

[KestellCH_01] C. Kestell, B. Cazzolato, C. Hansen: "Active noise control in a free field with virtual sensors", *Journal of the Acoustical Society of America*, 109(1), 232–243, 2001.

[Kociolek_02] R. Kociołek: *Tłumienie hałasu w aktywnym zagłówku fotela* (in Polish), M.Sc. Dissertation, Silesian University of Technology, Gliwice, 2002.

[Kucera_79] V. Kučera: *Discrete Linear Control. The Polynomial Equation Approach*, J. Wiley & Sons, Chichester, 1979.

[KuoM_96] S.M. Kuo, D.R. Morgan: *Active Noise Control Systems. Algorithms and DSP Implementations*, J. Wiley & Sons, New Jersey, 1996.

[Kwong_90] C.P. Kwong: "Control-theoretic design of the LMS and the Sign Algorithms in Nonstationary environments", *IEEE Trans. Acoustics, Speech, Signal Processing*, 38(2), 253-259, 1990.

[LjungS_83] L. Ljung, T. Söderström: *Theory and Practive of Recursive Identification*, MIT Press, Cambridge, MA, 1983.

[Lueg_36] P. Lueg: "Process of silencing sound oscillations", *U.S. Patent*, No 2,043,416, 1936.

[Maciejowski_89] J.M. Maciejowski: *Multivariable Feedback Design*, Addison-Wesley, 1989.

[Macchi_95] O. Macchi: *Adaptive Processing. The Least Mean Squares Approach with Applications in Transmission*, J. Wiley & Sons, Chichester, 1995.

[MacrosM_87] S. Macros, O. Macchi: "Tracking capabilities of the Least Mean Square algorithm: application to an asynchronous echo canceller", *IEEE Trans. Acoustics, Speech, Signal Processing*, 35(11), 1570-1578, Nov. 1987.

[Makarewicz_93] G.J. Makarewicz: *Problemy stabilności w układach aktywnej redukcji dźwięku* (in Polish), Ph.D. Dissertation, University of Mining and Metalurgy, Cracow, 1993.

[MarinoST_03] R. Marino , G.L. Santosuosso, P. Tomei: "Robust adaptive compensation of biased sinusoidal disturbances with unknown frequency", *Automatica*, 39, 1755-1761, 2003.

[Marvasti_01] F. Marvasti: *Nonuniform Sampling. Theory and Practice*, Kluwer, New York, 2001.

[Michalczyk_04] M.I. Michalczyk: *Adaptive Contol Algorithms for Three-Dimensional Zones of Quiet*, Ph.D. Dissertation, Jacek Skalmierski Computer Studio, 2004.

[MitraK_93] S.K. Mitra, J.K. Kaiser: *Handbook for Digital Signal Processing*, J. Wiley & Sons, New York, 1993.

[MorariZ_89] M. Morari, E. Zafiriou: *Robust Process Control*, Prentice-Hall, New Jersey, 1989.

[Morgan_80] D. Morgan: "An analysis of multiple correlation cancellation loops with a filter in the auxiliary path", *IEEE Trans. Acoustics, Speech, Signal Processing*, ASSP-28, 454-467, 1980.

[MunnCHK_02] J. Munn, B. Cazzolato, C. Hansen, D. Kestell: „Higher-order virtual sensing for remote active noise control", Proc. ACTIVE'02, Southampton, UK, 377-386, 2002.

[NelsonE_94] P.A. Nelson, S.J. Elliott: *Active Control of Sound*, Academic Press, Cambridge, 1994.

[Niederlinski_95] A. Niederliński: "An upper bound for the Recursive Least Squares estimation error", *IEEE Trans. Automatic Control*, 40(9), 1655-1661, 1995.

[NiederlinskiKF_93] A. Niederliński, J. Kasprzyk, J. Figwer: *EDIP – ekspert dla identyfikacji procesów. Podręcznik użytkownika* (in Polish), Silesian University of Technology Press, Gliwice, 1993.

[NiederlinskiKF_97] A. Niederliński, J. Kasprzyk, J. Figwer: *MULTI-EDIP – analizator wielowymiarowych sygnałów i obiektów* (in Polish), Silesian University of Technology Press, Gliwice, 1997.

[NiederlinskiMO_95] A. Niederliński, J. Mościński, Z. Ogonowski: *Regulacja Adaptacyjna*, WNT, Warszawa, 1995.

[NowlinGT_02] W.C. Nowlin, G.S. Guthart, G.K. Toth: "Noninvasive system identification for the multichannel broadband active noise control", *Journal of the Acoustical Society of America*, 107, 2049-2060, 2000.

[OaraV_99] C. Oară, A. Varga: "The general inner-outer factorisation problem for discrete-time systems", *www.er.robotic.dlr.de/control/publications/1999/varga_ecc99p1.pdf*.

[Ogonowski_94] Z. Ogonowski: "Adaptive noise control using direct method", Mat. XXII Zimowa Szkoła Zwalczania Zagrożeń Wibroakustycznych, Wisła, Poland, 65-66, 1994.

[OlsonM_53] H.F. Olson, E.G. May: "Electronic sound absorber", *Journal of the Acoustical Society of America*; 25, 1130-1136, 1953.

[OmotoE_97] A. Omoto, S.J. Elliott: "The effect of structured plant uncertainty on the stability and performance of multichannel feedforward controllers", Proc. ACTIVE'97, 825-836, Budapest, Hungary, 1997.

[OppenheimS_75] A.V. Oppenheim, R.W. Shafer: *Digital Signal Processing*, Prentice Hall, 1975.

[Orfanidis_88] S.J. Orfanidis: *Optimum Signal Processing*, Macmillan Publishin Company, New York, 1988.

[Papoulis_77] A. Papoulis: *Signal Analysis*, McGraw Hill, 1977.

[Park_02] C. Park: "Evaluation and demonstration of advanced active noise control in a passenger automobile", Proc. ACTIVE'02, Southampton, UK, 275-284, 2002.

[Pawelczyk_99a] M. Pawełczyk: *Active Noise Control for Compact Acoustic Plants*, Jacek Skalmierski Computer Studio, Gliwice, 1999.

[Pawelczyk_99b] M. Pawełczyk: "Minimum variance control for small acoustic plants", Proc. 6th Int. Congress on Sound and Vibration, Copenhagen, Denmark, CD-ROM, 1563-1570, 1999.

[Pawelczyk_99c] M. Pawełczyk: "Algorytmy tłumienia hałasu w aktywnym ochronniku słuchu", Mat. Przegląd Grantów KBN z Dziedziny Akustyki, 273-278, Kraków, Poland, 1999.

[Pawelczyk_00a] M. Pawełczyk: "Minimum variance control for acoustically-compact plants", *Int. Journal of Acoustics and Vibration*, 5(4), 183-189, 2000.

[Pawelczyk_00b] M. Pawełczyk: "Adaptive noise control for compact acoustic plants", Proc. of 6th International Conference on Methods and Models in Automation and Robotics – MMAR'2000, 1, 391-396, Międzyzdroje, Poland, 2000.

[Pawelczyk_00c] M. Pawełczyk: "Aktywne tłumienie hałasu w kompaktowych obiektach akustycznych - tematyka rozprawy doktorskiej" (in Polish), Mat. XXVIII Zimowa Szkoła Zwalczania Zagrożeń Wibroakustycznych, Wisła, Poland, 2000.

[Pawelczyk_01] M. Pawełczyk: "Analysis of active noise control plants using process identification and signal processing methodology, *Archives of Acoustics*, 26(2), 143-164, 2001.

[Pawelczyk_02a] M. Pawełczyk: "Feedforward algorithms with simplified plant model for active noise control", *Journal of Sound and Vibration*, 255(1), 77-95, 2002.

[Pawelczyk_02b] M. Pawełczyk "Analogue active noise control", *Applied Acoustics*, 63(11), 1193-1213, 2002

[Pawelczyk_02c] M. Pawełczyk: "Control algorithms for locating zones of quiet in the active headrest system", *Molecular & Quantum Acoustics*, 23, 339-350, 2002.

[Pawelczyk_02d] M. Pawełczyk "Analogue-digital control for active headsets", Proc. ACTIVE'02, 1219-1230, Southampton, UK, 2002.

[Pawelczyk_02e] M. Pawełczyk: "Control of sound in an active headrest system, Proc. 8th IEEE Conf. on Methods and Models in Automation and Robotics – MMAR'02, Szczecin, Poland, 1157-1162, 2002.

[Pawelczyk_02f] M. Pawełczyk "Aktywny zagłówek fotela" (in Polish), Mat. XXX Zimowej Szkoły Zwalczania Zagrożeń Wibroakustycznych, 109-114, Ustroń, Poland, 2002.

[Pawelczyk_02g] M. Pawełczyk "Projektowanie i realizacja analogowego układu sterowania dla aktywnego tłumienia hałasu w personalnym ochronniku słuchu" (in Polish), Mat. XIV Krajowej Konferencji Automatyki, 903 – 908, Zielona Góra, Poland, 2002.

[Pawelczyk_02h] M. Pawełczyk: "Research on active noise control" (a note), *Int. Sound & Vibration Digest*, 8(1/33), on-line edition (www.iiav.org), May 2002.

[Pawelczyk_02i] M. Pawełczyk "Identyfikacja niestacjonarnych modeli parametrycznych", chapter in J. Kasprzyk Ed. *Identyfikacja Procesów* (in Polish), Silesian University of Technology Press, 2002.

[Pawelczyk_03a] M. Pawełczyk, "Multiple input-multiple output adaptive feedback control strategies for the active headrest system: design and real-time implementation", *Int. Journal of Adaptive Control and Signal Processing*, 17(10), 785-800, 2003.

[Pawelczyk_03b] M. Pawełczyk: "A hybrid active noise control system", *Archives of Control Sciences*, 13(XLIX), 191-213, 2003.

[Pawelczyk_03c] M. Pawełczyk: "A double input – quadruple output adaptive controller for the active headrest system", *Mechanika*, 22(3), 367-374, 2003.

[Pawelczyk_03d] M. Pawelczyk: "Noise control in the active headrest based on estimated residual signals at virtual microphones", Proc. 10th Int. Congress on Sound and Vibration, Stockholm, Sweden, 251-258, 2003.

[Pawelczyk_03e] M. Pawelczyk: "Filtered-reference, Filtered-error and Shaped-error LMS algorithms for noise control in an active headrest system", Proc. 9th IEEE Conf. on Methods and Models in Automation and Robotics – MMAR'03, Międzyzdroje, Poland, 549-554, 2003.

[Pawelczyk_03f] M. Pawelczyk: "Comparison of two virtual microphone based adaptive systems for active noise control", Proc. 9th IEEE Conf. on Methods and Models in Automation and Robotics – MMAR 03, Międzyzdroje, Poland, 545-548, 2003.

[Pawelczyk_03g] M. Pawelczyk, "Advances in acoustic signal processing" (a note), *Int. Sound & Vibration Digest*, 9(1/51), on-line edition (www.iiav.org), 2003.

[Pawelczyk_04a] M. Pawełczyk, "Adaptive noise control algorithms for active headrest system", *Control Engineering Practice* 12(9), 1101-1112, 2004.

[Pawelczyk_04b] M. Pawełczyk, "Active Noise Control in a Phone", Proc. 11th Int. Congress on Sound and Vibration, St. Petersburgh, Russia, 523-530, 2004.

[Pawelczyk_04c] M. Pawełczyk, "Algorithms and applications in acoustic signal processing", (a note), *Int. Sound & Vibration Digest*, 10(1/53), on-line edition (www.iiav.org), 2004.

[Pawelczyk_05a] M. Pawelczyk: "Optymalny układ sterowania do generacji stref ciszy w żądanym położeniu" (in Polish), accepted to Krajowa Konferencja Automatyki KKA'2005, Warszawa, Poland, 2005.

[Pawelczyk_05b] M. Pawelczyk: "Design and analysis of a virtual-microphone active noise control system", accepted to the 12th Int. Congress on Sound and Vibration, Lisbon, Portugal, 2005.

[Pawelczyk_05c] M. Pawelczyk: "Analog active control of acoustic noise at desired location", submitted to *IEEE Trans. Control Systems Technology*, 2005.

[PawelczykW_01] M. Pawełczyk, P. Wicher: "Analogowo-cyfrowe algorytmy sterowania i realizacja praktyczna aktywnego personalnego ochronnika słuchu" (in Polish), Mat. XXIX Zimowa Szkoła Zwalczania Zagrożeń Wibroakustycznych, Wisła, Poland, 217-224, 2001.

[Rafaely_97] B. Rafaely: *Feedback Control of Sound*, PhD Dissertation, University of Southampton, 1997.

[Rafaely_01] B. Rafaely: "Zones of quiet in a broadband diffuse sound field", *Journal of the Acoustical Society of America*, 110(1), 296-302, 2001.

[RafaelyE_96] B. Rafaely, S.J. Elliott: "Adaptive internal model controller – stability analysis", Inter-Noise 96, Liverpool, UK, 983-988, 1996.

[RafaelyE_99] B. Rafaely, S.J. Elliott: "H_2/H_∞ active control of sound in a headrest: design and implementation", *IEEE Trans. Control Systems Technology*, 7(1), 79-84, 1999.

[RafaelyEG_99] B. Rafaely, S.J. Elliott, J. Garcia-Bonito: "Broadband performance of an active headrests", *Journal of the Acoustical Society of America*, 106(2), 787-793, 1999.

[RafaelyGE_97] B. Rafaely, J. Garcia-Bonito, S.J. Elliott: "Feedback control of sound in headrest", Proc. ACTIVE'97, Budapest, Hungary, 445-456, 1997.

[RamosSLM_02] P. Ramos, A. Salinas, A. López, E. Masgrau: "Practical implementation of a multiple-channel FxLMS active noise control system with shaping of the residual noise inside a van", Proc. ACTIVE'02, Southampton, UK, 303-314, 2002.

[RobertsV_73] A.W. Roberts, D.E. Varberg: *Convex Functions*, Academic Press, 1973.

[RoureA_99] A. Roure, A. Albarrazin: "The remote microphone technique for active noise control", Proc. ACTIVE'99, Fort Lauderdale, USA, 1233–1244, 1999.

[SaitoS_96] N. Saito, T. Sone: "Influence of modelling errors on noise reduction performance of active noise control systems using filtered-X LMS algorithm", *Journal of the Acoustical Society of Japan*, 17, 195-202, 1996.

[SakaiM_03] H. Sakai, S. Miyagi: "Analysis of the adaptive filter algorithm for feedback-type active noise control", *Signal Processing*, 83, 1291-1298, 2003.

[SastryB_89] S. Sastry, M. Bodson: *Adaptive Control. Stability, Convergence and Robustness*, Prentice-Hall, New Jersey, 1989.

[SeronBG_97] M.M. Seron, J.H. Braslavsky, G.C. Goodwin: *Fundamental Limitations in Filtering and Control*, Springer-Verlag, London, 1997.

[ShanK_98] T.J. Shan, T. Kailath: "Adaptive algorithms with an automatic gain control feature", *IEEE Trans. Circuit and Systems CAS-35*, 122-127, 1998.

[Shynk_89] J. J. Shynk: "Adaptive IIR filtering", *IEEE Acoustics Speech and Signal Processing Magazine*, 6(2), 4-21, April 1989.

[Shynk_92] J.J. Shynk: "Frequency-domain and multirate adaptive filtering", *IEEE Signal Processing Magazine*, 14-37, Jan. 1992.

[SkogestadP_96] S. Skogestad, I. Posltethwaite: *Multivariable Feedback Control*", J. Wiley & Sons, Chichester, 1996.

[SnyderH_94] S.D. Snyder, C. H. Hansen: "The effect of transfer function estimation errors on the Filtered-X LMS algorithm", *IEEE Trans. Signal Processing*, 42(4), 950-953, April 1994.

[SternadA_93] M. Sternad, A. Ahlén: "A novel derivation methodology for polynomial-LQ controller design", *IEEE Trans. Automatic Control*, 38, 116-121, Jan. 1993.

[TapiaK_90] J. Tapia, S.M.Kuo: "New adaptive on-line modelling techniques for active noise control systems", Proc. IEEE Conf. on Systems Engineering, 280-283, 1990.

[ToivonenM_03] H.T. Toivonen, A. Medvedev: "Damping of harmonic disturbances in sampled-data systems – parameterization of all optimal controllers, *Automatica*, 39, 75-80, 2003.

[TokhiL_92] M.O. Tokhi, R.R. Leitch: *Active Noise Control*, Clarendon Press, Oxford, 1992.

[TsengRE_02] W.K. Tseng, B. Rafaely, S.J. Elliott: "Performance limits and real-time implementation of a virtual microphone active headrest", Proc. ACTIVE'02, Southampton, UK, 1231-1242, 2002.

[VaudreyBS_03] M.A. Vaudrey, W.T. Baumann, R. Saunders: "Stability and operating constraints of adaptive LMS- feedback control", *Automatica*, 39, 595-605, 2003.

[VeenaN_04] S. Veena, S.V. Narasimhan: "Improved active noise control performance based on Laguerre lattice", *Signal Processing*, 84, 695-707, 2004.

[Vidyasagar_85] M. Vidyasagar: *Control Systems Synthesis. A Factorization Approach*, MIT Press, Cambridge, MA, 1985.

[WalachW_83] E. Walach, B. Widrow: "Adaptive signal processing for adaptive control", Proc. IFAC Workshop on Adaptive Systems in Control and Signal Processing, 1983.

[WangR_99] A. Kuo Wang, W. Ren: "Convergence analysis of the filtered-U algorithm for active noise control", *Signal Processing*, 73, 255-266, 1999.

[WangR_99b] A. Kuo Wang, W. Ren: "Convergence analysis of the multi-variable filtered-x algorithm with application to active noise control", *IEEE Trans. Signal Processing*, 47, 1166-1169, 1999.

[Weinmann_91] A. Weinmann: *Uncertain Models and Robust Control*, Springer-Verlag, Wien, 1991.

[Whittle_63] P. Whittle: "On the fitting of multivariate autoregressions and the approximate canonical factorization of a spectral density matrix", *Biometrika*, 50, 129-134, 1963.

[Widrow_86] B. Widrow: "Adaptive inverse control", 2nd IFAC Workshop on Adaptive Systems in Control and Signal Processing, 1986.

[WidrowS_85] B. Widrow, S.D. Stearns: *Adaptive Signal Processing*, Prentice Hall, Englewood, 1985.

[WidrowSS_81] B. Widrow, D. Shur, S. Shaffer: "On adaptive inverse control", Proc. 15th Conf. on Circuits, Systems and Computers, 185-195, 1981.

[Wilkosz_01] M. Wilkosz: *Active noise control in headrests* (in Polish), M.Sc. Dissertation, Silesian University of Technology, Gliwice, 2001.

[Wilson_72] G.T. Wilson: "The factorisation of matricial spectral densities", *Journal of Applied Mathematics*, 32, 420-426, 1972.

[WuB_04] B. Wu, M. Bodson: "Multi-channel active noise control for periodic sources – indirect approach", *Automatica*, 40, 203-212, 2004.

[Zawieska_91] W.M. Zawieska: *Analiza i Synteza Układu Aktywnej Redukcji Hałasu* (in Polish), Ph.D. Dissertation, University of Mining and Metalurgy, Cracow, 1991.

[ZhangF_92] Z. Zhang, J.S. Freudenberg: "Formulas for minimum-phase / all-pass factorization of discrete-time transfer functions", *Control Theory and Advanced Technology*, 8, 743-754, 1992.

[ZhangG_04] Q.Z Zhang, W.S. Gan: "A model predictive algorithm for active noise control with online secondary path modelling", *Journal of Sound and Vibration*, 270, 1056-1066, 2004.

[ZhangG_04b] Q.Z Zhang, W.S. Gan: "Active noise control usinga simplified fuzzy neural network", *Journal of Sound and Vibration*, 272, 437-449, 2004.

GLOSSARY

t	-	continuous-time variable
i	-	discrete-time variable
t_c	-	convergence time
τ	-	time constant
z	-	*Z*-transform variable, forward time-shift operator
z^{-1}	-	inverse of the *Z*-transform variable, backward time-shift operator, dropped if all the terms are of z^{-1} for the given equation
T_s	-	sampling period
f_s	-	sampling frequency
ω	-	angular frequency
Ω	-	frequency bin
n	-	frequency bin number
λ	-	eigenvalue of the cross-correlation matrix
j	-	$\sqrt{-1}$, index
l	-	index
β	-	weighting coefficient for filter parameters
μ	-	convergence coefficient (step size)
q	-	weighting coefficient
k	-	discrete time delay
N	-	number of control filter coefficients
M	-	number of plant (or plant model) parameters
P	-	number of tones in a multi-tonal noise
G	-	number of real or virtual microphones
I	-	number of secondary sources
Er, Ev	-	real and virtual microphones
G1-G4	-	secondary sources (loudspeakers)
$u(i)$	-	control signal
$r(i)$	-	filtered-reference signal
$r_\delta(i)$	-	modified filtered-reference signal
$x(i)$	-	reference signal, filter input signal

$d(i)$	-	disturbance signal
$y(i)$	-	general output signal, controlled signal
$y_r(i)$	-	output signal of the real microphone
$y_v(i)$	-	output signal of the virtual microphone
$y'(i)$	-	synthesised signal in the VMC3 system
$e(i)$	-	white noise signal
$e'(i)$	-	innovations process
S	-	transfer function of a general plant
S_o	-	transfer function of a nominal plant
δS	-	multiplicative uncertainty of plant S
$\overline{\delta S}$	-	upper bound of the multiplicative plant uncertainty
S_r	-	transfer function of the real path
S_v	-	transfer function of the virtual path
ΔS	-	difference path ($S_r - S_v$)
$\hat{\Delta S}$	-	difference filter (model of ΔS)
S_1, S_2	-	transfer functions used in the general notation
F, F_1, F_2	-	disturbance-shaping filter and its components
W	-	control filter
W_{opt+}	-	optimal causal control filter
W_∞	-	adaptive control filter, when converged
H	-	overall feedback controller
V, V_r, V_v	-	Sensitivity Function (General-Output, Real-Output, Virtual-Output)
T, T_r, T_v	-	Complementary Sensitivity Function (General-Output, Real-Output, Virtual-Output)
B_W	-	control path (BW)
K	-	additional filter in the VMC3 system
A, B, C	-	auxiliary transfer functions used for analysis of the adaptive systems
$S_\bullet(e^{j\omega T_s})$	-	frequency response of $S_\bullet(z)$
$S_{dd}(e^{j\omega T_s})$	-	Power Spectral Density of $d(i)$
L	-	cost function in the time domain
L_ω	-	cost function in the frequency domain
J	-	attenuation, measured by a sound analyser
$J(f)$	-	frequency-dependent attenuation
$\lVert\bullet\rVert_2$	-	H_2 norm of $\bullet$
$\lVert\bullet\rVert_\infty$	-	H_∞ norm of $\bullet$
$\hat{\bullet}$	-	model or estimate of $\bullet$

$\bullet(z)$	-	time-reversed form of $\bullet(z^{-1})$
$\bullet(n)$	-	response of $\bullet$ at the frequency bin n
$\bullet^{(i)}$	-	inner part of $\bullet$
$\bullet^{(o)}$	-	outer part of $\bullet$
$\{\bullet\}_+$	-	causal part of $\{\bullet\}$
$\{\bullet\}_-$	-	non-causal par of $\{\bullet\}$
$\bullet^*$	-	complex conjugate of $\bullet$
$\deg\bullet$	-	degree of polynomial $\bullet$
$\dim\bullet$	-	dimension of matrix $\bullet$
$\sigma\{\bullet\}$	-	singular value of matrix $\bullet$
$\bar{\sigma}\{\bullet\}$	-	largest singular value of matrix $\bullet$
$\mathrm{eig}\{\bullet\}$	-	eigenvalues of matrix $\bullet$
$\angle\{\bullet\}$	-	phase angle of $\bullet$
$\mathrm{Re}\{\bullet\}$	-	real part of $\bullet$
$E\{\bullet\}$	-	expected value of $\bullet$
$\underline{s}_\bullet$	-	vector of impulse response parameters of $S_\bullet$
$\underline{w}$	-	vector of control filter parameters W
$\underline{x}(i)$	-	vector of regressors of the reference signal
$\underline{r}(i)$	-	vector of regressors of the filtered-reference signal
$\underline{u}(i)$	-	vector of regressors of the control signal
$\underline{x}_j(i)$	-	vector of regressors of the j-th reference signal
$\underline{u}_j(i)$	-	vector of regressors of the j-th control signal
$\mathbf{d}(i)$	-	vector of multi-channel disturbance signal
$\mathbf{x}(i)$	-	vector of multi-channel reference signal
$\mathbf{u}(i)$	-	vector of multi-channel control signal
$\mathbf{y}(i)$	-	vector of multi-channel controlled (output) signal
$\mathbf{I}_G$	-	unity matrix of dimension G
$\mathbf{X}(i)$	-	matrix composed of identical vectors $\mathbf{x}(i)$
$\mathbf{Y}(i)$	-	matrix composed of identical vectors $\mathbf{y}(i)$
$\mathbf{W}$	-	matrix of control filters
$\mathbf{S}, \mathbf{S}_r, \mathbf{S}_v$	-	matrices of path responses
$\mathbf{W}_j$	-	constant matrix of j-th parameters of the control filters
$\{\bullet\}^H$	-	Hermitian of $\bullet$
$\mathbf{S}_{dd}$	-	matrix power spectral density of the disturbance signal

$\mathbf{R}_{dd}(m)$	-	matrix of autocorrelation function values
$\mathbf{V}$	-	matrix sensitivity function.
$\mathbf{T}$	-	matrix complementary sensitivity function
$\mathbf{H}$	-	matrix of the overall feedback controller
$\mathbf{w}_j$	-	constant vector of j-th parameters of the control filters
$\mathbf{w}$	-	concatenated vector of parameters of the control filters
$\mathbf{r}_j(i)$	-	concatenated vector of filtered-reference signals contributing to j-th output
$\mathbf{R}(i)$	-	block Toeplitz matrix of multi-channel filtered-reference signal
$\delta\mathbf{S}(e^{j\omega T_s})$	-	matrix of multiplicative unstructured plant uncertainties
$\mathbf{Z}$	-	matrix of backward shift operators
k_{jl}	-	discrete time delay of the $S_{2,jl}$-th element of matrix $\mathbf{S}_2$
$\mathbf{Q}_{IxG}$	-	matrix for weighting models of the cross paths by coefficient q
$\otimes$	-	product of corresponding matrix elements or blocks
A/D	-	Analogue-to-Digital (converter)
ANC	-	Active Noise Control
DIDO	-	Double-Input Double-Output
DIQO	-	Double-Input Quadruple-Output
DFT	-	Discrete Fourier Transform
D/A	-	Digital-to-Analogue (converter)
FELMS	-	Filtered-Error LMS
FULMS	-	Filtered Recursive LMS
FXLMS	-	Filtered-Reference LMS (Filtered-x LMS)
FFT	-	Fast Fourier Transform
FIR	-	Finite Impulse Response
IDFT	-	Inverse Discrete Fourier Transform
IIR	-	Infinite Impulse Response
IMC	-	Internal Model Control
LHS	-	Left-Hand Side
LFXLMS	-	FXLMS with Leakage, Leaky FXLMS
LMS	-	Least Mean Squares
LQ	-	Linear Quadratic
MIMO	-	Multi-Input Multi-Output
ODE	-	Ordinary Differential Equations
PSD	-	Power Spectral Density
QIDO	-	Quadruple-Input Double-Output
QIQO	-	Quadruple-Input Quadruple-Output
RHS	-	Right-Hand Side
RLS	-	Recursive Least Squares
SELMS	-	Shaped-Error LMS

SISO	-	Single-Input Single-Output
SPL	-	Sound Pressure Level
SPR	-	Strictly Positive Real
SSV	-	Structured Singular Value
VMC	-	Virtual Microphone Control
VMC1, 2, 3	-	VMC systems in different structures

Other symbols used in this monograph have only a local character.

Zastosowanie układów regulacji do tłumienia hałasu w zadanych położeniach

Streszczenie

Celem badań jest projektowanie i weryfikacja algorytmów sterowania ze sprzężeniem zwrotnym, umożliwiających tłumienie hałasu w żądanych miejscach w przestrzeni dla grupy obiektów elektro-akustycznych. Grupa ta została scharakteryzowana niewielkimi odległościami pomiędzy tymi punktami, a miejscami umieszczenia odpowiadających im mikrofonów rzeczywistych, w porównaniu do najmniejszej długości fali akustycznej istotnie wpływającej na poziom ciśnienia akustycznego hałasu.

Rozważane obiekty są nieminimalnofazowe (włączając opóźnienie), i dlatego osiągnięcie całkowitego tłumienia przy pomocy przyczynowego i stabilnego regulatora jest niemożliwe. Ze względu na swoje właściwości wybrano strukturę sterowania z modelem wewnętrznym obiektu – IMC, w której estymowany sygnał zakłócający wyjście obiektu, w tym przypadku hałas, stanowi wejście tzw. filtru sterującego. Chociaż algorytmy sterowania optymalnego w tej strukturze są znane, w niniejszej pracy zostały one usystematyzowane pod kątem aktywnego tłumienia hałasu. Projekt optymalnego filtru H_2 przeprowadzono korzystając z podejścia wielomianowego, częstotliwościowego i korelacyjnego, dla rzadko poruszanego w literaturze przypadku istnienia błędów modelowania obiektu. Równoważność (pod pewnymi warunkami) tych podejść zweryfikowano na drodze symulacji. Ich złożoność i przydatność zależy od konkretnej aplikacji. W przypadku podejścia wielomianowego wymagane jest przeprowadzenie faktoryzacji modelu toru rzeczywistego obiektu na część minimalnofazową (tzw. wewnętrzną) i wszechprzepustową (tzw. wewnętrzną), faktoryzacji oceny gęstości widmowej mocy zakłócenia oraz ekstrakcji części przyczynowej filtru lub rozwiązanie

równania Diofantycznego. Operacje te są mniej złożone w dziedzinie częstotliwości. Jednak w tym przypadku należy znaleźć parametry filtru sterującego o wyznaczonej odpowiedzi częstotliwościowej. Podejście korelacyjne wymaga z kolei wyznaczenia macierzy oceny autokorelacji i wektora oceny korelacji wzajemnej pewnych sygnałów, co ze względów obliczeniowych przeprowadza się często korzystając z transformaty Fouriera. Zaprezentowano również uproszczoną analizę stabilności optymalnego układu sterowania. Wynika z niej, że rozwiązanie bardziej odporne na błędy modelowania można uzyskać, uwzględniając w funkcji kosztów na przykład ważenie parametrów filtru sterującego.

Oddzielnie potraktowano problem tłumienia hałasu deterministycznego. Pokazano, że rozwiązanie w postaci optymalnego przyczynowego filtru sterującego zawsze istnieje i jest ono niejednoznaczne pod warunkiem, że wybrano odpowiednio bogatą strukturę tego filtru. Możliwe jest wówczas całkowite tłumienie hałasu (do poziomu tła akustycznego) niezależnie od właściwości obiektu, jeśli tylko w jego odpowiedzi częstotliwościowej nie ma głębokich dolin dla częstotliwości odpowiednich tonów.

W dalszej części rozważano regulację adaptacyjną. Do aktualizowania parametrów filtru sterującego o skończonej odpowiedzi impulsowej (strukturze FIR) wybrano algorytm FXLMS, najczęściej stosowany w literaturze poświęconej aktywnemu tłumieniu hałasu. Zaprezentowano również krótko inne reprezentacje i modyfikacje tego algorytmu, których wykorzystanie zależy od konkretnej aplikacji oraz wspomniano inne algorytmy adaptacji. Uporządkowano także znane z literatury wystarczające warunki zbieżności (zdefiniowanej w różnym sensie) tego algorytmu dla układów kompensacji i IMC. Istotny z praktycznego punktu widzenia tzw. fazowy warunek zbieżności w układzie kompensacji mówi, że błąd fazy pomiędzy modelem, a obiektem nie może być większy od $\pi/2$ dla częstotliwości obecnych w widmie sygnału. Warunki dotyczące układów ze sprzężeniem zwrotnym wymagają niestety założeń, które nie są spełnione przez obiekty elektro-akustyczne. Dlatego, aby skorzystać z wyników uzyskanych dla układów kompensacji, stosuje się linearyzację toru sterowania (od wejścia filtru sterującego do wyjścia obiektu). Podejście takie umożliwia wyprowadzenie fazowego warunku zbieżności, różniącego się od warunku dla układów kompensacji obecnością filtru sterującego. Warunek taki odzwierciedla istotną zależność pomiędzy stabilnością strukturalnej pętli sprzężenia zwrotnego, a zbieżnością algorytmu adaptacji, wprowadzającego dodatkową pętlę sprzężenia zwrotnego. Zależność ta maleje w przypadku niewielkich błędów modelowania i małego wzmocnienia filtru sterującego. Wówczas układ IMC można analizować, jak układ kompensacji, pamiętając jednak o strukturze regulatora zawierającej model obiektu i związanym z tym problemem dotyczącym wewnętrznej

stabilności. Pełna analiza takiego układu stanowi wciąż otwarty skomplikowany problem badawczy. Zmodyfikowanie funkcji kosztów, podobnie jak w przypadku algorytmów optymalnych, może poprawić zbieżność algorytmu adaptacji oraz stabilność całego adaptacyjnego układu sterowania. Uzyskany w ten sposób algorytm Leaky FXLMS został pozytywnie zweryfikowany w wielu aplikacjach.

Stabilność, zbieżność, czas zbieżności (w konsekwencji również szybkość zbieżności), śledzenie i poziom tłumienia hałasu zależą w zasadniczy sposób od doboru tzw. współczynnika zbieżności (kroku) w algorytmie FXLMS. Pokazano, że dla małych wartości tego współczynnika istnieje odwrotna zależność pomiędzy nim, a czasem zbieżności, niezależnie od błędów modelowania obiektu. Następnie występuje optymalna wartość tego współczynnika, dla której czas zbieżności jest najmniejszy. Zależy ona głównie od opóźnienia w obiekcie i rzędu filtru sterującego. Dalsze zwiększanie współczynnika zbieżności powoduje wzrost czasu zbieżności na skutek fluktuacji sygnału wyjściowego i w konsekwencji rozbieganie się parametrów filtru. W literaturze dostępnych jest wiele modyfikacji algorytmu FXLMS polegających na automatycznym strojeniu wartości współczynnika zbieżności w trakcie adaptacji. Wśród nich szczególnie przydatna okazała się tzw. modyfikacja korelacyjna – Correlation FXLMS.

Układ IMC rozważano również dla obiektów elektro-akustycznych o wielu wejściach i wielu wyjściach (MIMO). Zastosowano podobną metodologię projektową do wykorzystanej dla obiektów o jednym wejściu i jednym wyjściu (SISO). Dyskutowano zarówno rozwiązania optymalne, jak i adaptacyjne. Przywołano warunki stabilności oraz modyfikację służącą jej poprawie. Zaprezentowano także znany wystarczający warunek na zbieżność wielokanałowego algorytmu FXLMS dla układów kompensacji. Brak jest jednak zarówno odpowiedniego warunku dla układów regulacji w przypadku obiektów nieminimalnofazowych, jak i pełnej analizy stabilności takiego układu.

Układ IMC poddano weryfikacji eksperymentalnej w zastosowaniu do sterowania aktywnym zagłówkiem fotela. Celem aktywnego zagłówka fotela jest generacja stref największego tłumienia hałasu (tzw. stref ciszy) wokół uszu osoby zajmującej miejsce na fotelu. Ze względu na zastosowane rozmieszczenie geometryczne głośników i mikrofonów należy on do rozważanej grupy obiektów elektro-akustycznych. Występuje w nim dodatkowo silne oddziaływanie kanałów, które w przypadku sterowania zdecentralizowanego może prowadzić do niestabilności. Przeprowadzone badania wykazały, że tłumienie hałasu mierzone dla danego kanału jest wówczas znacząco mniejsze w porównaniu do uzyskiwanego w przypadku sterowania uwzględniającego obecność sprzężeń skrośnych. Dlatego we wszystkich eksperymentach laboratoryjnych stosowano struktury MIMO, chociaż w literaturze powszechnie korzysta się z niezależnych układów SISO. Na drodze symulacji i eksperymentów z obiektem rzeczywistym pokazano, zgodnie z oczekiwaniami, że zarówno optymalny, jak i adaptacyjny układ IMC generuje strefy ciszy w otoczeniu mikrofonów rzeczywistych umieszczonych w obudowie zagłówka. Tłumienie w okolicach uszu użytkownika jest znacznie mniejsze. Ponadto przestrzenny gradient tłumienia jest wysoki, co jest przyczyną nieprzyjemnych efektów akustycznych odbieranych przez użytkownika w przypadku nawet niewielkich ruchów głowy.

Powyższe wnioski uzasadniają potrzebę projektowania układów sterowania umożliwiających generację stref ciszy w żądanych miejscach, w których umieszczenie mikrofonów rzeczywistych jest często z wielu powodów nie do zaakceptowania. Właściwości rozważanej grupy obiektów elektro-akustycznych ułatwiają jednak estymację sygnałów (efektów interferencji) w tych miejscach, zwanych sygnałami mikrofonów wirtualnych, w oparciu o pomiary dokonane mikrofonami rzeczywistymi.

W pierwszej z proponowanych struktur układu sterowania z mikrofonami wirtualnymi, nazwanej VMC1, estymowany sygnał jest przetwarzany tak, jak w klasycznej strukturze ze sprzężeniem zwrotnym. Z uwagi na zerowy sygnał zadany stanowi on wejście filtru sterującego i zarazem poddawany jest minimalizacji. Oprócz faktoryzacji pewnej transmitancji na część minimalnofazową i wszechprzepustową, faktoryzacji oceny gęstości widmowej zakłócenia i ekstrakcji części przyczynowej optymalnego filtru, projekt optymalnego filtru sterującego przeprowadzono, korzystając z równania Diofantycznego „rozbijającego" minimalnofazowy filtr kształtujący zakłócenie. Analiza adaptacyjnego układu sterowania z algorytmem FXLMS udowodniła, że do uzyskania zbieżności algorytmu w tym przypadku wymagane jest spełnienie silnego warunku fazowego. Ponadto, jedno z założeń niezbędnych do wyprowadzenia tego warunku, dotyczące korelacji pomiędzy sygnałem wejściowym filtru sterującego, a zakłóceniem, może zostać naruszone dla sygnałów deterministycznych lub wąskopasmowych. Znalazło to potwierdzenie w przeprowadzonych eksperymentach. W konsekwencji, mimo iż układ optymalny generuje strefy ciszy w żądanych miejscach, układ adaptacyjny nie spełnia swego zadania. Dla tej struktury zaproponowano również inny projekt regulatora bazujący na minimalizacji pewnego wskaźnika jakości w zadanym paśmie częstotliwości przy ograniczeniach dotyczących zapasu stabilności oraz maksymalnego dopuszczalnego wzmocnienia dźwięku poza tym pasmem.

Aby rozwiązać problem związany z realizacją adaptacyjną, zmodyfikowano strukturę sterowania. W układzie VMC2 minimalizowany jest estymowany sygnał mikrofonu

wirtualnego, ale wejście filtru sterującego stanowi estymowany sygnał zakłócenia. Optymalny filtr sterujący zaprojektowano stosując te same podejścia, jak w przypadku układu IMC. Wykorzystano do tego celu ogólną formę zapisu. Realizacja adaptacyjna w tym układzie wymaga dla poprawnej pracy dużo słabszych warunków zbieżności, niż w przypadku układu VMC1. Weryfikacja eksperymentalna również potwierdziła oczekiwania. Zarówno w przypadku układu optymalnego, jak i adaptacyjnego generowane strefy ciszy ulokowane są w żądanych miejscach. Dodatkowo, przestrzenny gradient tłumienia jest znacznie mniejszy, niż w przypadku układu IMC. W konsekwencji, tłumienie hałasu w okolicach uszu użytkownika jest zadowalające nawet wobec znaczących ruchów głowy. W tym samym czasie tłumienie przy mikrofonach rzeczywistych jest zdecydowania mniejsze lub obserwowane jest nawet wzmocnienie dźwięku.

Istnieje wiele aplikacji aktywnego tłumienia hałasu, w których zmiany zarówno hałasu, jak i parametrów obiektu są niewielkie. Zaproponowano więc układ VMC3, w którym można wyróżnić dwa etapy pracy. W etapie strojenia minimalizowany jest bezpośrednio sygnał z mikrofonu tymczasowo umieszczonego w żądanym miejscu. W tym samym czasie strojony jest dodatkowy filtr. Filtr ten jest następnie wykorzystywany w etapie sterowania, w którym nie korzysta się ze wspomnianych mikrofonów, do wypracowania wartości zadanej dla sygnału mierzonego przez mikrofon rzeczywisty. Dla układu VMC3 fazowy warunek zbieżności jest najsłabszy. Zatem w układzie tym możliwe jest uzyskanie zbieżności algorytmu adaptacji w warunkach, dla których w pozostałych układach algorytm taki jest rozbieżny. Układ VMC3, zarówno w wersji optymalnej, jak i adaptacyjnej, potwierdził swoje zalety w konfrontacji z obiektem rzeczywistym. Uzyskane tłumienie hałasu w żądanych miejscach oraz strefy ciszy są największe.

Dla wszystkich omawianych układów sterowania wyprowadzono zależność wyrażającą zmiany poziomu tłumienia hałasu w przestrzeni, związane ze zmianą toru wirtualnego. Pokazano również, że zwiększenie liczby mikrofonów i głośników umożliwia zwiększenie rozmiarów stref ciszy oraz poprawę tłumienia hałasu. Jednak takie rozwiązanie komplikuje układ sterowania, negatywnie wpływa na jego odporność w przypadku zmian parametrów obiektu oraz istotnie zwiększa złożoność obliczeniową.

Rozważano również problem tłumienia hałasu w większych odległościach od mikrofonu rzeczywistego, niż założono na samym początku. W takim przypadku, zarówno w projekcie układów optymalnych, jak i adaptacyjnych należy zastosować filtr pozwalający na estymację hałasu w punkcie mikrofonu wirtualnego na podstawie pomiarów dokonanych mikrofonem rzeczywistym. Jednak, filtr taki silnie zależy od położenia źródła pierwotnego względem tych mikrofonów oraz od środowiska akustycznego, co uniemożliwia jego znalezienie w ogólnym przypadku. Zastosowanie tablicy mikrofonów rzeczywistych nie rozwiązuje problemu. Dlatego, jeśli zachodzi potrzeba tłumienia hałasu w większej odległości od źródła wtórnego, zaleca się zastosowanie mikrofonu bezprzewodowego (na przykład przymocowanego do ubrania), a następnie ewentualnie przesuwanie stref ciszy o niewielkie odległości względem długości fali z wykorzystaniem omawianych układów VMC.

Dla celów projektowania i analizy omawianych algorytmów założono, że obiekt jest liniowy. Założenie to można uznać zwykle za spełnione. Istnieją jednak pewne aplikacje, w których nieliniowości obiektu mogą mieć istotne znaczenie, szczególnie dla bardzo niskich częstotliwości hałasu oraz przy bardzo małej odległości mikrofonu rzeczywistego od źródła wtórnego [Pawelczyk_01]. Wówczas, tłumienie uzyskiwane w wyniku pracy omawianych algorytmów może ulec pogorszeniu. Problem ten można rozwiązać stosując nieliniowe techniki sterowania. W ostatnich latach prowadzono prace nad wykorzystaniem sieci neuronowych do zagadnień aktywnego tłumienia hałasu. Głównym problemem jest wówczas powolny proces uczenia, który można przyspieszyć stosując odpowiednie modyfikacje [Bouchard_01]. Można również zastosować rozmyte sieci neuronowe oraz modelowanie rozmyte [ZhangG_04b], [BottoSC_05]. Umożliwiają one włączenie informacji lingwistycznej do procesu przetwarzania numerycznego.

Spis rysunków

Spis tabel

Wydano za zgodą
Rektora Politechniki Śląskiej

WYDAWNICTWO POLITECHNIKI ŚLĄSKIEJ
ul. Akademicka 5, 44-100 Gliwice; tel. (0-32) 237-13-81
http://wydawnictwo.polsl.pl

Sprzedaż i Marketing
tel. (0-32) 237-18-48
wydawnictwo_mark@polsl.pl

Nakł. 120+50	Ark. wyd. 11	Ark. druk. 11,5	Papier offset. 70x100,80g
Oddano do druku 30.06.2005 r.	Podpisano do druku 30.06.2005 r.		Druk ukończ. w lipcu 2005 r.

Wydrukowano w Zakładzie Graficznym Politechniki Śląskiej w Gliwicach, ul. Kujawska 1
zam. 298/05